Doctoral theses at NTNU, 2017:342

Michele Baravalle

Risk and Reliability Based Calibration of Structural Design Codes

Principles and Applications

ISBN 978-82-326-2752-3 (printed ver.)
ISBN 978-82-326-2753-0 (electronic ver.)
ISSN 1503-8181

NTNU
Norwegian University of
Science and Technology

NTNU
Norwegian University of Science and Technology
Thesis for the Degree of
Philosophiae Doctor
Faculty of Engineering
Department of Structural Engineering

Doctoral theses at NTNU, 2017:342

NTNU
Norwegian University of
Science and Technology

Michele Baravalle

Risk and Reliability Based Calibration of Structural Design Codes

Principles and Applications

Thesis for the Degree of Philosophiae Doctor

Trondheim, December 2017

Norwegian University of Science and Technology
Faculty of Engineering
Department of Structural Engineering

NTNU
Norwegian University of
Science and Technology

NTNU
Norwegian University of Science and Technology

Thesis for the Degree of Philosophiae Doctor

Faculty of Engineering
Department of Structural Engineering

ISBN 978-82-326-2752-3 (printed ver.)
ISBN 978-82-326-2753-0 (electronic ver.)
ISSN 1503-8181

Doctoral theses at NTNU, 2017:342

Printed by NTNU Grafisk senter

To you, who will be born soon. I can't wait!

Table of Contents

Table of Contents ..... **iii**
Preface ..... **vii**
Abstract ..... **ix**
Acknowledgments ..... **xi**
Outline of the Thesis ..... **xiii**
List of Papers ..... **xv**
Abbreviations ..... **xvii**

Chapter 1 Introduction **1**

1.1 Background and research objectives 1
1.2 Limitations 22
1.3 Highlights and main findings 23
1.4 Conclusions and discussion 25
1.5 Future research 29

Part I Calibration of Codified Design **33**

Chapter 2 Paper I: A Risk-Based Approach for Calibration of Design Codes **35**

2.1 Abstract 35
2.2 Introduction 36
2.3 Background 37
2.4 Methods 40
2.5 Case study 49
2.6 Summary and discussion 59
2.7 Conclusions 63

Chapter 3 Paper II: Generic Representation of Target Values for Structural Reliability **65**

3.1 Abstract 65
3.2 Introduction 66
3.3 Structural design as an optimisation problem 67
3.4 Risk acceptance criteria 70
3.5 The plot for optimal and acceptable reliabilities 72
3.6 Illustrative examples 78
3.7 Conclusions 82
3.8 Appendix to Chapter 3 – Plots for different distribution types 83

Chapter 4 Paper III: A Framework for Estimating the Implicit Safety Level of Existing Design Codes 87

4.1 Abstract 87
4.2 Introduction 88
4.3 Target safety levels from monetary optimisation 88
4.4 Estimation of the implicit target reliability of existing codes 90
4.5 Comparison with another method 95
4.6 Conclusions 96

Part II Specific Study Cases 99

Chapter 5 Paper IV: Calibration of Simplified Safety Formats for Structural Timber Design 101

5.1 Abstract 101
5.2 Introduction 102
5.3 Eurocode safety format 103
5.4 Proposed simplified safety formats 104
5.5 Calibration of safety formats 105
5.6 Results and discussion 109
5.7 Conclusions 114
Acknowledgments 114

Chapter 6 Paper V: On the Probabilistic Representation of Wind Climate for Calibration of Structural Design Standards 115

6.1 Abstract 115
6.2 Introduction 116
6.3 Representation of the wind climate 117
6.4 Inclusion of wind climate spatial variation in code calibration 129
6.5 Discussion 133
6.6 Conclusions 134
6.7 Appendix I to Chapter 6 - Equations and formulas 135
6.8 Appendix II to Chapter 6 - Stochastic models used in the example calibration 136

Chapter 7 Paper VI: Risk and Reliability-Based Calibration of Design Codes for Submerged Floating Tunnels 137

7.1 Abstract 137
7.2 Introduction 138
7.3 Design approaches and code calibration 139
7.4 Case study: SFT with reinforced concrete structure 142
7.5 Conclusion 146
Acknowledgments 147

References 149

Appendix A Penalty Functions for GOM and AM 157

A.1 Penalty functions 157
A.2 Comparison of calibration methods and penalty functions 159

Appendix B Reliability-Based Calibration of Partial Safety Factors in the Eurocodes 163

B.1 Introduction 164
B.2 Methods 164
B.3 Calibration of the partial safety factors on the load side 165
B.4 Evaluation of the reliability of the design with the calibrated load partial safety factors for cases with two variable loads acting simultaneously 178
B.5 Calibration of the partial safety factor for a generic load 181
B.6 Calibration of the partial safety factor for a generic material 182
B.7 Summary and future work 185

Preface

This doctoral thesis is submitted in partial fulfilment of the requirements for the degree of Philosophiae Doctor (Ph.D.) in Structural Engineering at the Norwegian University of Science and Technology (NTNU). The research was carried out at the Department of Structural Engineering at NTNU in Trondheim, Norway.

The project was founded by the Department of Structural Engineering at NTNU. The project started in October 2013 and the thesis was submitted in September 2017. The founding included one year of teaching assistance at the Department of Structural Engineering. This activity was mostly concentrated in the first three years. A part of this research work has been supported by the Norwegian Public Roads Administration (NPRA) as part of the "Ferry-free coastal route E39" project.

The main supervisor of the project was Professor Jochen Köhler (NTNU, Norway). The co-supervisor was Professor John Dalsgaard Sørensen (Aalborg University, Denmark).

Michele Baravalle
Trondheim, September 2017.

Abstract

Structures and infrastructures are essential for most societal activities and are required to be safe, as well as economically and environmentally sustainable. At the same time, societal resources of all kinds are limited. Thus, it is of vital importance that these resources are allocated optimally, not only financially but also in terms of reduction of risk to life. A logical point to start from in approaching this complex optimization problem is with our building codes that constitute the primary decision support for structural engineers. Therefore, it is essential that the building codes are optimised or calibrated for this perspective. The design with optimised codes balances investments into safety and expected adverse consequences.

This work contributes to the development of theoretical methods for code making. The aim is to reduce the subjectivity involved in the process and, consequently, to make more solid, transparent and optimal decisions.

The primary objective is to provide rational methods, frameworks and principles for optimizing the design requirements. For this purpose, in the first part of the work, code optimization is seen as a decision problem under risk, where society is the rational decision maker. Indeed, the outcomes of a decision, such as the assignment of safety factor values, are not known with certainty. Therefore, the basis is exclusively taken from the normative decision theory, which provides a strategy ensuring minimal use of resources over time. Three main methods are proposed: i) a generic and comprehensive risk-based calibration approach for calibrating the design requirements, ii) a generic representation of target values for structural reliability and iii) a method for estimating the implicit safety level of existing optimal codes.

The secondary objective is to address the current code calibration and code-related tasks and to provide objective bases for decision making. Four tasks are addressed: i) the calibration of simplified safety formats for the design of common timber structures, ii) the probabilistic modelling of the wind climate for code calibration, iii) the discussion of the optimality of designing extraordinary structures using common design codes, iv) the assessment and eventual re-calibration of the partial safety factors in the Eurocodes.

In conclusion, the present work represents a substantial step forward towards a more rationally based code making. The methods proposed in the first part might support code committees in the fundamental decision of selecting target reliabilities and differentiating them among structures with diverse characteristics. The second part proposes solutions to current calibration tasks applying existing methodologies.

Acknowledgments

I would like to warmly acknowledge Professor Jochen Köhler for starting this project and selecting me as a student. In addition, I would like to thank the Department of Structural Engineering at the Norwegian University of Science and Technology (NTNU) for financing the project and providing all of the facilities a Ph.D. candidate needs. In addition, I would like to acknowledge the Norwegian Public Roads Administration (NPRA) for financing part of the work.

I would like to thank my main supervisor, Prof. Jochen Köhler, and my co-supervisor Prof. John Dalsgaard Sørensen. Thank you for guiding me during these four years of intense work, learning and transformation. You have taught me a lot and you have introduced me to a very interesting subject and research community.

I would like to acknowledge all the people I met during these four years: PhD students, colleagues, department employees, professors, students and all of the people I got to know. I consider the new relationships and friendships established with all of you as more valuable than any research achievement. Among my colleagues, I would like to thank Klodian, Martin and Mirko for all the time we spent together, for proofreading my manuscripts, exchanging precious advice and sharing this once-in-a-lifetime experience that we will never forget.

Finally, a special thanks to all my family. The biggest thank goes to Eleonora. Besides our wonderful private life, you substantially contributed to this work by helping me to overcome the most demanding and stressful periods with support and patience.

Grazie!

Michele Baravalle
Trondheim, September 2017.

Outline of the Thesis

This thesis is a collection of scientific papers. The first Chapter of this thesis presents an introduction to this research work and a review of the principles and methods of code calibration. The following Chapters are divided into two parts: the first provides rational methods, frameworks and principles for optimizing the requirements in the design codes; the second includes some current code calibration and code-related tasks.

Chapters 2, 3, 5 and 6 are papers published in, or submitted to, international scientific journals. Chapters 4 and 7 are papers presented at international conferences. The results of the calibration work performed for the CEN\TC 250 Sub-Commission 10 Working Group 1 are included in Appendix B since they are still in a preliminary status.

List of Papers

Papers included in the thesis

The thesis includes the following papers written by the author. These papers are referenced in this thesis with roman numbers.

Paper I: A Risk-Based Approach for Calibration of Design Codes
Baravalle, Michele; Köhler, Jochen
Submitted to an international scientific journal on September 8th, 2017.

Paper II: Generic Representation of Target Values for Structural Reliability
Baravalle, Michele; Köhler, Jochen
Submitted to an international scientific journal on September 22nd, 2017.

Paper III: A Framework for Estimating the Implicit Safety Level of Existing Design Codes
Baravalle, Michele; Köhler, Jochen
Proceedings of the 12th International Conference on Structural Safety & Reliability (ICOSSAR 2017), Vienna, Austria.

Paper IV: Calibration of Simplified Safety Formats for Structural Timber Design
Baravalle, Michele; Mikoschek, Michael; Colling, François; Köhler , Jochen
In *Construction and Building Materials.* Volume 152, 2017, pp. 1051-1058.

Paper V: On the Probabilistic Representation of Wind Climate for Calibration of Structural Design Standards
Baravalle, Michele; Köhler, Jochen
In *Structural Safety.* Volume 70, 2018, pp. 115-127.

Paper VI: Risk and Reliability-Based Calibration of Design Codes for Submerged Floating Tunnels
Baravalle, Michele; Köhler, Jochen
In *Procedia Engineering*. Volume 166, 2016, Pages 247-254.

Declaration of authorship

Michele Baravalle conducted the research, wrote the manuscripts, performed the calculations, worked out the examples and case studies and analysed the results in all of the work included in this thesis. The co-authors of the papers contributed with constructive criticism and discussions, and proofread the manuscripts.

In paper IV, M. Baravalle proposed the calibration framework and procedure, wrote most of the manuscript and performed the majority of the calculations with the contribution of Michael Mikoschek. The simplified safety format SFI was proposed earlier by Michael Mikoschek and François Colling [1]; the simplified safety format SFII was an idea of Jochen Köhler. All four authors participated to the assessment of results, the individuation of the most common design scenarios, proofread the manuscript and contributed with constructive discussions.

The calculations in Appendix B were conducted by Michele Baravalle, the selection of the input and the evaluation of the results were jointly performed by M. Baravalle, Jochen Köhler and John D. Sørensen; the constructive criticism of the CEN Sub-Committee 10 Working Group 1 contributed to improving the work significantly.

Abbreviations

ALS	Accidental limit state
AM	Approximate method (see [2])
ASD	Allowable stress design
CDF	Cumulative probability distribution function
COV	Coefficient of variation
EN	European Standard
EU	Expected utility
FORM	First order reliability method
GOM	Global optimization methods (see [2])
ISO	International Organization for Standardization
JCSS	Joint committee on structural safety
LQI	Life quality index
LRFD	Load and resistance factor design
LSF	Limit state function
MU	Monetary unit
PMC	Probabilistic model code
PDF	Probability density function
PSF	Partial safety factor
PV	Present value
SLS	Serviceability limit state
SWTP	Societal willingness to pay
ULS	ultimate limit state

Chapter 1 Introduction

1.1 Background and research objectives

1.1.1 The need for safe, optimal and sustainable structures

The built environment constitutes the basis for our economy and contributes to the continuous development of our society. In this respect, structures play an important role, since their primary purpose is to provide the functionality of the built environment and the safety of its users. Consequently, a significant portion of societal economic and natural resources is invested in the continued development, maintenance and renewal of structures. In the European Union, for example, the construction industry consumes between 1200 and 1800 Million tonnes of building materials per annum [3].

The total used resources and the total costs of a generic structure over time are not predictable with certainty. Indeed, different hazards exist during the activities of building, using, maintaining and decommissioning of the structure. The harm that might result from these hazards has a social cost that might be expressed in terms of fatalities, monetary units or greenhouse gas emissions. Hazard indicates here a potential source of harm or damage to life, the environment or property. The ground motion caused by an earthquake (the hazard), for example, might lead to the event of structural failure and associated consequences such as loss of lives and financial losses. The magnitude of a hazard is measured in terms of risk that is the product of the probability of the damaging event occurring and the average damage given that the event has occurred. Therefore, the risk is expressed in the same units as the consequences.

The uncertainty regarding the consequences of adverse events and the probability of their occurrence have been traditionally “compensated” by engineers with a conservative design or, equivalently, a risk-averse behaviour [4]. In other words, engineers prefer more safe structures that have more certain, but often higher, expected lifetime cost rather than less safe structures that have more uncertain, but possibly lower, expected cost. Thus, rare events with high consequences are over-weighted. The resulting actual level of risk associated with the use of structures is significantly lower than the risk involved in most human activities [5], and appears to be widely accepted by society. This risk-averse strategy might be tolerated by society because the waste of resources associated with over-designed structures is lower than the waste associated with under-designed structures since the risk function for over-designed structures

is relatively flat [5]. Nevertheless, decision strategies based on conservativeness and risk aversion are irrational from the perspective of society when all of the hazards and the uncertainties, as well as the risk to life, are included in the decision making. Indeed, these strategies lead to a waste of resources and, thus, might not fulfil the requirement for financial and environmental sustainability. Since society's economic and natural resources are limited, their use should be optimised, i.e. directed to efficient life-saving and risk-reducing measures. The optimal allocation of the resources guarantees that, with the given budget, the maximum possible number of fatalities is avoided and that the societal needs for structures and infrastructures are satisfied with the least amount of resources over time.

The first principles of financial optimisation regarding structural design codes date back to 1924, when Forssell [6] argued that resources should be expended for increasing safety against fire in houses only when the corresponding reduction of the expected consequences is larger than the resources invested. As later introduced, this principle is applicable for levels of risk to life and limb that are above a certain absolute acceptable level. Environmental sustainability is a more modern, but certainly relevant, requirement. In fact, it is estimated that, in Europe, the emissions from the (cradle-to-gate) production of materials used in construction for buildings correspond to about 3 to 5 % of the annual greenhouse gas emissions [3]. Therefore, the decisions taken in this sector have a significant impact on emissions and environmental policies.

A logical point to start approaching the ambiguous and complex optimisation of our structures is the main interface between research and practical decision making: the structural design codes, or standards. The codes constitute the primary decision support for practising structural engineers since the clear majority of structures are designed and controlled according to these legal regulations. Therefore, it is essential that structural design codes represent a rationale leading to design solutions that balance expected adverse consequences (e.g., in case of failure or deterioration) with investments into safety. Structural design codes should, therefore, be calibrated based on the associated risks or, in the same vein, based on the related failure probability.

1.1.2 Structural design codes

Codes provide standardisation of structures and facilitate the daily work of engineers [7]. They are also referred to as norms, standards or regulations. Modern codes guarantee, besides safety, a certain level of serviceability, durability and sustainability.

In the broader societal context introduced previously, the ultimate objective of the standards is "*to guard the interests of society*" [8, p.4] by guiding decision makers to the optimal allocation of societal resources in structures. The structural optimisation is reached in two stages [9]: first, the optimisation of each structure and, second, the optimisation of design norms, which are the constraints placed on the first. In this broader perspective, the codes play a major role in terms of economic competitiveness and decision making in engineering [5]. They influence, indeed, part of the construction sector that is a major sector in all developed countries.

Codes covering structural design are tightly interconnected with other standards regulating, for example, material production, grading and acceptance or construction and installation tolerances. Consequently, design codes should not be seen as singular regulatory documents, but rather as elements of a regulatory framework.

Structural design and assessment of decisions can be performed with three main approaches [10]. Every approach is limited to certain engineering problems and is supported by a specific kind of standard, as illustrated in Figure 1.1.

- **Level 4 or risk-informed approach.** The first, most general and widely applicable, approach consists in making decisions based on full-risk analyses. The international standard ISO 2394 [10] provides the principles to be followed.
- **Levels 3 and 2 or reliability-based approach.** The second approach consists of reliability-based design and assessment. It can be used as a simplification of the first when the consequences of failure and damage are well understood and within ordinary ranges. Reliability analyses are based on reliability theory and probabilistic modelling of the involved random variables and stochastic processes [5, 11, 12]. The Probabilistic Model Code (PMC) [13] issued by the Joint Committee on Structural Safety (JCSS) codifies and standardises the modelling approaches and philosophy. Although the PMC has no regulatory validity to date, it has reached a broad consensus in the last decades.
- **Level 1 or semi-probabilistic approach.** The third approach consists in the design and assessment of decisions by means of semi-probabilistic design codes. This approach is a further simplification of the second one, and it applies to categorised and standardised consequences, failure modes and uncertainty representation.

The mentioned approaches make use of different analysis techniques which are often referred to as Levels 4, 3, 2 and 1 [5, 14]. Consequently, the codes regulating their application are here also referred to as Levels 4, 3, 2 and 1, see Figure 1.1. A thorough description of the fundamental aspects of the three approaches is given in [I] and in [10].

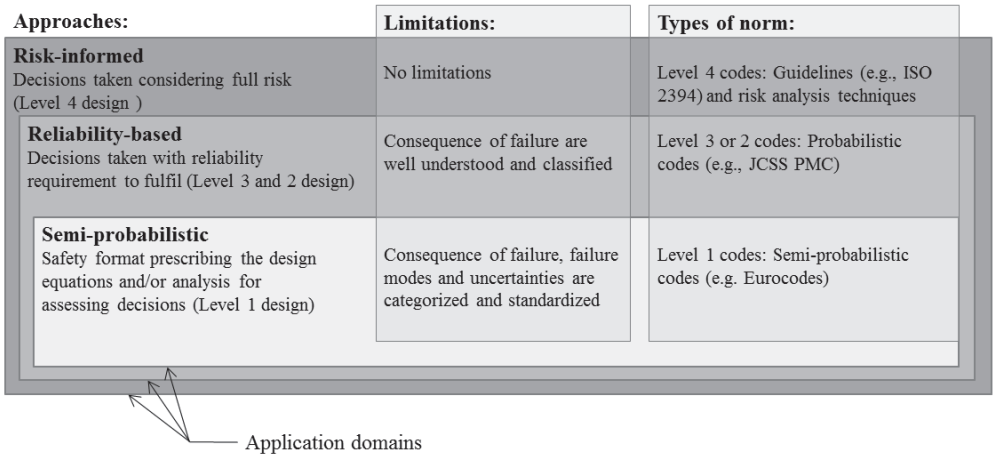

Figure 1.1. Design and assessment approaches with limitations [10] and regulating norms.

The simplification of higher design approaches is performed for specific classes of similar decision problems. For example, semi-probabilistic codes reduce the assessment of structural design to a "*routine"* procedure [9] and are specifically developed for the design of common structures under normal loading, operational and environmental conditions (see e.g., the Eurocode 1 Part 1-4 [15] that is limited to structures up to 200 m high). Consequently, they are only applicable in the domain they have been developed and calibrated for. The semi-probabilistic and the probabilistic codes should, therefore, state all relevant information concerning possible limitations and assumptions. Their validity and application should be specified including legal, temporal and geographical constraints, types of structures, materials, uses and loads [10]. The philosophy behind the simplification and the following limitations are

described in [I]. The mentioned simplifications come at the cost of a reduction of design optimality or, equivalently, an economic loss. This loss is partly or totally balanced by the reduction of the effort in the design. The balance between code simplification and optimality is discussed in [I] and [IV] where a simplified safety format for timber design is calibrated and compared with the existing format.

Semi-probabilistic codes are the most used standards for structural design. The reasons are that they apply to all ordinary structures, their simplicity reduces the engineering costs and the design checks are highly reproducible (or at least it is believed so) in the sense that they weakly depend on the engineer performing them. On the contrary, reliability- and risk-based design approaches require engineers to have information (e.g., consequences of failure, stochastic models) and knowledge (e.g., reliability methods, probabilistic modelling) that they seldom have. Moreover, in most cases, reliability analyses' results depend on the person performing the analysis since they are conditional on the information available to that person. The possibility of including all the available information is, indeed, one of the strengths of the method. At the same time, it is one of the reasons for its limited application, as common engineers interpret the failure probability as a property of the structure and, therefore, do not trust design methods that provide different results for the same structure. Consequently, reliability-based assessment and design are not accepted by the majority of authorities and professionals [16]. Nevertheless, it should be noted that the semi-probabilistic codes are calibrated with the probabilistic codes and structural reliability methods. Thus, there are in principle no differences between the two codes, except the fact that the former simplifies the design at the cost of an optimality loss. Although the Probabilistic Model Code [13] was introduced for mitigating these disadvantages, the two higher methods are mainly used at present for cases that are not covered by semi-probabilistic codes (e.g., the use of new materials) or when the simplifications of the latter are too conservative, leading to excessive over-design. However, the conversion of a probabilistic code, such as [13], to a standard and the inclusion of structural reliability as a basic subject in all structural engineering study programs are seen as essential requisites for reaching a more extensive use of Level 2 and 3 methods in the future [17].

Semi-probabilistic formats have been developed and improved continuously over time. The safety factor was applied originally on the strength side only in the so-called allowable stress design (ASD) format. Later, the safety factor was applied on the loading side allowing for, e.g., the plastic design. The most modern codes (e.g., [18, 19, 20, 21, 22]) are written in the Load and Resistance Factor Design (LRFD) format with the partial safety factors on both sides [23]. This format was first introduced by Ravindra and Galambos in 1978 [24]. Compared to the previous semi-probabilistic formats, the LRFD format provides more uniform reliability among structures, has higher flexibility in introducing a new technology or material and can easily accommodate adaptions for different geographical areas and uses.

In the LRFD format, random variables are represented by characteristic values, which are then transformed into design values using partial safety factors (PSFs) [5, 11, 14, 23]. The structural dimensions (e.g., element cross-section, reinforcement area) are selected to satisfy the design equations which are often similar to the corresponding limit state functions even though this is not strictly necessary and may not be optimal [25]. In general, the load PSFs are material independent, and the material PSFs are load independent. Moreover, the load combination is independent of the safety check. Besides the PSFs associated with defined characteristic values, the LRFD safety format includes other *reliability elements* [10] that

control the reliability of the design; these include the load reduction factors and the modification factors.

Semi-probabilistic codes usually implement the single-failure-mode checking format applied at the structural element level. Therefore, system effects are not directly considered. Nevertheless, the reliability of the resulting structural systems is often larger than the component reliability due to several reasons such as the contribution of non-structural elements, the requirements on serviceability and structural redundancy, the hidden safety reserves and the discretisation of the structural element sizes [23, 26]. However, in some cases, these effects are not present, and the resulting system reliability might be lower than the reliability of the components. Therefore, robustness requirements are usually present for limiting the contribution of the indirect risk to the total risk [27].

1.1.3 Code writing and code revision

The process of writing new codes and revising the existing ones is continuous. In Europe, for example, European standards for structural design [18] were released between 1998 and 2006, maintained and evolved in the following years and a major revision work (started in 2012) is ongoing at present [28]. In detail, new codes or review of the existing ones are needed for different reasons including:

- Technology developments such as new or improved: production methods, structural analysis tools (e.g., non-linear Finite Element analyses tools), quality control tools, materials and material properties (e.g., structural glass and cross-laminated timber), installation procedures and structural concepts (e.g., the submerged floating tunnel [29]).
- The requirement for an extension to new applications (e.g., longer bridges [29], higher buildings, more slender structures).
- The inclusion of the experience gained using the existing standards (e.g., excessive failure rates or construction costs).
- The harmonisation with other standards or sectors.
- The implementation of new findings in research.
- The socio-economic changes that lead to different levels of risk acceptance and requirements.
- The variation of climatic actions induced by climate change (see, e.g. [30]).
- Other requirements from professionals, industry, society or the authorities.

Theoretically, the optimal rate of code change might be estimated by solving an adaptive control problem since the effects of code changes are not predictable and are evident only after a certain time [9]. Small changes might be introduced at optimal points in time starting from an over-optimal code. In fact, frequent changes may lead to overshooting of the optimal safety level, while slow changes might cause a waste of materials. However, the revision process is (and was) never planned so rigorously due to practical reasons such as the organisation of code committees and the availability of resources. Moreover, code changes must be introduced gradually over time to avoid mistrust and uncertainty of the engineers [5]. In practice, the code revisions were usually undertaken when one or several of the reasons listed at the beginning of this Section were present.

Review of structural standards usually consist of one of the following main actions or a combination of them:

- **Change of code format** might be performed for converting the ASD to the LRFD format or to the probabilistic format. It is often performed under the postulate that the existing code is optimal since, in the contrary case, it would have been revised. It follows that the reliability elements of the new format are calibrated to lead, as far as possible, to the same level of safety or same design as the existing code. For converting a LRFD format code into a probabilistic code, the cost of failure and the reliability level implicit in the LRFD code can be back calculated by assuming probabilistic models representing the random variables. When several probabilistic codes are available, the "prudency principle" was proposed for selecting the best one [31].
- **Code calibration or optimisation** is the most significant revision action since it changes the code safety level. Details on code calibration are given in the following Section.
- **Introduction of new principles, requirements and reformulation of text** are performed subjectively by experts in the field since no objective real alternatives exist.
- **Extension to new applications** (e.g., materials, failure modes, loads, types of structures) is characterised by a lack of experience. Therefore, analytical calibration methods assume higher importance than experience.

1.1.4 Code calibration or optimisation

1.1.4.1 Motivation

The Level 4 approach consists in making decisions that minimise the risk. In very simplified terms, the risk associated with a certain decision parameter p (e.g., the cross-sectional dimension of a column) is $\Re(p) = C_C(p) + E[H] \cdot P_f(p)$. The first addend represents the cost of safety, a larger p costs more but also reduces the likelihood of structural failure. The second addend is the product between the expected consequences given the failure occurs $E[H]$ and the probability of failure occurrence $P_f(p)$. The product represents the risk associated with the structural failure event, which decreases with p. Consequently, the sum of the two addends (i.e., the risk function) is typically convex. Provided that $E[H]$ and the functional relationships $C_C(p)$ and $P_f(p)$ are known, the optimal design is individuated minimising the risk. The designer can minimise the risk by reducing the consequences given failure, by reducing the failure probability or both.

For the Level 3 or 2 approaches, the consequences given failure are not directly considered in the design. Instead, the probability of failure minimising the risk (for the expected consequences of failure characterising the problem at hand) is given. This probability of failure is referred to as the target or optimal probability of failure ($P_{f,t}$ and $P_{f,opt}$, respectively). Alternatively, the target reliability index is given, which is one-to-one related to $P_{f,t}$ by $\beta_t = -\Phi^{-1}(P_{f,t})$, where Φ is the standard normal cumulative probability distribution function. Subsequently, the designer selects a p value that satisfies $P_f(p) = P_{f,t}$. In practice, target probabilities of failure are not differentiated for each specific engineering problem since this would correspond to a risk-based design, and it would not simplify the design. Instead, a unique $P_{f,t}$ is given for each class of engineering problems; within each class the characteristics of the problems that influence the location of the risk function minimum are similar, although not identical. In the example introduced before, the structures in a class shall be similar regarding $C_C(p)$, $E[H]$ and $P_f(p)$. Thus, the optimal $P_{f,t}$ has to be calibrated by answering the question "given that a unique $P_{f,t}$ is sought for a class of similar structures, what $P_{f,t}$ minimises the risk?" The structures designed with the calibrated $P_{f,t}$ will not all be optimal, but the $P_{f,t}$ will regulate the reliability-based approach optimally.

For the Level 1 approach, neither the P_f nor the consequences are directly considered in the design. The designer selects p by satisfying a certain design equation, $f(p,\mathbf{r}) \geq 0$, where $\mathbf{r}$ is a vector of reliability elements. The values of the reliability elements are selected so that if p satisfies $f(p,\mathbf{r}) = 0$, then $P_f(p) = P_{f,t}$ and thus the risk is minimum. As before, a unique set of reliability elements is given in practice for each class of engineering problems which have similar $C_C(p)$, $E[H]$ and $P_f(p)$. This requires the reliability elements to be calibrated, answering the question "given that a unique set of reliability elements is sought for a class of similar structures, what set minimises the risk?" Again, the design with the calibrated $\mathbf{r}$ will not lead to optimal structures in all cases, but the optimal $\mathbf{r}$ will regulate the design optimally with the semi-probabilistic approach.

As described in this Section, the different approaches are interconnected and all based on higher levels. This interconnection is described rigorously in [I], where a generic calibration approach is proposed allowing for a consistent calibration of the different codes. It is also important to note that the only rational approach satisfying "rigorously" the requirements for sustainable and optimal structures is the Level 4 approach. All other approaches are simplifications of this level. This implies that higher levels are implicitly accepted when using lower levels.

1.1.4.2 Definition

Code calibration or optimisation is defined in the literature as "[…] *the process of assigning values to the parameters in a design code* […] *with a view to achieve a desired level of reliability in error-free structures* " [12, p.126]. Parameters are here considered to be the reliability elements which in general can be intended to be the partial safety factors, load reduction factors and modification factors for semi-probabilistic codes or the target failure probabilities for probabilistic codes.

Calibration of semi-probabilistic codes also includes the selection of the safety format, the characteristic values, the partial safety and load combination factors, the load combination rules and all the other reliability elements "*such that the level of reliability of all structures designed according to the design codes is homogeneous and independent of the choice of material and the prevailing loading, operational and environmental conditions.* […] *including the choice of the desired level of reliability or "target reliability*"" [32, p.2].

1.1.4.3 Modern techniques and past experience

Structures designed in the past, with a specific code, have been evaluated and represent full-scale "experiments" providing information, or "*past experience*" [9], to be considered during a code revision. In the past, codes were revised based solely on experience through a "trial-and-error strategy" since no other rational methods were available. This method is here referred to as experience-based code calibration. The safety level was changed every time a non-acceptable lack of balance between construction costs and safety was observed.

Modern code calibration techniques have been developed over the last decades for overcoming the limitations of experience-based calibration. The methods are essentially based on the structural reliability and decision theories. They are referred to as reliability-based and risk-based code calibration. These techniques consider only correctly implemented measures to take hazards into account. In other words, they do not consider the effects of human errors. The core of the calibration is essentially to define the extent of the fraction of the hazards that is taken as risk and the fraction that is taken into account by safety measures, see Figure 1.2.

Although modern calibration methods are available and widely accepted, experience remains an important part of the code-making process. The reasons are that, as illustrated in Figure 1.2, neither experience-based calibration nor calibration with modern methods is complete. On the one hand, i) modern calibration techniques do not account for the human errors (of any type), ii) the effects of code changes are rather difficult to predict, iii) the substantial simplification of the complex calibration problem which is indispensable for applying the calibration techniques might reduce the accuracy of the results, iv) the accepted risk includes epistemic uncertainties and v) the models adopted might include some hidden safety. On the other hand, observation of the built environment is not always possible (as in the case of calibration of a code for a new material or for including the predicted effects of climate change) and, when possible, it requires a rather extended period of observation. The observed failure rates in the typical time intervals between two code revisions are characterised by a large statistical uncertainty due to the low failure rate of typical structures. In addition, the amount of statistical information obtained from the observation is limited by the fact that the population of built structures is highly non-homogeneous and that it is difficult to exclude from the assessment aspects such as human errors and the contributions of the non-structural components.

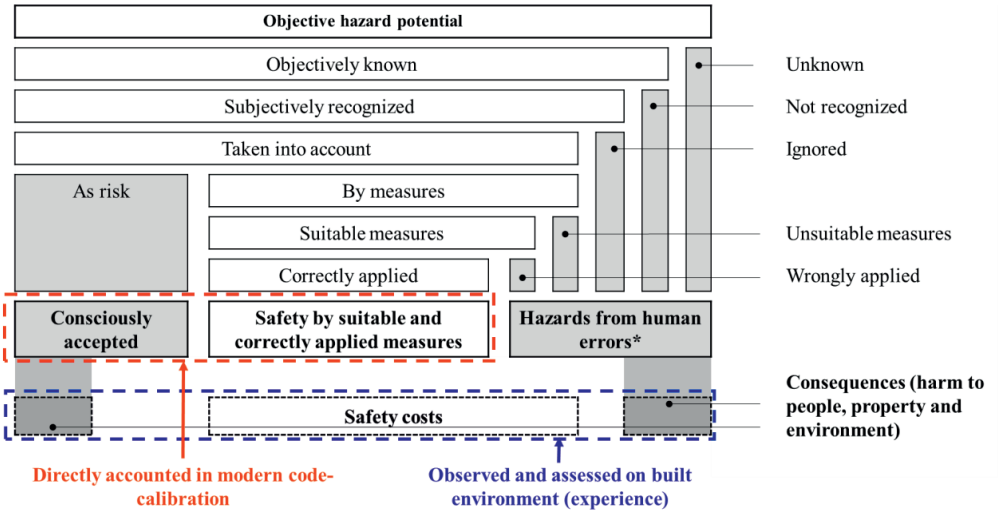

*Including human errors in code-calibration as well as errors in design, construction, use and maintenance of the structure.

Figure 1.2. Risk picture for structures (adapted from [14]).

The human errors represent a hazard which might result in adverse events and, thus, future losses. Nevertheless, the objectives of structural reliability and probability theory are not to treat and prevent human errors in design, construction, maintenance, use and decommissioning of structures. Gross human errors in these phases are prevented by robustness requirements; the other minor errors are "controlled" by quality assurance and quality checks. These errors are not considered in the code-optimization under the assumption that, in the vicinity of the optimum, the optimal probability of failure or the optimal set of reliability elements is unaffected by the errors [33]. Under this assumption, the nominal probability of failure is utilised and different $P_{f,t}$ or different $\mathbf{r}$ values are compared and the most optimal selected.

However, errors can be made in the process of code making and code calibration, for example, in the application of the optimisation techniques, in modelling the random phenomena or variables probabilistically, in recognising the hazards, in applying and selecting the reliability methods and so forth. The consequences of these types of errors might be observed in the existing structures and provide input for an improvement of the calibration. Nevertheless, it has to be mentioned that it might be difficult to distinguish human errors, which should be prevented by quality control, from human errors involved in the calibration. In fact, events of structural damage or failure are often triggered by a combination of several factors and errors as well as the unfavourable realisations of the loads and the material properties.

In conclusion, it is important to highlight that the design codes are tools supporting decision making in structural engineering. Between the models implemented in the code and the real behaviour of structures (e.g., the failure rate, the costs of construction and so forth) there is a series of elements that are impossible to account for rigorously but that certainly affect the performance of the structure. These elements include, for example, the human errors not discovered during the quality control, the contribution of non-structural elements and the system effects. The code for structural design represents a set of principles and rules that support decisions independently of these aspects, but these aspects are implicitly accounted when evaluating the performance of a code by assessing the structures built following its implementation.

1.1.4.4 Methods

Code calibration strategies have been formally divided into three main methods [11, 12]. Usually, their combination is adopted.

- **Judgment** was the first method used when probability and structural reliability theories were not yet developed. It consists of modifying codes and/or changing reliability elements based on observations following a 'trial-and-error' strategy. The method cannot be used for writing codes covering new materials, technologies and types of structures due to the lack of related experience.
- **Fitting** consists in calibrating the new code in order to achieve the same reliability or same design as the old code. It is mostly used when rewriting a code considered "optimal" in a new format. An example regarding the British standards is reported in [34] and [35].
- **Optimisation** is the highest level and most modern approach consisting in defining risk-acceptance criteria and an optimal design concerning a certain utility function (e.g., expected benefits) and consequently calibrating the reliability elements. Application examples are reported in, e.g., [2, 7, 23, 35, 36, 37, 38, 39, 40, 41, 42, 43, 44].

Calibration of design codes is the exclusive competence of the so-called code committees appointed by national or international regulatory bodies and composed of established experts in the field. The reason for this is that most of the decisions involved in this complex problem can only be taken wholly or partly based on subjectivity, experience and engineering judgment. In fact, the existing rational and objective methods are not sufficient to represent the whole problem due to its complexity. Henderson and Blockley [34] proposed a logical model of the process of code calibration and showed, in an example application, that the statements and assumptions outside the detailed reliability-based calibration process were less dependable than those inside the calibration procedure (e.g., models, weights and penalty functions). The agreement among the code-committee members on the less dependable statements and assumptions is the best available method ensuring that best decisions are taken. Critical

decisions not fully supported by objective methods include: the simplification of the real problem to a simplified one to which rational methods can be applied, the selection of the representative structures, the formulation of the design requirements, the definition of the safety format and load combination rules, the writing of the requirements and principles, the selection of the level of detail and sophistication, etc. Thus, **the general aim of this work is to provide and extend methods and frameworks based on rational principles and, in particular, on normative decision theory for supporting code committees in their decision-making process.**

A (limited) part of the decisions involved in code calibration is based on objective calculations of which a theoretical background and principles have been established in the past decades. Practical calibration of codes can be performed in several consecutive steps, as proposed in [12, 45], and standardised in the International Standard ISO 2394:2015 [10], see Section 1.1.4.7. Other similar procedures are proposed in the literature [11]. Although code calibration concepts are well established, two main tasks still present difficulties: *i)* the selection of the target probability of failure or the corresponding target reliability and *ii*) the detailed calibration procedure with the individuation of simplified models reflecting the best practice.

1.1.4.5 Code optimisation as a decision problem

Calibration of design codes can essentially be seen as a decision problem under risk. In fact, the decision does not lead to a certain and unique outcome, but rather to several outcomes with known probabilities. The general decision to be taken is the selection of a code and, in detail, the specification of the code requirements, the safety format and the reliability elements. The decision maker is society since the objectives are set at the societal level. The aim of the decision is to provide codes that guide engineers to design safe, optimal and sustainable structures. The rigorous formulation of the entire decision problem is presented and applied to a relevant case study in [I]. The outcome of a decision in code making depends on variables describing the "state of the world" which are divided into two groups: i) variables that neither the code maker nor the designer knows with certainty (e.g., the exact material strength in a given structure) and ii) variables whose realisations are known with certainty by the designer but not known with certainty by the code maker (e.g., the number of elements in the structural systems). The consideration of the latter group introduced in [I] allows taking into account the difference among the structures covered by the same reliability elements. Differences in system layout, number of components, material and loads are specifically considered.

The normative decision theory for an individual under risk provides a rational support for taking the optimal decision [4] and, thus, for allocating societal resources in efficient risk-reducing measures. This decision strategy is also referred to as risk-based or risk-informed decision making. Its application to code making is named risk-based code calibration. The code maker aims at selecting the preferable code within the code space. The code is here intended generally, i.e., including the design principles and requirements, the format, the reliability elements and so forth. For a selected code, different consequences are possibly obtained depending on the state of a world that is not known with certainty. However, the probability distribution of the different states of the world – and hence of the various consequences – is considered known for any selected code. Thus, choosing a code corresponds to picking up a specific probability distribution over the possible consequences or, in formal words, to choose a lottery between the consequences. The comparison of the different selections can then be performed based on the utility function defined by the decision maker. Finally, the optimal

decision is the one that selects the lottery with the largest expected utility. This decision strategy is rational under the assumption that the decision maker agrees with the axioms stated by von Neumann and Morgenstern [46]. The strategy ensures that the mean utility approaches the expected utility (i.e. the maximum) with probability one when several independent decisions are made.

Various types of resources might enter the utility function including economic, natural, human, tangible and intangible resources. These resources need to be expressed in the same units in an optimisation problem. Often, the monetary value is utilised. Therefore, the term "resources", of all kinds, and "cost" are interchanged from now on. The conversion to monetary value is also performed when assessing the risk to life and the efficiency of risk-reducing measures. The use of monetary units (MU) in this context should not be misunderstood. Indicators such as the cost of a statistical life or the money society is willing to pay for saving one additional life ($SWTP$) is not to be considered the cost of a person's life. A person's life has no value. Nevertheless, these costs are necessary for comparing life-saving measures and, thus, allocating resources in the most efficient way for saving most lives within a given budget. The mentioned indicators are derived from small probabilities of missing life. As an example, consider a device that costs 100 MU and that reduces the chance of missing life by 10^{-5} for each person using it (e.g., a bike helmet). For this specific device, the cost of saving one statistical life is equal to $100/10^{-5} = 10^7$ MU since a reduction of one fatality is expected for each 10^7 MU spent. This indicator can be used for comparing life-saving measures. For example, the mentioned device should be preferred to other ones that cost more than 10^7 MU for statistical life. Further, if a society is willing to pay for this device, it can be said that the society is willing to (or, better, it can afford to) pay 10^7 MU for saving one statistical life. Consequently, all other life-saving measures that cost less than 10^7 MU per statistical life should be implemented for the society to be consistent.

1.1.4.6 Code optimisation

The concept of "optimal code" as that optimising the use of societal resources was developed in the early seventies [9, 47]. Semi-probabilistic codes and probability codes were seen as development steps toward the ideal code format [8]. The theoretical concepts proposed by Lind [9] regarding codes and their optimality are briefly summarised here (the notation is slightly modified). Essentially, structural design consists in mapping the space of all possible structural layouts $\{S\}$ in the space of all bearing structure proportions $\{P\}$. This correspondence is not uniquely defined by the norms since a given layout can be mapped to different structures. Nevertheless, a one-to-one correspondence might be established between $\{S\}$ and the space of optimal structures $\{P_{opt}\}$ under the assumption that only one of these structures is optimal. Therefore, P_{opt} can be written as a function of S and N, $P_{opt} = P_{opt}(S, N)$, where N is the norm used for the design that belongs to the space of all possible norms $\{N\}$. Each norm leads to different structural safety levels and has an associated level of risk $\mathfrak{R}(N) = \sum_i H_i \cdot P_{f,i}\left(P_{opt}(S_i, N)\right)$, where: H_i is the socio-economic expected loss related to failure of the structure i and $P_{f,i}$ is the related probability of failure. The sum is extended to all structures covered by the code. The optimal norm is defined as that minimising the total risk $\mathfrak{R}_{tot}(N) = \mathfrak{R}(N) + \sum_i C\left(P_{opt}(S_i, N)\right)$, where the second addend represents the total construction costs calculated as the sum of the costs over all structures [9].

Lind's general method for optimising codes is hardly applicable in practice. Therefore, the simplified methods listed below and illustrated in Figure 1.3 are often utilised in practical

calibration of codes. Both of these simplified methods are included in the generic calibration approach in [I].

- A **practical application of the decision-theoretic approach** that consists in pre-selecting a code N from $\{N\}$ and then calibrating the reliability elements in the code by maximising a utility function [32, 36]. The method applies to code Levels 1, 2 and 3; the principles of code optimisation were extended by Rackwitz [48] and are further developed in [I].
- **Simplified methods for calibration of Level 1 codes** that consist in pre-selecting a code N and then dividing the problem into two independent steps. First, the target reliability level is derived based on the decision-theoretic method described above or on the current practice, see [48]. The second step consists in calibrating the reliability elements ($\mathbf{r}$), and it can be performed with two methods [2]:
    - global optimisation methods (GOM); and
    - approximate methods (AM).

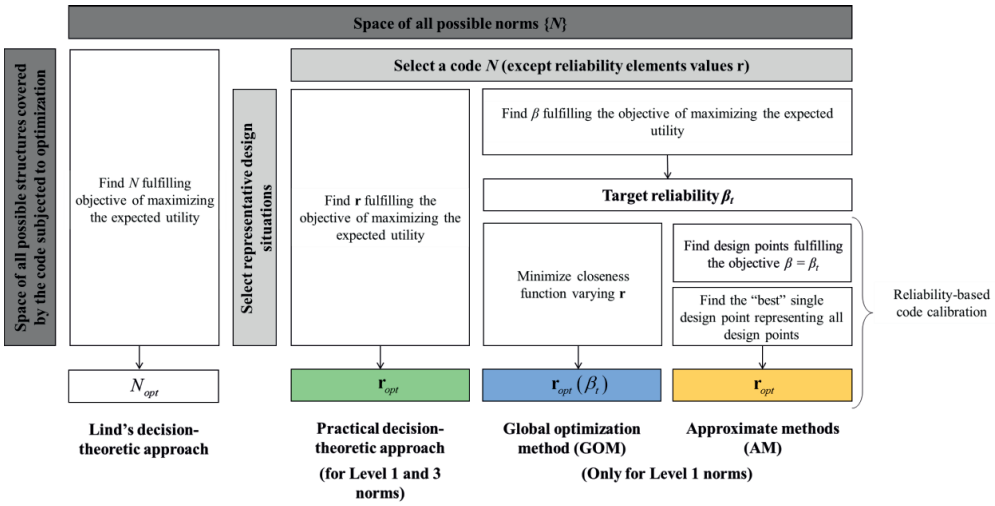

Figure 1.3. Summary of different optimisation methods for code levels 1, 2 and 3.

1.1.4.7 The seven-steps procedure for optimisation

A seven-steps procedure for code optimisation was proposed in [12, 45] and was standardised in the international standard ISO 2394:2015 [10]. Other similar procedures were proposed in the literature such as the five points procedure in [11]. The seven-step procedure is slightly generalised here in order to attempt to fit in it the different calibration approaches illustrated in Figure 1.3. A summary of the procedure is given in Table 1.1, detailed descriptions of the steps are given in the remaining part of this Section.

Table 1.1. Application of the seven-steps procedure to difference calibration problems.

Approach		***Practical decision-theoretic approach***			***Reliability-based calibration***	
Calibration problem		***Calibration of Level 3 (or 2) codes***	***Calibration of β_t for reliability-based calibration of Level 1 codes***	***Calibration of Level 1 codes***	***GOM for cal. of Level 1 codes***	***AM for cal. of Level 1 codes***
Reliability elements $\mathbf{r}$ to be calibrated		Target probabilities of failure ($P_{f,t}$) or target reliabilities (β_t)		PSFs, sensitivity factors, load reduction factors and modification factors		PSFs or sensitivity factors
Steps	1. Scope	Define the structures covered by the code				
	2. Objective	Minimise the use of societal resources			Target reliabilities β_t	
	3. Format	Define a set of rules Define groups of design situations covered by the same reliability elements		Define a set of rules, including which and how many reliability elements (PSFs, load comb. factors, mod. factors), how they are used in design equations and load combinations. Define groups of design situations covered by the same $\mathbf{r}$		
	4. Failure modes and models	System effects might be accounted in design	Single mode and element level only			
	5. Closeness	Expected utility or risk function like in Eq. (1.1)			Penalty functions in Appendix A	
	6. Optimum	Find $\mathbf{r}_{opt}$				Find $\hat{\boldsymbol{\alpha}}_{opt}$ or then $\mathbf{r}_{opt}$
	7. Verification	Evaluate solution of step 6 Decide values for $\mathbf{r}$ to include in the code				
	(8. Check)	Design some selected structures with the selected $\mathbf{r}$ and assess the design with higher methods				

Step 1 - Definition of the scope of the code

Level 1 and Level 3 codes consist of simplified design requirements that are developed for and limited to a specific class of structures (see Figure 1.1). The first step consists in defining this class. The types of structures, materials, failure modes, the geographical domain of validity, the types of loads and accidental scenarios are the principal elements to define. In general, a broader class of structures implies a larger average difference between each structure and the code objective. On the contrary, restricted classes allow a higher level of optimality, see [11] and [I].

Step 2 - Definition of the code objective

The code objective is defined at a higher level. For calibration of Level 3 codes or calibration of target reliabilities (β_t) for reliability-based calibration of Level 1 codes, the objective is set at Level 4 and consists in minimising the risk or, equivalently, minimising the expected use of resources over time. For reliability-based calibration of Level 1 codes, the code's objective is the target reliability that might be: i) derived minimising the risk (see [I]), ii) taken from standards such as [10, 13] or iii) adopted as equal to the safety level of an existing code covering similar structures and considered optimal (see [III]). Target values may not be

unique since different optimal reliabilities are associated with different failure modes (e.g., plastic and brittle failures), consequence classes and other aspects discussed later. Acceptability criteria must also be defined, the application of the marginal life saving principle is recommended in [10], and further details are given in Annex G of [10].

The target reliability levels were first implicitly defined as the intrinsic reliability level of the "best practice" corresponding to the design codes in use [9, 31]. These codes are the results of past developments and adjustments based on observations of real structures. The evaluation of the code implicit safety level is an underdetermined problem since the simplified code formats in use (e.g., load and resistance factor design format, LRFD) lead to variable reliability levels, as shown in, e.g., [23, 49]. Several calibration works reported in the literature use the mean reliability or other fractiles as targets. Alternatively, the problem is approached in [11, 31] with the decision-theoretical principles assuming a simplified calculation of the risk as a function of the reliability index of the corresponding probability of failure. The degree of freedom is fixed by postulating that the code in use provides optimal structures or, equivalently, minimal risk [31]. These methods lead to different results, particularly when the existing code leads to a large scatter in the reliability of the structures. A different approach was proposed in [III] where decision-theoretic methods were applied under the assumption that the code leads to optimal structures on average. As a result, the implicit safety level of the existing codes is lower than the mean reliability level of the structures designed with it. This is a consequence of the fact that i) the reliability variation caused by the simplified safety format needs to be accommodated and ii) the risk function is skewed. Plots for direct implementation of the method are provided in [III].

Target reliabilities were later derived from risk or monetary optimisation [47, 50, 51] interpreting design codes as tools for decision making that guarantee optimal use of societal resources. Rackwitz brought together these concepts and further developed them in a seminal article [48] where different objective functions are derived for various scenarios. The case of structures that are systematically reconstructed after failure, also referred to as the infinite renewal case, is the most relevant in code making. An example of the calculation of the optimal failure rate and its sensitivity to the probabilistic models and the safety and failure costs, is presented in [48].

A single value of target reliability does not satisfy the requirement of an economic optimum since different structures have in general different optimal reliabilities. It follows that a set of target reliability indices, or better a "target safety index function" is preferred to reflect the highest requirement of optimisation [25]. Target reliability indices provided by design codes are in general differentiated based on the consequences and the safety costs only. Tentative target reliabilities proposed by the Joint Committee on Structural Safety (JCSS) [13] are the result of this innovative approach. These values are based on Rackwitz's work [48], are widely accepted in the field of structural reliability and they have been included in the International Standard ISO 2394:2015 [10]. Nevertheless, detailed background calculations are missing, making these values less transparent and open to misinterpretation. In addition, the attempts to back calculate these values using Rackwitz's objective functions lead to several discussions since they require a significant number of subjective choices. The main discussed and misinterpreted points are:

- the part of the structure the targets refer to, i.e., the structural system as a whole, a part of it or a single structural component;

- the estimation of the failure costs and safety costs for individuating the consequence class and the cost-of-safety class;
- the selection of the appropriate reference period for the target reliability: 1-year and lifetime reference periods are discussed;
- the reliability differentiation based on aspects different than the consequences and safety costs, i.e., involved uncertainties, service life, limit state functions;
- the selection of a structure representing the whole structural class to be used in the optimisation.

These points were addressed in [I] were the code-optimisation principles were clarified, synthesized and extended to reduce the level of subjectivity involved, accounting for the differences among structures within the structural class and accounting for the system effects. The method proposed allows for the classification of structures in classes with more similar characteristics to increase the level of code optimality. For example, reliability differentiation between series and parallel systems was proposed and compared with a single reliability target covering all of them simultaneously.

The reliability is differentiated in current codes based solely on the consequences given failure (see, e.g., [18]) or based on the consequences and cost of safety (see, e.g., [10, 13]). The values are given in the form of tables for three consequence and safety cost classes. However, as discussed in [II], the optimal reliability depends on the four most important aspects:

- the ratio between total failure costs and marginal safety costs;
- the uncertainty involved in the problem;
- the obsolescence rate (i.e., the inverse of the expected design life); and
- the discounting rate.

The current tables for target reliabilities only provide differentiation based on the first aspect. The remaining aspects are accounted for approximately. For example, the target for a structure with a short design life is obtained from the tables considering the cost of safety to be larger than "normal". This reliability differentiation is quite approximate and sub-optimal. Therefore, simplified plots for communicating target reliabilities are proposed in [II]. The plots can account for all of the four aspects listed above.

Step 3 - Definition of the code format

The code format "*[...] is a formal system of variables together with a set of rules*" [11, p.315]. In practical calibration procedures, the set of rules is usually fixed first (when selecting N from $\{N\}$) and the definition of the code format is limited to the selection and definition of the reliability elements. Moreover, groups of structures or failure modes to be covered by the same set of reliability elements need to be defined balancing code simplicity and optimality. In fact, a larger number of reliability elements leads, in general, to more optimal structures but makes the code more sophisticated. The problem is illustrated in [11] for semi-probabilistic codes and more generically in [I].

Current design standards have reached a high level of sophistication, at the cost of increasing their complexity and probably the engineering costs. Several discussions on what constitutes an adequate level of code sophistication are ongoing [1, 52, 53, 54], and a major aim of the code revision works, among other objectives, is to improve the ease-of-use of codes [28]. Simplified safety formats may either be included in codes as alternatives to more detailed formats or be used in the early design stages for pre-design. Simplified safety formats might be

calibrated so to lead always to an equal or a larger design (i.e. equal or larger cross-sections) compared to the more sophisticated ones. This calibration might not be optimal since it leads to an excessive level of safety. At present, no rational methods have been proposed for supporting decisions on the simplification of design formats. An approach for this purpose was proposed in [IV] and applied for calibrating a simplified safety format for the design of common timber structures. The work aimed at calibrating these formats minimising the increase in expected costs compared to the detailed formats, without compromising the safety level. The simplified safety formats were calibrated for a specific sub-class of structures representing the most common timber structures. The reduction of the structural class allowed to obtain a relatively low scatter of reliability from the target even though the safety formats were greatly simplified. The calibrated simplified formats were then compared with the existing code to assess the differences in design, in the number of load combinations used and the reliability level. These three indicators can support code committees in assessing and comparing safety formats with different levels of detail.

Step 4 - Identification of typical failure modes and stochastic models

In practice, code calibration is a complex problem that requires a significant amount of simplification before the existing calibration methods can be applied. In fact, codes are complex tools applicable to a broad range of different failure modes, structural layouts, materials and material grades, analysis techniques, system configuration and relevant actions. The reduction of complexity from the code to the calibration exercise can be observed in several reports [23, 37, 49]. The reduction is based on numerous subjective assumptions, agreements among experts, simplified representations of phenomena and generalisations that are still a topic of research. Practical issues arise in conjunction with: selecting the representative structural elements to be used in the calibration, deciding between more detailed or more general limit state functions, estimating the uncertainties affecting the resistance and load models proposed in the code and individuating their hidden safety, simplifying the models representing the loads and their combination, selecting the reference time interval for reducing time-variant problems to time-invariant ones, proposing a safety format for more advanced analysis tools such as non-linear finite element software and several others.

The typical failure modes within the class of structures selected are identified, and the relative limit state equations are formulated. Two different approaches are found in the literature:

- the use of limit state functions representing some specific failure modes of selected elements (see, e.g., [23, 36, 37, 55]); and
- the use of generalised limit state functions (see, e.g., [7, 35]) where only the variables dominating the failure modes are represented.

While the former method is more detailed for each specific case considered, the latter allows the covering of approximatively all failure modes governed by the same set of random variables with a unique limit state function. Thus, it is more general.

Failure modes at element level are often considered. This might seem more appropriate for the calibration of Level 1 codes that set the design requirements at the component level. On the other hand, reliability analyses at Level 3 design permit consideration of system effects explicitly. Therefore, it might be more appropriate to evaluate the reliability at the system level in calibrating Level 3 codes. In fact, the consequences associated with the failure of a component and those associated with the failure of the system might be equal (for series

systems) or substantially different (for robust parallel systems). The inclusion of the system effects in code optimisation was proposed in [I] also for the calibration of component target reliabilities to include the system effects.

The representative design situations are individuated, and the associated frequencies of practical occurrence (named the *demand function* in [12]) are estimated. The limit state function g_j for the design situation j is a function of the design parameters $\mathbf{p}$ (e.g., structural dimensions and specifications) and some random variables $\mathbf{X}$. In addition, the design depends on the reliability elements $\mathbf{r}$, $g_j = g_j\left(\mathbf{p}(\mathbf{r}), \mathbf{X}\right)$. In general, $\mathbf{r}$ includes:

- the target reliability indices, the minimum acceptable reliability indices and the requirements on robustness when Level 3 codes are optimised; or
- the PSFs, the load reduction factors and the modification factors when Level 1 codes are optimised.

A crucial part of a calibration exercise is the selection of the probabilistic models representing the random variables included in the selected limit states. The stochastic models representing actions, material properties and degradation are selected based on: measurements, the literature [56, 57, 58] and probabilistic codes such as [13]. In Level 1 codes, these models are only used in the calibration, while in Level 3 codes they are also used in the reliability analysis performed during design. Simplified models need to be considered for simplifying the problem without compromising the calibration accuracy. Their selection is often a topic of discussion at code committees. These models should reflect the best practice and represent all sources of uncertainty that are associated with: the material properties, the geometry, the load effects, the deviation of the material strength in the structural elements from the tested specimens, the deviations of the resistance models from the resistance derived from tests and the deviations of the action models from the real actions. Models on the load side often depend on the geographical location and should consider the variations within the domain of applicability of the code (e.g., snow load models vary significantly with climate type, altitude, latitude, vicinity to the sea and so forth). The analyses and the proposal of stochastic models to represent the wind climate in Norway for the calibration of PSFs were presented in [V]. In [V], a method accounting for the variation over the territory covered by the same reliability elements was also proposed, and the uncertainties on the characteristic values provided by the wind maps in the standards were included in the calibration.

The stochastic models representing the material properties and geometrical imperfections might change among countries due to different habits, production methods and quality control routines. In addition, the model uncertainties express the deviation between the measurements and the values predicted by the models in the code at hand. Therefore, the model uncertainties are specific for each design code.

Step 5 - Definition of a "measure of closeness" to the optimum [7] or "degree of fit" or "penalty function" [11]

This step depends on the calibration method and strategy adopted.

Step 5 for calibration of Level 3 codes or target reliabilities for Level 1 codes by risk minimisation uses the risk or expected utility function as a measure of closeness. In fact, this function has a unique minimum corresponding to the optimal risk level. Different utility functions were derived in [36, 47, 48] and the detailed optimisation problem is extended and discussed in detail in [I]. In brief, when the benefits from the existence of a structure (given the structure performs as it should) are independent of the structural safety, the maximum expected

utility corresponds to the minimum expected costs. The total risk associated with a given code is approximated by the risk associated with some selected representative structures designed to just satisfy the code's requirements in Eq. (1.1), where: $\mathbf{r}$ is the vector of reliability elements, $C_{C,j}$ are the construction costs, $C_{R,j}$ are the reparation costs and $C_{f,j}$ are the failure costs associated with the j^{th} representative structure that occurs with relative frequency w_j. Other costs might be considered such as obsolescence, serviceability limit state violation and environmental costs.

$$\Re(\mathbf{r}) \cong \sum_{j=1}^{n} w_j \left[C_{C,j}(\mathbf{r}) + C_{R,j}(\mathbf{r}) + C_{f,j} P_{f,j}(\mathbf{r}) \right] \tag{1.1}$$

Step 5 for reliability-based calibration of Level 1 codes (i.e., the second part of the AM and GOM methods) requires a function to measure the closeness to the target reliability. Several penalty functions have been derived from different objectives. Their main distinguishing characteristic is the skewness, i.e., the degree of asymmetry around the target value. Highly skewed functions lead to almost no values below the target. The different penalty functions found in the literature are reported in Appendix A together with a comparative calibration example. In general, the final result of code optimisation is not very sensitive to the choice of penalty function [11]. Nevertheless, significant differences might be observed when the reliability index scatter among the selected structures is large, or when highly skewed functions are utilised. The penalty functions $M = M(\mathbf{r}, \beta_t)$ are functions of the target reliability β_t, the reliability elements $\mathbf{r}$ and eventually other parameters.

Step 6 - Determination of the optimal reliability elements $\mathbf{r}$ for the chosen code format

For calibration of Level 3 codes or target reliabilities for Level 1 codes, the optimal reliability elements are found solving an optimisation problem like the one in Eq. (1.2).

$$\mathbf{r}_{opt} = \arg\min_{\mathbf{r}} \left\{ \sum_{j=1}^{n} w_j \left[C_{C,j}(\mathbf{r}) + C_{R,j}(\mathbf{r}) + C_{f,j} P_{f,j}(\mathbf{r}) \right] \right\} \tag{1.2}$$

For reliability-based calibration of Level 1 codes, the GOM and the AM approach this step differently. The former provides more precise and optimal reliability elements, while the latter requires fewer evaluations of the reliability index and is preferred for cases with computationally expensive reliability analyses [2]. Further, the GOM allows for the calibration of the PSFs, load combination factors and modification factors, while the AM is limited to the PSFs only. This is seldom a relevant limitation since the load combination factors and the modification factors are calibrated with alternative techniques, see e.g., [58, 59, 60].

In the GOM, the representative structures are first designed as "just safe" for a given $\mathbf{r}$ i.e., just satisfying the design equations defined in Step 3. Then, the reliability of the designs is evaluated with structural reliability methods. The First Order Reliability Method (FORM) is often adopted for its low computational cost since a large number of evaluations are required in the calibration. Successively, the weighted sum of the selected penalty function M is evaluated to quantify the closeness to the code objective, see Eq. (1.3), where the weights w_j have been defined in Step 4 and the penalty function in Step 5. Finally, the optimal set of reliability elements $\mathbf{r}_{opt}$ is found, solving the minimisation problem. The number of times the reliability index is calculated is equal to n times the number of iterations necessary to solve the minimisation problem.

$$\mathbf{r}_{opt} = \arg\min_{\mathbf{r}} \left\{ \frac{1}{\sum_{j=1}^{n} w_j} \sum_{j=1}^{n} w_j M\left(\beta_j\left(\mathbf{r}\right), \beta_t\right) \right\} \tag{1.3}$$

The AM is divided into two parts. In the first part, the representative structures are designed fulfilling the code objective, i.e., giving $\beta = \beta_t$. The methods proposed in [2] might be used for this purpose. The selection of the method depends on the problem at hand and mainly on the computational cost of the reliability analyses. For each design situation considered, the set of reliability elements $\mathbf{r}_j$ fulfilling the code's objective is calculated knowing the design point $\mathbf{x}_{d,j}$. In detail, the i^{th} partial safety factor in $\mathbf{r}_j$, $r_{i,j}$, is calculated as $x_{d,i,j}/x_{k,i,j}$ (for load variables) or $x_{k,i,j}/x_{d,i,j}$ (for resistance variables), where $x_{k,i,j}$ and $x_{d,i,j} = F_{X_i}^{-1}\left(\Phi\left(\alpha_{i,j}\beta_t\right)\right)$ are the characteristic and the design values of the random variable i in the design situation j, respectively, and $\boldsymbol{\alpha}_j$ is the vector of FORM sensitivity factors. In the second part of the AM, a unique set of reliability elements $\mathbf{r}_{opt}$ is sought with different methods. Gayton, Mohamed [2] propose choosing the most conservative reliability elements (i.e., $r_{opt,i} = \max_j\left\{r_{i,j}\right\}$) or choosing the weighted mean (i.e., $r_{opt,i} = \sum_{j=1}^{n} w_j r_{i,j} \Big/ \sum_{j=1}^{n} w_j$). Alternatively, a unique and optimal vector of sensitivity factors $\hat{\boldsymbol{\alpha}}_{opt}$ is sought to represent all sensitivity factors $\boldsymbol{\alpha}_j$ corresponding to the design just satisfying the code objective. Ditlevsen and Madsen [11] proposed an improved approximate optimisation method for finding the vector $\hat{\boldsymbol{\alpha}}_{opt}$ solving the linear problem in Eq. (1.4). The linearity significantly reduces the computational cost. However, the problem should be constrained to avoid $\hat{\boldsymbol{\alpha}}_{opt}$ vectors outside the cluster of the $\boldsymbol{\alpha}_j$ vectors [61] since the error introduced by the approximation leads, in some cases, to erroneous optima. The partial safety factors are calculated once the $\hat{\boldsymbol{\alpha}}_{opt}$ vector and the target reliability are defined following the first-order reliability theory, see [12].

$$\hat{\boldsymbol{\alpha}}_{opt} = \arg\min_{\hat{\boldsymbol{\alpha}}} \left\{ \frac{1}{\sum_{j=1}^{n} w_j} \sum_{j=1}^{n} w_j M\left(\hat{\boldsymbol{\alpha}}, \boldsymbol{\alpha}_j, \beta_t\right) \right\} \tag{1.4}$$

The $\hat{\boldsymbol{\alpha}}_{opt}$ vector is almost independent of β_t in most practical cases. This property allows for linearisation of the problem and, more importantly, it allows the use of the same vector $\hat{\boldsymbol{\alpha}}_{opt}$ for the calibration of safety factors with different target reliabilities. This is expedient when PSFs are to be calibrated, for example, for various consequence classes and hence different target reliabilities. An application of the method is included in Annex C of EN 1990:2002 [18].

Vrouwenvelder and Siemes [23] proposed an approximate method for calibrating the partial safety factors by solving the linear problem $\mathbf{A} \cdot \mathbf{r} = \mathbf{b}$. The $m \times m$ matrix $\mathbf{A}$ and the $m \times 1$ vector $\mathbf{b}$ are given in Eq. (1.5) and (1.6), where: $i = 1,...,m$, $l = 1,...m$ and $\mathbf{r} = \left[r_1, r_2, ..., r_m, r_{m+1}, ..., r_{m+t}\right]$ has m free PSFs to be calibrated for t fixed. In these equations, the α factors for resistance variables are positive, and they are evaluated from the design corresponding to the reliability elements in the existing code, from a design fulfilling the code's objective or being close to doing so. The $\boldsymbol{\alpha}$ vectors are assumed constant, i.e., independent of the reliability level. In addition, the PSFs are defined as $r_i = x_{d,i}/x_{k,i}$ both for resistance and load variables.

$$A_{il} = \sum_{j=1}^{n} \frac{\alpha_{ji} x_{k,i}}{\sigma_{X_i}} \frac{\alpha_{jl} x_{k,l}}{\sigma_{X_l}} \tag{1.5}$$

$$b_l = \sum_{j=1}^{n} \left\{ \sum_{i=1}^{m+t} \frac{\left[\mu_{X_i} - \alpha_{li} \beta_t \sigma_{X_i} \right]}{x_{k,i}} \frac{\alpha_{ji} x_{k,i}}{\sigma_{X_i}} \frac{\alpha_{jl} x_{k,l}}{\sigma_{X_l}} - \sum_{i=m+t}^{m+t} \frac{\alpha_{ji} x_{k,i}}{\sigma_{X_i}} \frac{\alpha_{jl} x_{k,l}}{\sigma_{X_l}} r_i \right\} \tag{1.6}$$

Independently of the method selected, the optimisation problem might be subject to constraints including:

- Lower bounds on the reliability level β_{acc} derived, for example, from applications of acceptance criteria such as the marginal life saving costs principle when the risk to life is an issue.
- Constraints on the reliability elements: $\mathbf{r}^l \le \mathbf{r} \le \mathbf{r}^u$ where $\mathbf{r}^l, \mathbf{r}^u$ are the lower and upper bounds for $\mathbf{r}$. This constraint may be included to limit changes in the PSFs and to maintain historical habits (e.g., use of material PSFs larger than unity in Europe).
- Upper bounds for $\sum_j w_j M\left(\beta_j(\mathbf{r}), \beta_t\right)$ which suggest, when exceeded, a change of safety format [25]. The author has not found in any practical calibration reported in the literature using the application of these constraints. This may be due to the difficulty in the selection of the bound.
- Limit to the probability of having a reliability index below the target [2] by imposing: $\beta_t \equiv \mu_{\mathrm{B}}(\mathbf{r}) - \eta \sigma_{\mathrm{B}}(\mathbf{r})$, where $\mu_{\mathrm{B}}(\mathbf{r})$ and $\sigma_{\mathrm{B}}(\mathbf{r})$ are the mean and standard deviation of the reliability indices for the different design situations considered, and η is a parameter. For a reliability index represented by a normal distribution ($\mathrm{B} \sim N(\mu_{\mathrm{B}}, \sigma_{\mathrm{B}})$), for example, a 5 % probability of having $\mathrm{B} < \beta_t$ is obtained with $\eta = 1.64$.
- Other constraints on, for example, the costs, the weight of the structure and the greenhouse gas emissions.

Step 7 - Verification.

The results from the previous step are assessed by the code committee, and the final reliability elements are decided with engineering judgment considering traditions and other relevant considerations. This may lead to adopting reliability elements quite different from the optimal ones due to different reasons, including the necessity of changing the codes gradually to avoiding mistrust among the users. An example is reported in [23] where the reliability elements minimising changes from previous codes were preferred to the ones providing maximum reliability homogeneity among all considered structures.

Step 8 - Checking of results.

This final step consists essentially in checking some randomly selected structures designed with the calibrated reliability elements with higher level methods. This step is not included in the standardised procedure in ISO 2394:2015, and was proposed by Gayton et al. [2] for the specific case of PSFs calibration. This point may be important when calibration is performed using generalised limit state functions (e.g., [7]), simple representative structural elements (e.g., [37]) or any other types of simplifications, approximations and generalisations.

1.1.5 Current code-related activities

1.1.5.1 Calibration of Eurocodes and background documentation

Calibration of codes plays a key role in the ongoing major revision of the European standards for structural design [28]. The second generation of Eurocodes is expected to be published in the early 2020s and will extend the scope of the existing ones. The revision includes tasks of code calibration such as the differentiation of the partial safety factors for the

environmental actions, the revision of the load combination rules, the revision and extension of Annex C and the documentation of background calculations. It is an objective of the present work to **contribute to the ongoing discussions, code revision and calibration. The calibration tasks specifically addressed in this work are described in the following paragraphs.**

The current revision of the Eurocode 0 (EN 1990:2002) includes tasks such as the assessment of the current partial safety factors, the differentiation of the partial safety factors for the different actions such as snow, wind, self-weight and permanent loads and the documentation of the background calculations. In the current version of the Eurocodes, the same partial coefficient is used for imposed, wind and snow loads that are characterised by different uncertainties and represented by different models. In addition, there is a necessity to assess and eventually recalibrate the sensitivity factors for the so-called design value method to calculate the design values proposed in Annex C to Eurocode 0 [18]. The method makes use of the standardised sensitivity, or influence factors, α. The α-factors given in [18] are $\alpha_R = -0.8$ and $\alpha_E = 0.7$ for random variables dominating the resistance and the load, respectively. Non-dominating variables have lower sensitivity factors, more details are given in Annex C to [18]. The current factors were calibrated considering lifetime reliability in [62], i.e., 50-year target reliability. The absolute value of the α-factors is proportional to the contribution of the corresponding variable to the total uncertainty in the problem. Yearly maxima have larger coefficients of variation than lifetime maxima. Consequently, $|\alpha_E|$ corresponding to yearly maxima are greater and, as the sum of the squared α factors is close to 1, the $|\alpha_R|$ are smaller. Thus, the sensitivity factors need to be assessed and eventually re-calibrated in case the design value method is to be used with yearly target reliabilities as proposed for the new version of the Eurocode 0. The reliability based calibration of the partial safety factors and the sensitivity factors is reported in Appendix B. Although the work is still in an early stage, the methodology and some main results are presented and discussed.

The partial safety factor recommended in [18] for the wind load is $\gamma_Q = 1.50$. It has been shown in [63] that a wind load dominated structure designed with $\gamma_Q = 1.50$ has a reliability lower than the Eurocode target, which requires a yearly target reliability index β_t equal to 4.70. The calibration of the partial safety factor for wind action requires detailed probabilistic models representing the different aspects of the wind action on the structure. One of these aspects is the wind climate, which represents the free-field wind speed. The probabilistic modelling of the wind speed extremes presents several challenges including i) the extrapolation to high fractiles where no observations are available, ii) the inclusion of the variability over the territory covered by the same partial safety factor and iii) the estimation of the systematic error affecting the georeferenced characteristic wind speeds given in the national Annexes to the Eurocodes. Consequently, there is a need to represent the wind climate variability in time and space, and to calibrate the partial safety factor for wind action on structures.

1.1.5.2 E39 Ferry free project in Norway

The *Coastal Highway Route E39* project includes several crossings of major fjords in Norway [64]. The characteristic of these fjords requires bridges much longer than the existing ones or new types of crossings such as floating bridges and submerged floating bridges (Archimedes' bridge). The design of these bridges presents several challenges not only to the prediction of their mechanical behaviour but also to the identification of their optimal level of

safety. These structures differ from common structures on many aspects that affect the optimal reliability level; in general, compared to common structures, these structures have:

- different relevant limit states;
- different magnitudes of the consequences associated with failure and different marginal safety costs;
- different accuracy of the models predicting the structural response. The models are thus characterised by large epistemic uncertainty as a consequence of the lack of experience since only one pedestrian Submerged Floating Tunnel (SFT) has been built so far;
- different load scenarios such as the simultaneous action of traffic, currents, tide etc. leading to load combinations which rarely occur in other structures.

Therefore, the applicability and optimality of the existing codes should be assessed. Eventually, the design requirements can be specifically calibrated for these structures in case the existing codes are found not to be optimal.

1.2 Limitations

This thesis focuses on the risk-based calibration of design codes to optimise the use of societal resources in structures. Financially optimal solutions do not necessarily guarantee that the associate level of risk to life and limb is acceptable from the societal point of view. Risk acceptance criteria should, therefore, be applied and represent a constraint to resource optimisation. A common representation of the risk to life associated with a given activity makes use of the so-called Farmer diagrams. These diagrams divide the risk domain into three regions: i) the non-acceptable region characterised by combinations of consequences and probabilities that are never acceptable; ii) the acceptable region and iii) the region in between where the risk should be As Low As Reasonably Possible (ALARP). The marginal life saving cost principle can be applied to assess whether a risk-reducing measure is "reasonably possible" or not, and thus deriving the risk acceptance limits [10]. The principle ensures that societal resources are allocated to efficient risk-reducing measures, i.e., to measures providing a gain larger than the costs. The principle have been implemented in this work by means of the Life Quality Index (LQI) [65]. Codes are optimised from the societal perspective and, therefore, harm to people and environment are directly accounted for in the risk optimisation. Consequently, the optimum, in most cases, also satisfies the risk-acceptance criteria [66]. However, as discussed in [I], the application of the risk acceptance criteria to code-calibration require some further research and investigation that was not part of this work.

This research work focused on the Ultimate Limit States (ULS) and the associated target reliability levels, while serviceability limit states (SLS) and accidental limit states (ALS) have been disregarded. As known, serviceability requirements are in some cases more demanding than ultimate limit states. Therefore, a complete optimisation of design norms should consider SLS and ALS requirements, as well as all other code requirements regarding, for example, quality control and structural analysis methods. Such a comprehensive calibration would also balance the different risk components associated with different hazards such as overload, fire and explosions. Nevertheless, the optimisation of all these aspects simultaneously is a complex task. Therefore, for simplification purposes, these aspects are usually optimised individually. However, the calibration methods proposed in this work might be applied to the calibration of all code requirements. In fact, SLS and ALS differ from ULS mainly in the types of limit states and the consequences associated with their violation.

The results of the examples/study cases presented in this work are conditional on the stochastic models and the assumptions adopted. Therefore, their validity is restricted to cases where the selected models are representative. The case studies should be seen primarily as illustrations of the proposed methods rather than attempts to provide final values for target reliabilities or partial safety factors. Final values can only be decided by code committees based on the results of agreed analyses and inputs. For this reason, all Matlab scripts utilised in this work are published online with the intent of providing tools for supporting the decision-making process within the code committees. The Matlab® scripts are freely downloadable at [67] under the GNU General Public License Version 3.

This work often refers to the European Standards (the Eurocodes) [18]. This is because of geographical location and the ongoing revision of these standards [28] that has opened the possibility of re-discussing several principles and concepts that were not optimal in the existing version or that needed to be changed. However, the main research findings are of general validity and therefore applicable to any standard for structural design.

1.3 Highlights and main findings

In the following, the highlights and the main findings for each Chapter are summarised.

1.3.1 Chapter 2. Paper I: A Risk-Based Approach for Calibration of Design Codes

- A conceptual and generic formulation of the code calibration based on decision theoretical principles is presented with the use of decision trees.
- The method avoids the subjective selection of one structure to represent the whole class of structures for which the optimal reliability target or reliability elements are sought.
- The method accounts for the system effects; consequently, it is able to calibrate target reliabilities at the component and system level.
- The method accounts for the code's safety format and, given the format (e.g., the reference time for target reliabilities), it allows calibration of the most optimal reliability elements.
- The method applies to different calibration tasks (optimisation of system and component reliability, calibration of rel. elements) allowing to perform them consistently.
- The method is applied to a case study where a class of structures with different characteristics are considered; the component and system reliabilities are optimised.
- The results show that an equal target reliability might be optimal for system and component level; this result is reasonable under specific circumstances but needs careful interpretation.
- The method allows quantification of the loss/gain in optimality when structural classes are enlarged/reduced and, therefore, it can support the definition of the structural classes.
- Target values obtained in a case study are relatively close to the values proposed by the JCSS. Thus the method might serve as a transparent and solid background to these values.
- Designs with target reliabilities at the system and the component level might be equivalent regarding expected costs and robustness.
- Neglecting system effects gives larger optimal component reliabilities; nevertheless, when a more accurate method exists, conservativeness in optimisation is a contradiction.
- Yearly and lifetime target reliabilities optimised with the proposed method are financially equivalent, i.e. they lead to different design but same total expected costs over the class.
- The differentiation of the target reliability at the system level for classes of series and parallel systems is proposed, and tentative target values are optimised.

1.3.2 Chapter 3. Paper II: Generic Representation of Target Values for Structural Reliability

- The principles of structural reliability optimisation are discussed from a practical perspective with the aim of supporting practitioners.
- Target reliabilities depend on: the failure cost to marginal safety cost ratio, the amount of uncertainty, the obsolescence and the discounting rates.
- Current target reliability tables allow accounting only for the first two aspects, while the others are accounted for in an approximate way "adjusting" the safety and failure costs.
- A simple plot for communicating target reliabilities that allows accounting for all of the four aspects mentioned above is proposed.
- The financially optimal design does not necessarily guarantee an acceptable risk to life; the risk acceptance criterion based on the marginal life saving cost principle is described.
- The risk acceptance thresholds depend on societal wealth, the marginal safety costs, the expected number of fatalities and the interest and obsolescence rates.
- The plots proposed also allow for evaluation of the acceptable reliability levels accounting for all of the aspects listed above.
- The proposed plots might complement the target reliability tables in the current standards and result in a higher reliability differentiation among structures, i.e., higher optimality.
- Guidance for estimating the parameters affecting the optimal reliability target are discussed with the aim of helping their estimation in practical design works.
- The optimal target and acceptable reliabilities are calculated in two illustrative examples concerning real structures.

1.3.3 Chapter 4. Paper III: A Framework for Estimating the Implicit Safety Level of Existing Design Codes

- Target safety levels for the calibration of design codes or reliability-based design are derived from monetary optimisation or the best practice (the existing codes).
- A method for deriving the implicit safety level of existing codes is proposed, and is based on the assumption that the existing code is, on average, providing optimal structures.
- The code mean reliability is larger than the implicit reliability because the reliability variation resulting from the code simplified safety format needs to be accommodated.
- Thus, the reliability-based design of structures similar to the ones covered by the code at hand should be performed with a target reliability lower than the code mean reliability.
- Ready-to-use plots are provided for calculating the implicit reliability level for different sets of parameters.
- The proposed and existing methods are compared: significant differences are obtained for large coefficients of variation of the rel. index over the design cases covered by the code.

1.3.4 Chapter 5. Paper IV: Calibration of Simplified Safety Formats for Structural Timber Design

- A framework for calibrating the reliability elements in simplified semi-probabilistic design safety formats is presented.
- The objective of the calibration is to minimise the increase in construction costs compared to the non-simplified safety format, without reducing the level of structural safety.
- Simplified safety formats present large reliability variations. Thus, the penalty function should be selected carefully since it affects the calibration results significantly.

- The framework is applied to the calibration of two simplified safety formats for the design of common timber structures.
- The simplified plots are calibrated for a restricted class of structures (most common structures) for reducing the scatter of reliability w.r.t. the target reliability.
- The detailed and the simplified safety formats are compared in terms of reliability, simplicity and dimensions of structural elements.

1.3.5 Chapter 6. Paper V: On the Probabilistic Representation of Wind Climate for Calibration of Structural Design Standards

- The requirements for the stochastic models representing the wind climate for code calibration are discussed.
- Real data are analysed with different techniques to find the probabilistic model representing the wind climate in Norway with the specified characteristics.
- Analyses of data from the Norwegian territory with different techniques support the use of the Gumbel distribution to represent the yearly wind speed squared maxima.
- The uncertainty related to the poor rounding affecting the recorded wind speeds was taken into account in the estimation of the distribution parameters.
- The wind climate coefficient of variation is seen to vary over the territory covered by the same design code and is, thus, covered by the same safety factor.
- A method is suggested to account for the spatial variability of the wind climate considering the coefficient of variation as a random variable.
- The results show that the calibrated partial safety factor corresponds approximately to the one obtained considering the coefficient of variation known and equal to its mean value.
- In addition, the uncertainty on the wind load maps given in the standard is modelled probabilistically and included in the calibration of the safety factor.

1.3.6 Chapter 7. Paper VI: Risk and Reliability-Based Calibration of Design Codes for Submerged Floating Tunnels

- The article discusses whether the use of design standards that were developed for common structures for the design of submerged floating tunnels (SFT) is optimal or not.
- SFTs are characterised by failure modes, consequences of failure, accuracies of the mechanical models' and loads scenarios different than common structures.
- Optimal target reliabilities depend on all these aspects; thus, the reliability levels of common design standards might not be optimal for SFTs.
- A case study considering the reversible water tightness limit state is presented and the need for further detailed assessments and calibrations is highlighted.

1.4 Conclusions and discussion

1.4.1 Conclusions

The fundamental aim of the design codes is to simultaneously support and simplify the decision making in structural design and to regulate design in order to obtain safe and optimal structures. The most comprehensive and generic design method that guarantees safe and optimal structures is the risk-based approach. Its application requires knowledge and information which are scarcely available.

Simplified design approaches have proven to perform satisfactorily for common classes of design problems. The simplified approaches are derived from the risk-based approach and are achieved by:

1) **Simplifying the design and assessment methods** by avoiding estimation of the consequences given structural failure and the probability of structural failure explicitly.
   On one hand, reliability-based design (Levels 2 and 3) avoids the direct consideration of the consequences given failure. The consequences are indirectly accounted for by selecting the appropriate reliability target. To date, a large number of methods and computer programs is available for solving most reliability analyses. The reliability-based design is regulated in standards such as the ISO 2394:2015.
   On the other hand, the semi-probabilistic approach (Level 1) avoids both the direct estimation of the consequences given failure and the reliability analyses since the target probability of failure is achieved by using the calibrated safety factors. This format is implemented in several modern design codes.
   These simplified assessment methods ease the calculations that engineers need to perform during the design.
2) **Providing the same design requirements for classes of similar, but not identical, structures** (e.g., same reliability elements or reliability targets).
   Uniform design requirements over classes of structures simplify first and foremost the design standards, and second the practical design. The differences among the structures in the regulated class have frequently been considered in the reliability-based calibration of the semi-probabilistic design formats. However, its consideration in the calibration of the target reliabilities was firstly proposed in Chapter 2 [I].

The measures for simplifying the design mentioned above are implemented in modern design standards and have been addressed in this work. The main conclusions are summarized below.

- The codes regulating the different design and assessment levels should be calibrated consistently from higher levels to lower levels as illustrated in [I]. The Level 1, 2, 3 and 4 approaches are consistent only if calibrated in this manner. Under these conditions, the use of the semi-probabilistic method implies the acceptance of the higher methods.
- The reliability elements should be optimised for structural classes and should account for the safety format and the design approach. This optimisation can be performed by monetary optimisation [I] or based on the existing best practice [III]. The first method does not rely on the accumulated experience and is based on sound principles of decision and probability theories. The second approach relies on experience in using an existing standard. The "performance" of the standard is assessed observing the structures that comply with it.
- Design codes tend to be more sophisticated to cover more design cases, types of materials and technologies. Code sophistication might not be necessary for the most common and frequent design problems. Since code simplicity is one of the two elements for simplifying design, there might be a need to assess whether a simplification is necessary, quantify the loss of optimality that a code simplification implies and eventually calibrate the simplified formats as illustrated in [IV]. Further, the risk-based code-calibration approach proposed in [I] allows to optimize the level of code sophistication, including the classification of structures under the same design requirements.

- The probabilistic models should include the variation over the class of structures regulated by the same code. The example of the space variation of the wind characteristics over the territory covered by the same reliability elements was presented in [V].
- A careful assessment and eventually a re-calibration of the design codes should be performed when they are used to design structures outside of the class they have been developed and calibrated for [VI]. In short, structures that differ in those characteristics affecting the optimal and acceptable reliability levels should not be treated by the same reliability requirements or reliability elements.

1.4.2 Discussion

Design codes regulate design approaches by providing sets of rules and requirements that have been agreed by society. It is noteworthy to make clear that design codes are not a series of mathematically derived design requirements that show the absolute "right" design or the absolute "right" safety level. A significant part of the codes is based on statements, hypotheses or decisions that are not falsifiable. Thus, important parts of the codes do not have a scientific basis. This statement should not be misunderstood: scientific (falsifiable) methods and theories are used in code making but not exclusively.

Concepts such as the higher requirement of minimising the use of societal resources are certainly rational but not falsifiable. Thus, they do not have scientific validity. However, they are the "rules of the game" agreed within the society and thus preferred to any other rules. Consequently, design codes should be interpreted as such and they should be modified from this perspective. This core characteristic of the design codes should be transparently communicated by, for example, making all of the background documentation and calculations available to anyone in order to avoid misinterpretation of the code users and, sometimes, of the code makers. These misinterpretations are discussed in the following.

Although some design requirements (particularly in the semi-probabilistic codes) are written in a mathematical language, they should not be confused with scientific (falsifiable) statements. They are only the rules of the game written in a mathematical language. Consequently, design codes can and should be continuously updated, refined and improved based upon the gained experience and technological and scientific advancements. These characteristics should be clearly communicated. To quote a pioneer in the field of structural reliability, "[…] *progress is no more than a continuous refinement of operational procedures ("rules for a game") that capture just enough reality to protect the public and profession from low quality practice, on one hand, and, on the other, to be supportive of the competent engineering designer who wants to check himself or to roughly calibrate his new design relative to others where we have experience*" Cornell [68].

The understanding of the above concepts will help to trust and to increase the use of higher level design methods which are consistent with the widely accepted semi-probabilistic method. Nevertheless, when the background to the design codes and their philosophy are not understood, the interpretation is radically different: semi-probabilistic design codes are seen as a collection of scientific, exact, reproducible and falsifiable principles while higher design approaches are not, since "you can get any result you want out of them". Practically, the differences between the approaches are that:

1) The outcome of a semi-probabilistic design is (or, better, it seems) more reproducible since a significant number of decisions are taken once and for all by the code committees. On the other hand, higher level approaches leave a larger number of decisions to the

engineering designers who possess different information and thus make different decisions. However, it must be remarked that the same decisions must be made in the three approaches. The only difference is who is taking them. This problem can be overcome by standardising reliability-based design by providing the probabilistic models and methodologies [17] and by making the decisions made during code calibration publicly available and transparent.

2) The deterministic models can be put to the test of falsification, while the falsification of the probabilistic models is slightly more complex. Nevertheless, a "pragmatic falsification" can be utilised to assess the objectivity of a probabilistic model [69].

If the higher requirement is to design financially optimal structures with acceptable levels of risk of loss of life and limb, the alternatives discussed in code making should be ranked with respect to their optimality and acceptability. Thus, within reasonable limits, there are no "right" and "wrong" design requirements, but there are more or less optimal design requirements, broader or smaller domains where the design requirements can be efficiently applied. Decisions of the code committee should be based on these aspects.

Apparently, the risk-based design approach was developed historically after the deterministic codes and semi-probabilistic codes. Practically, a risk-based approach was implicitly used in the past for tuning the design codes and this resulted in the current design codes. When calibration was performed by trial and error, in fact, the code safety level was increased any time the failure events were observed too frequently, and it was lowered any time the construction costs (i.e., safety costs) were considered too high to satisfy societal needs. We can say, at least for some cases, that this process resulted in codes that were risk optimal or close to it. Modern techniques provide theories and more rigorous methods for undertaking the same risk optimisation. The trial and error strategy that correspondeds to build and assess the consequences over time is now replaced by risk analyses based on decision and probability theories that partly avoid the trials and, more importantly, the errors. These modern techniques are necessary to address new problems that are not covered by current standards. These problems include: design against terror attacks, the calibration of design rules for new materials (e.g., structural glass and cross-laminated timber), the design of new types of structures (such as suspension bridges with floating towers and Archimedes' bridges), the assessment of existing structures and so on. Existing structures represent a tremendous challenge that our society must face since they are continuously increasing in number and age, and because they often do not satisfy the current design requirements. Risk-based assessments could be utilised, for example, at societal level to make decisions on whether to retrofit the existing structures with new technologies to make them earthquake resistant or not. It could be further evaluated whether it is acceptable not to retrofit the structures with respect to the established risk acceptance criteria and whether it is financially beneficial for society to invest in the retrofitting. In the case that the retrofit must be performed, the level of intervention should be calibrated. Without higher level approaches these societal challenges are difficult to address.

1.5 Future research

1.5.1 The inclusion of risk-acceptance criteria in the proposed risk-based approach for calibration of design standards

The most interesting continuation of the work presented in this thesis would be the inclusion of the risk acceptance criteria in the framework for risk-based calibration of codes presented in [I]. In detail, it should be investigated if it is the acceptability of the decision rule itself that should be assessed or the acceptability of each single structure designed with it that should be considered.

In the first case, the decision rule is the decision variable, and the acceptability of the decision is evaluated with the marginal life saving cost principle over the entire class of structures. In this case, a simple risk acceptance analysis could be requested for subclasses of design problems that could result in a non-acceptable level of safety. The categories of design problems for which a risk acceptance assessment is necessary should be individuated (e.g., temporary tribunes) and the method presented in [II] could be applied for estimating the minimum acceptable reliability.

In the second case, it should be checked that all possible structures designed with the calibrated design rule have an acceptable level of safety. Besides the obvious difficulty in assessing all the possible cases covered by the design rule (including the extreme cases), the design rule could result in significantly over-designed structures just to accommodate some critical cases.

1.5.2 Optimal level of code detail

An interesting additional continuation of this work is the investigation of the code optimal level of detail including the subdivision of structures into classes with uniform design requirements. The principles exposed in [I] could be applied for this purpose. The result could be a further differentiation of the design requirements in comparison to the current standards. For example, as shown in [I], target reliability levels for parallel and series system could be differentiated.

1.5.3 Identification of the hidden safety

Regarding the practical code calibration, a key research objective would be the identification of the hidden safety, i.e. the bias of the models for calculating the load effects and the load-bearing capacities. The bias is significantly affecting the output of the calibration. The absolute bias should be estimated when the calibration is performed with the objective of reaching an absolute level of safety. On the contrary, the bias relative to all the other resistance models or load models simultaneously accounted in the calibration is of importance when the calibration aims at making the reliability more uniform over structures built with different materials or dominated by different actions. For example, in the calibration of the load factors in Appendix B, the “redistribution of safety” from one load to another for reaching a more homogeneous reliability is significantly affected by the safety hidden in the models for representing the effects of actions. However, there is scarce information about the safety hidden in the models included in the Eurocodes.

1.5.4 The modernisation of design codes

Besides the work presented in this thesis, there are, in the author's view, several interesting research areas related to code making and to the design approaches that are worthy of further investigation and modernisation. Their common denominator is the need to adapt current codes to the technological and scientific advancements of the last decades. To date, these advancements are not been reflected in the structural design codes. The civil engineering branch and, in particular, the structural engineering branch are too static and conservative in the author's opinion. The available technology could be applied to change the form of the codes and their content, as well as to simplify the calculations performed by the engineers. Two proposals are discussed in the following.

1.5.4.1 ***Dynamic* design codes**

A first interesting area worth exploring is how the current technology could be used to radically modernise the design codes. Except for the content and the safety formats that have changed considerably, the codes in use are documents with static text similar to the first building regulations that appeared some centuries ago. Since then, several technological revolutions have taken place. Codes might be made more dynamic utilising the available technology.

The use of technologies such as hypertext and online resources might change the codes and their use substantially. For example, online calculations might provide the design wind speed for a specific site and continuously update it based on field measurements at the specific site. Similar modifications of the design codes could allow for a higher level of detail, continuous updating, a lower likelihood of human errors and possibly also catch some of the trends of climate change.

Dynamic codes might also simplify design and minimize the disadvantages associated with the use of simplified design approaches. Consider, for example, a *dynamic* design standard that provides partial safety factors optimised online and in real time for each specific case at hand. The code would automatically update the partial safety factor values, the characteristic loads and the requirements on robustness based on the information provided by the designer including the type of structure, the material utilized, the geographical location, its intended use, the design service life and so forth. This could essentially eliminate the main drawback of the simplified design methods by providing optimised reliability elements for each design case. The benefits that technology could bring to the design codes seem worth a more detailed investigation.

1.5.4.2 **The use of the information technology to simplify the higher design approaches**

My second research interest consists in developing the technologies for supporting and increasing the use of higher design approaches. The use of reliability-based design could be increased by:

- Making a standard regulating this approach, as suggested in [17]. The JCSS Probabilistic Model Code [13] could be converted into a standard. An extensive application of the reliability-based design method might require differentiating the reliability target even more compared with the existing model code where only nine structural classes are included. For this purpose, the plots in [II] might be of use, and the work in [I] might serve as a basis for treating system effects and grouping structures in classes in an optimal way.
- Developing simplified and user-friendly software for reliability-based design. The existing computer programs for reliability analyses are quite advanced and made for users that are

expert in reliability methods. Easy-to-use programs for reliability-based design should simplify reliability-based design by allowing engineers with some basic knowledge of reliability analysis and probabilistic modelling to perform reliability analyses. The development of such "user-friendly" software should initiate from the research community since the industry does not see the need for program development since they are not aware of the benefits. The reader can think of a finite element software that performs reliability analyses which require only the input of the type of material utilised and that has in-built probabilistic models to represent the random variables on the resistance side. The software could, for example, update the models automatically when the user provides some field measurements without requiring the user to master advanced statistical methods. At the same time, the software could allow the expert users to insert the specific probabilistic model if known. This would simplify the use of the methodology significantly. The available technology seems sufficient for these advancements. The inspiration could be taken from the non-linear finite element programs that are used more and more and also from engineers that have basic knowledge of finite element methods.

- The two points above might also support the attempt to even out the level of detail of the models describing the structural response, the component capacities and the effects of actions. It is the author's opinion that, to date, there is a tendency to perform structural analyses with very accurate mechanical models and structural analysis methods together with (extremely) poor modelling of the uncertainties on the material properties, models and loads. The reason is perhaps that the analysis methods and the mechanical models are theoretically sound and "deterministic" while the other variables need to be modelled with probabilistic models. In this respect, it is to be observed that probabilistic modelling is just a methodology necessary for modelling phenomena whose "*experimental data in our possession are compatible with such and such a probabilistic model* […]*, and we do not have any deterministic model which can account for them in a more satisfactory fashion*" [70, p.10]. Consequently, there should not be such a difference of detail among models or variables that require stochastic models and the ones that do not. This is, perhaps, a change that should start with the education of future engineers. Probabilistic modelling and reliability methods should not only be present in a course during the degree, but should be considered in all subjects that require their application.

Part I

Calibration of Codified Design

Chapter 2 Paper I: A Risk-Based Approach for Calibration of Design Codes

Paper

Authors: M. Baravalle[a], J. Köhler[a]
[a] Department of Structural Engineering, Norwegian University of Science and Technology, Trondheim

Submitted to an international scientific journal in September 2017.

2.1 Abstract

This paper contributes to the ongoing discussion on the tentative target reliability levels for the design of structures and calibration of codes. An extension of the existing approach for code optimisation is proposed. The basis is taken from the normative decision theory as the rational strategy for taking a decision under risk. The proposed method allows to explicitly account for the structural system effects and the differences among the structures belonging to the same class in the code optimisation. The theoretical decision aspects that are often misunderstood and object of discussions in the research community are clarified. The work contributes to a more robust and transparent background to target reliabilities in design standards.

Keywords: risk, design codes, code calibration, target reliability, decision theory, optimisation.

Is not included due to copyright

Chapter 3 Paper II: Generic Representation of Target Values for Structural Reliability

Paper

Authors: M. Baravalle[a], J. Köhler[a]

[a] Department of Structural Engineering, Norwegian University of Science and Technology, Trondheim

Submitted to an international scientific journal in September 2017.

3.1 Abstract

A simple plot for communicating target and acceptable reliabilities is proposed in this article. The plot might supplement the tables for target reliabilities in existing design codes. The optimal target reliability is derived with the objective function suggested by Rackwitz. The parameters entering the function are discussed for guiding their estimation. The acceptable reliability is derived with the marginal life saving cost principle implemented using the Life Quality Index. The plot allows differentiating target reliabilities concerning the failure costs, the relative safety costs, the obsolescence rate, the interest rate used by the decision maker for discounting future cash flows and the uncertainty characterising the problem at hand. The acceptable reliabilities are distinguished with respect to the number of expected fatalities given failure, the societal willingness to pay for saving one additional life, the type of uncertainties, the relative safety costs, the obsolescence rate and the societal interest rate. The proposed plot allows for higher reliability differentiation and consequently higher levels of structural optimisation compared with the tables in current design codes.

Keywords: design codes, code calibration, target reliability, acceptable reliability, reliability differentiation, plot.

Is not included due to copyright

Chapter 4 Paper III: A Framework for Estimating the Implicit Safety Level of Existing Design Codes

Paper

Authors: M. Baravalle[a], J. Köhler[a]
[a] Department of Structural Engineering, Norwegian University of Science and Technology, Trondheim

Proceedings of the 12th International Conference on Structural Safety & Reliability (ICOSSAR 2017), Vienna (Austria), August 6th-10th 2017.

4.1 Abstract

Target safety levels (β_t) are key elements for reliability-based design and calibration of design codes. They are derived by monetary optimization or from existing codes. The current article discusses these two approaches and proposes a novel method for estimating β_t from existing codes, based on a specific optimality assumption. The method leads to implicit target reliabilities lower than the existing code's mean reliability. It further estimates how much a simplified safety format can increase the cost of structures compared to codes of higher levels, and also can reduce the code's mean reliability when a more homogeneous safety level is reached through the optimization of the partial safety factors. The results are compared with the ones obtained from another method presented in literature.

Keywords: target reliability, code calibration, existing codes, decision theory, best practice.

Is not included due to copyright

Part II

Specific Study Cases

Chapter 5 Paper IV: Calibration of Simplified Safety Formats for Structural Timber Design

Paper

Authors: M. Baravalle [a,*], M. Mikoschek [b], F. Colling [b], J. Köhler [a]
[a] Department of Structural Engineering, Norwegian University of Science and Technology, Trondheim
[b] University of Applied Science Augsburg, Institut für Holzbau, An der Hochschule 1, 86161 Augsburg, Germany

In *Construction and Building Materials*. Volume 152, 2017, pp. 1051-1058.

5.1 Abstract

A framework for calibrating the reliability elements in simplified semi-probabilistic design safety formats is presented. The objective of calibration is to minimize the increase of construction costs, compared to the non-simplified safety format, without reducing the level of structural safety. The framework is utilised for calibrating two simplified safety formats which aim at reducing the number of load combinations relevant in structural timber design. In fact, the load-duration effect makes the design of timber structures more demanding since a larger number of load combinations need to be considered compared with other construction materials.

Keywords: simplified safety formats, code calibration, timber, reliability, load-duration effect.

5.2 Introduction

Current standards for timber design, such as the Eurocode 5 [87], have reached a high level of sophistication, extensiveness, efficiency and completeness at a cost of increasing the number and complexity of design rules, principles and requirements. This is the result of a code-development process driven mainly by the need to extend the standards to new materials, solutions, technologies, calculation tools and mechanical models. The associated drawback is an increased, and sometimes unnecessary, complexity of structural design, particularly for common and simple structures. Therefore, code provisions should balance simplicity, economy, comprehensiveness, flexibility, innovation, and reality [88]. These properties are usually mutually exclusive and their adjustment must not affect the safety level of the design. In addition, the adequate complexity level depends on manifold factors, including the types of structures designed, the materials and technological solutions adopted, the design phase, and the experience of the engineers [53, 54, 88]. For example, complex structural solutions require detailed codes, while simple structures do not. Consequently, discussions about the adequate level of code sophistication are ongoing [1, 52, 53, 54].

Simplification and improvement of the ease of use of codes are essential criteria in all code development projects, including the publication of the second generation of European structural design codes [28]. Sophistication is obviously required only when bringing benefits since unnecessary detailing will solely increase bureaucracy. Therefore, two research directions are of interest. The first is the assessment of modern codes, the quantification of the benefits given by sophistication compared with existing simpler alternatives. The second is the proposal of less complex solutions that can either substitute the complex ones (when the latter brings no benefits) or work as alternatives when the engineer needs a simpler and faster design for different reasons [1, 52, 53, 54].

Part of the complexity of timber design standards is due to the wide range of material-specific phenomena, which can lead to a more demanding structural engineering design compared to other building materials. The most important phenomena are anisotropy, grain deviation, shrinkage, creep and the load-duration effect. These phenomena are influenced by the environmental conditions. The load-duration effect is considered in the ultimate limit state design with modification factors, as k_{mod} in Eurocode 5 [87], and has an effect on the determination of the decisive load combination. For other building materials, the load combination with the maximum load is automatically decisive for the design. This is not equally applicable to timber structures. In fact, due to the influence of load duration and service class - accounted for by the corresponding values for k_{mod} - the decisive load combination could also result in a lower absolute sum of loads if it has to be divided by a smaller modification factor. As a consequence, a larger number of relevant load combinations must be considered during structural design. This increases the engineering effort significantly, especially when hand calculations are performed, as is often the case for simple structures or structural components.

Beside the time-consuming search of the decisive load combination, there are further demanding aspects of the design of timber structures. There are a large number of values for timber specific factors (especially k_{mod}), depending on the materials and the regulations of the different countries. Thus, a harmonization and reduction of the corresponding values seem to be necessary and helpful.

Different simplifications of load combination rules for timber design have been discussed and proposed in the literature [52, 54]. This article proposes two simplified safety formats that

facilitate the detection of the decisive load combination. The work is partly a result of the European Cooperation in Science and Technology (COST) Action FP1402. Preliminary formats and concepts were developed and proposed in [1]. Previous investigations in the field of simplified rules for load combinations in structural timber design led to good results, comparing the design and economic aspects with the Eurocodes [18, 87]. First rough calculations regarding reliability aspects showed that the designs identified by simplified rules led to higher reliability indices than the ones identified by the present Eurocodes [89]. However, further reliability analyses and calibrations were necessary for more profound results. Therefore, this article attempts to provide a more scientific basis for further discussions in code committees.

5.3 Eurocode safety format

The Eurocodes [18, 87] comprise the Load and Resistance Factor Design format (LRFD) as several other modern codes (see e.g. [19, 20, 21]). It is referred to as semi-probabilistic, i.e. the safety assessment of structural members is simplified and reduced to a comparison of the resistance design value r_d with the design value of the effect of actions e_d, i.e. the former has to be larger than the latter in order to provide appropriate reliability ($r_d > e_d$).

In Eurocode 0 [18], r_d is written in general terms as in Eq. (5.1) where $\mathbf{z}_d$ is the vector of design values of geometrical data, $f_{k,i}$ are the characteristic values of the material properties involved, $\gamma_{M,i}$ are the partial safety factors and η is the mean value of the conversion factor that keeps into account several effects including the load-duration effect. The partial safety factor γ_M is dependent on: the uncertainties on the material property, the uncertainties on η, the uncertainty on the resistance model as well as the geometric deviations.

$$r_d = r\left\{\eta \frac{f_{k,i}}{\gamma_{M,i}}; \mathbf{z}_d\right\} \tag{5.1}$$

For the ultimate limit state design of timber elements, the conversion factor η is represented by the modification factor k_{mod} that considers the time-dependent decrease of the load bearing capacity of timber. It depends on the moisture content of the timber elements (defined in service classes) and the type of load or, more precisely, the load duration. Generally, the strength reduction is greater when the moisture is high and the load is being applied for longer periods. The values of the factors are usually determined empirically by experience or by using probabilistic methods, which are referred to as damage accumulation models (see e.g. Gerhards model [90] or Barrett and Foschi's model [91, 92]), example values are given in Table 5.1.

Table 5.1. Values for the modification factor k_{mod} for solid timber and glulam according to [93].

Moisture content	***Service class***	***Load-duration class of action***				
		Permanent	***Long-term***	***Medium-term***	***Short-term***	***Instantaneous***
< 12%	1	0.60	0.70	0.80	0.90	1.10
12-20%	2	0.60	0.70	0.80	0.90	1.10
> 20%	3	0.50	0.55	0.65	0.70	0.90

The effect of action e_d for the verification of structural ultimate limit states can be written in general terms as presented in Eq. (5.2), where one variable load is dominant and the

remaining ones are accompanying. The partial safety factors for permanent actions γ_G and variable actions γ_Q cover the uncertainties on the actions, their effects and models. The load combination factors ψ_0 reduce the effect of accompanying actions since the coincidence of maxima has a low probability of occurrence.

$$e_d = e\left\{\gamma_{G,j}\, g_{k,j}; \gamma_{Q,1} q_{k,1}; \gamma_{Q,i}\psi_{0,i} q_{k,i}\right\} \quad (j \geq 1, i > 1) \tag{5.2}$$

The design effect of action shall be determined for each relevant load case by combining the effects of actions that can occur simultaneously. The combination of actions in curly brackets in Eq. (5.2) might be expressed as in Equation 6.10 of EN 1990:2002 (see Eq. (5.3) below), where the symbol "$_+$" means "to be combined with". The k_{mod} on the resistance side should be chosen as the one corresponding to the load with the shortest duration considered in the combination.

$$\sum_{j\geq 1} \gamma_{G,j} g_{k,j} + \gamma_{Q,1} q_{k,1} + \sum_{i>1} \gamma_{Q,i}\psi_{0,i} q_{k,i} \tag{5.3}$$

For resistance models which are linear in the material property, the design check can be rewritten as in Eq. (5.4), where the resistance side is independent of the load duration and moisture content. The assumption of linear models is maintained hereinafter.

$$r_d > e_d \rightarrow r\left\{\frac{f_{k,i}}{\gamma_{M,i}}; \mathbf{z}_d\right\} > \frac{e_d}{k_{\text{mod}}} = e_d^* \tag{5.4}$$

As is clear from Eq. (5.4) the load case with highest e_d^* is decisive for design. This requires the consideration of a larger number of load combinations compared to other construction materials where the combination giving the largest e_d is decisive. For the case with permanent loads and two variable loads ($n_Q = 2$), five load combinations should be considered, see Eq. (5.5) to (5.7). The notation $k_{\text{mod},[\cdot]}$ stands for the k_{mod}-value corresponding to the action $[\cdot]$.

$$e_{d,1}^* = \frac{e\left\{\sum_{j\geq 1} \gamma_{G,j} g_{k,j}\right\}}{k_{\text{mod,G}}} \tag{5.5}$$

$$e_{d,1+i}^* = \frac{e\left\{\sum_{j\geq 1} \gamma_{G,j} g_{k,j} + \gamma_{Q,i} q_{k,i}\right\}}{k_{\text{mod},Q_i}} \quad (i = 1,2) \tag{5.6}$$

$$e_{d,3+i}^* = \frac{e\left\{\sum_{j\geq 1} \gamma_{G,j} g_{k,j} + \gamma_{Q,i} q_{k,i} + \gamma_{Q,h}\psi_{0,h} q_{k,h}\right\}}{\max\left\{k_{\text{mod},Q_1}, k_{\text{mod},Q_2}\right\}} \quad (i = 1,2; h = 1,2; h \neq i) \tag{5.7}$$

For $n_Q > 2$ the number of load combinations becomes $1 + 2n_Q + n_Q\left(n_Q - 1\right)$.

5.4 Proposed simplified safety formats

5.4.1 General

In order to facilitate the search for the decisive load combination, two simplified rules for structural timber design are proposed below. The proposals are intended to simplify the design of structures when there are two or more variable loads in addition to permanent loads. For the case with one variable load, the simplification is not needed because two load combinations are to be considered only.

5.4.2 Simplified safety format I (SFI)

The simplified safety format in [1] is proposed and reviewed here. It is in accordance with the rules in the German standard DIN 1052:2004-08 [94] in § 5.2 (1). However, additional restrictions and statements are introduced for a better understanding and larger conservatism. A total of $1+n_Q$ load combinations is to be considered for a structural element loaded by n_Q variable loads, see Eq. (5.8) and (5.9). The first equation introduces a "global" safety factor γ_F multiplying the sum of all characteristic values of loads. In previous investigations, 1.40 or 1.35 were used as values for γ_F with respect to $\gamma_G = 1.35$ and $\gamma_Q = 1.50$ [1, 89]. The second equation combines the permanent load and only one variable load at a time.

$$e^*_{d,1} = e\left\{\gamma_F \left(\sum_{j\geq 1} g_{k,j} + \sum_{i=1}^{n_Q} q_{k,i}\right)\right\} \Big/ \max\left\{k_{\mathrm{mod},Q_1},\ldots,k_{\mathrm{mod},Q_{nQ}}\right\} \tag{5.8}$$

$$e^*_{d,1+i} = e\left\{\sum_{j\geq 1} \gamma_{G,j} g_{k,j} + \gamma_{Q,i} q_{k,i}\right\} \Big/ k_{\mathrm{mod},Q_i} \quad \left(i = 1,\ldots,n_Q\right) \tag{5.9}$$

5.4.3 Simplified safety format II (SFII)

A second simplified format is proposed consisting of the load combination rules of the Eurocodes [18] with a fixed value of the modification factor $k_{\mathrm{mod}} = k'_{\mathrm{mod}}$. This format reduces the number of different load duration factors, which is indeed the cause of the additional effort for finding the decisive load combination in structural timber design. In addition, this format requires considering the same number of load combinations as for any other construction material (e.g., structural steel and reinforced concrete). A total of n_Q load combinations is to be taken into account, see Eq. (5.10).

$$e^*_{d,i} = e_{d,i} / k'_{\mathrm{mod}} = e\left\{\sum_{j\geq 1} \gamma_{G,j} g_{k,j} + \gamma_{Q,i} q_{k,i} + \sum_{h\neq i} \gamma_{Q,h} \psi_{0,h} q_{k,h}\right\} \Big/ k'_{\mathrm{mod}} \quad \left(i = 1,\ldots,n_Q\right) \tag{5.10}$$

5.5 Calibration of safety formats

5.5.1 General

The reliability level associated with the proposed simplified safety format are assessed and compared with the safety level given by the Eurocodes. In general, when the complexity of a code brings benefits, such as higher structural efficiency, any simplification will reduce the engineering costs, but likely also reduce the efficiency of the resulting design and/or limit the code's application domain. Consequently, the safety factor γ_F introduced in *SFI* and the k'_{mod} introduced in *SFII* are calibrated by established techniques ([5, 7, 10, 11, 36, 95]) applied in a novel manner to satisfy the objective of minimizing the reduction of structural efficiency without compromising the structural safety level. For this purpose, the safety level associated with the design just satisfying the design equations (i.e. $e_d \equiv r_d$) is evaluated using the First Order Reliability method (FORM). The FERUM package [73] is used in Matlab® [96] for this purpose. First rough calculations regarding the reliability analysis of the simplification (*SFI*) were performed and published in [89]. These calculations are extended and performed more precisely. As in [89], the work is restricted to:

- service classes: 1 and 2 (see Table 5.1),
- two variable loads: wind (Q_1) and snow (Q_2),
- two materials: solid timber (ST) and glulam (GL), and

- three ultimate limit state failure modes at the full member level (i.e., excluding joints and construction details): bending, tension and compression parallel to the grain.

These restrictions represent the most common cases of typical wooden structures (e.g. roof constructions) for which the simplifications are aimed at.

5.5.2 Reliability analyses and probabilistic models

Normalized and standardized limit state functions (LSFs) in Eq. (5.11) to (5.15) have been considered for the reliability analyses as in [7]. $\mathbf{X}=\left[F,\Theta_R,G,\Theta_{Q_1},Q_1,\Theta_{Q_2},Q_2\right]^T$ and $\mathbf{p}=\left[z,k_{\text{mod}},\alpha_G,\alpha_Q\right]^T$ are the vectors of random variables and deterministic parameters, respectively. All random variables in $\mathbf{X}$ are considered uncorrelated. The description of the random variables and the stochastic models representing them are summarized in the Appendix. The limit states functions are normalized implying that the random variables have all unitary mean except for the model uncertainties which might have different mean values for representing biased models. In this way, different load scenarios (i.e. different ratios between actions induced by self-weight, first and second variable loads) are represented by varying the parameters α_Q and α_G in the limit state functions. The equations are standardized meaning that they can represent different failure modes. For example, the representation of failure in bending considers the general material property F to be the bending strength F_m and the design parameter z to be the cross-section modulus. Geometric properties are assumed deterministic and equal to their nominal or design value. The k_{mod}-values included in the limit state functions are assumed to be known (deterministic) and equal to the ones given in the Eurocodes. Their uncertainty is assumed to be included in the resistance model uncertainty (Θ_R). Therefore, the load damage models are not considered explicitly. The probability of failure of the structural element is the union of the failure events represented by the five limit state functions. For the specific problem at hand, it is observed that the failure probability of the union is always governed by one of the five limit states. Hence, for simplification purposes, the reliability index is calculated as the minimum reliability index among the ones obtained from the five limit state functions.

$$g_1(\mathbf{x},\mathbf{p})=z\,k_{\text{mod,G}}f\theta_R-\alpha_G g\le 0 \tag{5.11}$$

$$g_2(\mathbf{x},\mathbf{p})=z\,k_{\text{mod},Q_1}f\theta_R-\alpha_G g-(1-\alpha_G)\left[\alpha_Q\theta_{Q1}q_1\right]\le 0 \tag{5.12}$$

$$g_3(\mathbf{x},\mathbf{p})=z\,k_{\text{mod},Q_2}f\theta_R-\alpha_G g-(1-\alpha_G)\left[\left(1-\alpha_Q\right)\theta_{Q2}q_2\right]\le 0 \tag{5.13}$$

$$g_4(\mathbf{x},\mathbf{p})=z\max\left\{k_{\text{mod},Q_1},k_{\text{mod},Q_2}\right\}f\theta_R-\alpha_G g-(1-\alpha_G)\left[\alpha_Q\theta_{Q1}q_{1L}+(1-\alpha_Q)\theta_{Q2}q_{2A}\right]\le 0 \tag{5.14}$$

$$g_5(\mathbf{x},\mathbf{p})=z\max\left\{k_{\text{mod},Q_1},k_{\text{mod},Q_2}\right\}f\theta_R-\alpha_G g-(1-\alpha_G)\left[\alpha_Q\theta_{Q1}q_{1A}+(1-\alpha_Q)\theta_{Q2}q_{2L}\right]\le 0 \tag{5.15}$$

The five LSFs represent different failure events due to: only permanent load G (LSF g_1), permanent load with a single variable load (LSFs g_2 and g_3), and permanent load with the simultaneous occurrence of the two variable loads (LSFs g_4 and g_5). The yearly maxima of the variable loads (Q_1, Q_2) are used in the LSFs g_2 and g_3. The Ferry Borges and Castanheta load combination rule is applied in the LSFs g_4 and g_5 (see e.g. [11]) combining together the loads' maxima over reference periods of different length. This is done considering one load as leading (q_L) and the other one as accompanying (q_A). The two loads are represented by a Poisson rectangular pulse process. The loads are present n_p days a year and have a number of independent realizations a year equal to n_r, a similar combination model is included in e.g. [97].

Four major types of climate are regarded by combining snow and wind actions with different characteristics. The parameters of the processes representing the loads, the associated modification factors, and load combination factors are reported in Table 5.2. For the snow load on the ground, a fundamental distinction is made between continental climate (covered by Cases 2 and 4) and maritime or mixed climates (Cases 1 and 3) [58]. Continental climate is characterised by snow accumulation through the winter and is typical for European sites above 1000 m a.s.l., and for the Nordic countries Finland, Iceland, Norway, and Sweden. Maritime and mixed climates are characterised by significant melting between snow events and are typical for European sites below 1000 m a.s.l. Wind action is represented by 365 independent repetitions a year based on the macro-meteorological period, i.e. the period of passage of a fully developed weather system, that is typically between 1 and 7 days in Europe (see e.g. [98]). According to Eurocode 5, wind action can be considered as short-term or instantaneous with corresponding recommended k_{mod}-values given in Table 5.1. Classifying wind as short-term, i.e. load-duration up to one week, seems very conservative. This is supported by the fact that several European countries classify wind as instantaneous. Other countries, including Germany and Austria, classify wind as short-term/instantaneous. For all these reasons wind is considered, in this work, short-term/instantaneous (Cases 1 and 2) and instantaneous (Cases 3 and 4). The national choices might be considered including the country-specific climate characteristics. The four cases might represent the climates and the national choices for, in order: Germany (locations below 1000 m a.s.l.), Austria (locations above 1000 m a.s.l.), Denmark and Norway.

The self-weight of structural and non-structural parts (G) is classified as permanent action and therefore has a modification factor $k_{\mathrm{mod}} = 0.60$ for service classes 1 and 2 (see Table 5.1).

Table 5.2. Different climatic conditions and relative parameters of the load models and recommended ψ_0 and k_{mod} values from Eurocodes.

Case	***Wind***					***Snow***				
	Load dur.	k_{mod}	ψ_0	n_p	n_r	***Load dur.***	k_{mod}	ψ_0	n_p	n_r
1 - Germany	Short /inst.	1.00	0.60	365	365	Short	0.90	0.50	100	11
2 - Austria	Short /inst.	1.00				Medium	0.80	0.70	150	
3 - Denmark	Inst.	1.10				Short	0.90	0.50	100	
4 - Norway	Inst.	1.10				Medium	0.80	0.70	150	

5.5.3 Reliability level of the current Eurocodes

The proposed simplified load combinations are calibrated in order to provide safety levels which are equal to or larger than the safety levels implicitly provided by the Eurocodes. The partial safety factors recommended in the Eurocodes are:

- $\gamma_G = 1.35$ for all permanent loads (self-weight of structural and non-structural parts),
- $\gamma_Q = 1.50$ for all variable loads,
- $\gamma_{M,ST} = 1.30$ for the strength of solid timber, and
- $\gamma_{M,GL} = 1.25$ for the strength of glulam timber.

The weighted mean and standard deviation of the reliability indices obtained for different material properties and different load scenarios are calculated. The weights for the different material properties (w_F) are assigned with engineering judgment representing the frequency of occurrence in real structures, see Table 5.3. Two cases have been investigated. The first

considers solid timber as dominant material. The simplified design equations presented in this article are expected to be applied in the design of simple housing structures that are mostly made of solid timber. The second considers glulam timber as the dominant material representing industrial buildings. The first case can also be considered as a conservative selection of w_F-values since it weighs more the material presenting the largest uncertainties.

Table 5.3. Weights for material properties (w_F) for ST dominating (case of GL dominating in brackets).

Material	***Bending*** F_m	***Tension*** $F_{t,0}$	***Compression*** $F_{c,0}$	***Total (per material)***
Solid Timber (ST)	0.42 (0.06)	0.07 (0.01)	0.21 (0.03)	0.70 (0.10)
Glulam (GL)	0.18 (0.54)	0.03 (0.09)	0.09 (0.27)	0.30 (0.90)
Total (per failure mode)	0.60	0.10	0.30	

Different load scenarios are included in the study. They are characterised by the proportions between the different loads expressed as $\chi_G = g_k / \left(g_k + q_{1,k} + q_{2,k}\right)$ and $\chi_Q = q_{1,k} / \left(q_{1,k} + q_{2,k}\right)$. The required values of χ_G and χ_Q are obtained by varying the parameters α_G and α_Q in the limit state functions (Eq. (5.11) to (5.15)). Load scenarios are divided into two domains as listed below, representing different typologies of structures:

- Structures with dominating permanent loads (e.g. green roofs): $\chi_G \geq 0.6$ and $0 \leq \chi_Q \leq 1$;
- Structures with dominating variable loads (e.g. common buildings): $0 \leq \chi_G \leq 0.6$ and $0 \leq \chi_Q \leq 1$.

All load scenarios are equally weighted, i.e. the weights associated with different χ_Q and χ_G values are equal ($w_{\chi_G} = w_{\chi_Q}$). This considers the load scenarios equally frequent. The sum of all weights is fixed to unity ($\sum_i \sum_j \sum_k w_{F,i} w_{\chi_G,j} w_{\chi_Q,k} = 1$).

5.5.4 Calibration objective

Tentative values of the reliability elements γ included in the proposed simplified safety formats (γ_F, k'_{mod}) were calibrated solving the minimization problem in Eq. (5.16). The term in squared brackets is a skewed penalty function proposed in [11]. It penalizes under-design ($\beta < \beta_t$) more than over-design ($\beta > \beta_t$). In fact, under-design is associated with larger expected costs due to larger expected failure costs, see e.g. [48] for more details. The sums are extended over the six considered material properties (or failure modes) and the different values of χ_G and χ_Q. The objective of the calibration was to obtain a level of safety equal to or larger than the level given by the current standard. Therefore, the target reliability index was selected as $\beta_t = E\left[\beta_{EC}\right]$, where $E\left[\beta_{EC}\right]$ is the weighted mean reliability index associated with the design given by the Eurocode.

$$\min_{\boldsymbol{\gamma}} \left\{ \sum_{i=1}^{6} \sum_{j=1}^{10} \sum_{k=1}^{10} w_{F,i} w_{\chi_G,j} w_{\chi_Q,k} \left[\frac{\beta_{ijk}(\boldsymbol{\gamma}) - \beta_t}{d} - 1 + \exp\left(-\frac{\beta_{ijk}(\boldsymbol{\gamma}) - \beta_t}{d} \right) \right] \right\} \quad (d \approx 0.23) \tag{5.16}$$

It is to be highlighted that the estimation of the target reliability β_t from the existing codes and the calibration of reliability elements are performed with the same probabilistic models. Therefore, the (nominal) reliability indices are used to compare safety levels rather than expressing the "exact" level of safety. As expected, the absolute value of $E\left[\beta_{EC}\right]$ is sensitive to the stochastic models adopted. Nevertheless, the calibrated reliability elements are seen to

be almost insensitive to changes of the coefficients of variation of the distribution functions within the realistic domain. For this reason, the random variables are represented by simplified stochastic models (Table 5.4). For the same reason, the biases of the resistance and load models were not considered. Beside the difficulty of their estimation, their inclusion will affect the values of β considerably, but not the values of the calibrated reliability elements. Larger reliability indices are expected due to the conservativeness (bias larger than 1) of the Eurocode models (see e.g. [99] for wind load model).

*Table 5.4. Stochastic models for the reliability analysis from [13] unless otherwise specified (§[37], *yearly maxima).*

Random variable		***Symbol***	***Type***	***Mean***	***COV***	***Characteristic fractile***
Solid timber (ST)	Resistance model uncertainty	$\Theta_{R,ST}$	Lognormal	1.00	0.07	/
	Bending strength	$F_{m,ST}$	Lognormal	1.00	0.25	0.05
	Tension parallel to grain	$F_{t,0,ST}$	Lognormal	1.00	1.2·0.25	0.05
	Compression parallel to grain	$F_{c,0,ST}$	Lognormal	1.00	0.8·0.25	0.05
Glulam (GL)	Resistance model uncertainty	$\Theta_{R,GL}$	Lognormal	1.00	0.07	/
	Bending strength	$F_{m,GL}$	Lognormal	1.00	0.15	0.05
	Tension parallel to grain	$F_{t,0,GL}$	Lognormal	1.00	1.2·0.15	0.05
	Compression parallel to grain	$F_{c,0,GL}$	Lognormal	1.00	0.8·0.15	0.05
Dead load		G	Normal	1.00	0.10	0.5
Wind time-invariant part (gust c_g ,pressure c_{pe} and roughness c_r coefficients)		Θ_{Q_1}	Lognormal	1.00	0.27	0.78 (c_{pe}) (μ for c_g,c_r)
Wind mean reference velocity pressure *		Q_1	Gumbel	1.00	0.25	0.98
Snow time-invariant part (model uncertainty and shape coefficient)		Θ_{Q_2}	Lognormal	1.00	0.20§	(μ)
Snow load on roof *		Q_2	Gumbel	1.00	0.35§	0.98

5.6 Results and discussion

5.6.1 Results

The calibrated reliability elements are calculated for the different cases included in the study and summarized in Table 5.5. The influence of the dominating material on the calibrated reliability elements is observed to be of little importance within each case. The differences in the calibrated values of k'_{mod} among the 4 different cases are considered small for dominating permanent load. All k'_{mod} -values are indeed close to $k_{\mathrm{mod},G}$ that is 0.60. This might suggest the use of a single value for all four cases. In contrast, larger differences are observed for dominating variable loads. In fact, the reliability level was observed to be quite sensitive to small variations of k'_{mod}. This suggests representing the suggested k'_{mod} values, as precise as practically feasible in the possible revision of the design format. In general, the calibrated modification factors are all within the range of the standardized values in Table 5.1. For *SFI*, γ_F is varying in the same magnitude among the four cases. For permanent load dominating, the calibrated γ_F are close to $\left(\gamma_G \cdot k_{\mathrm{mod},Q}\right) / k_{\mathrm{mod},G}$ as expected.

Table 5.5. Calibrated reliability elements.

Dominant material	***Dominant loads***	***Rel. element (Safety format)***	***Case***			
			1 Germany	***2 Austria***	***3 Denmark***	***4 Norway***
ST	Permanent	γ_F (SFI)	2.14	2.17	2.35	2.38
		k'_{mod} (*SFII*)	0.63	0.62	0.63	0.62
	Variable	γ_F (SFI)	1.46	1.48	1.56	1.58
		k'_{mod} (*SFII*)	0.89	0.84	0.92	0.86
GL	Permanent	γ_F (SFI)	2.16	2.18	2.37	2.39
		k'_{mod} (*SFII*)	0.63	0.62	0.63	0.62
	Variable	γ_F (SFI)	1.42	1.42	1.51	1.53
		k'_{mod} (*SFII*)	0.90	0.82	0.93	0.84

The two proposed formats and the Eurocode format are compared in terms of safety levels, structural dimensions and number of relevant load cases.

The reliability levels associated with the calibrated reliability elements are compared with the Eurocode format in Figure 5.1 for solid timber (ST) dominating. Detailed plots are illustrated in Figure 5.2 for a selected case. The boxplots for the case with dominant glulam (GL) are very similar to the ones in Figure 5.1 in terms of minimum, maximum, average and skewness of the reliability indices. For this reason, they are not shown in the paper. Both cases show larger safety level and scatter in reliability indices compared to the considered design code due to the selected objective function. The performance of *SFI* and *SFII* are quite similar and no significant differences in terms of reliability are observed for the case with dominant permanent loads.

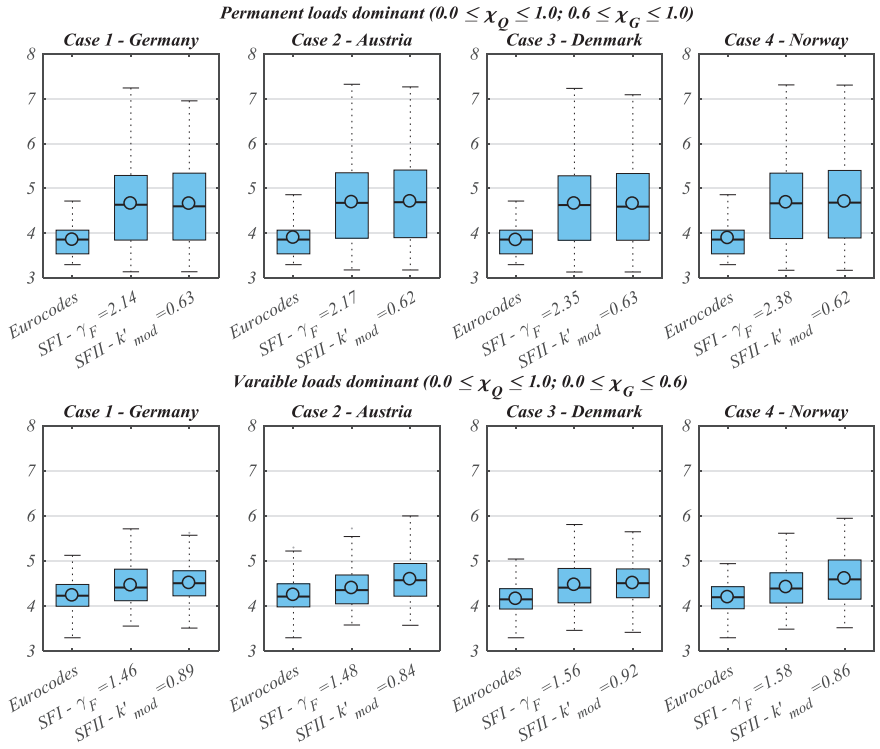

Figure 5.1. Reliability indices corresponding to the design performed with Eurocodes and the two simplified safety formats with calibrated reliability elements for ST dominating (Box-and-whisker plot with boxes from first to third quartiles with median (line) and mean value (circle), whiskers from minimum to maximum).

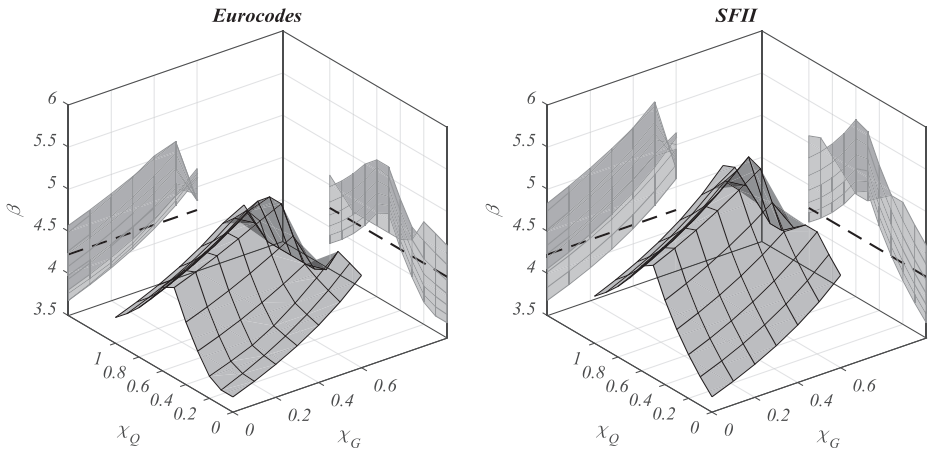

Figure 5.2. Reliability indices for Case 1, compression parallel to grain $F_{c,0}$, dominating variable loads and solid timber: Eurocodes (left), calibrated SFII (right) and Eurocodes weighted average (dashed line).

The proposed simplified formats drastically reduce the number of load combinations as summarized in Table 5.6. The reduction is increasing with the number of variable loads n_Q. *SFII* always requires one load combination less compared to *SFI* and, as already mentioned, it requires the same number of load combinations for any other construction material.

Table 5.6. Number of relevant load combinations to consider in design.

n_Q	***Eurocodes***	***SFI***	***SFII***
1	2	2	1
2	5	3	2
3	13	4	3
4	21	5	4

The proposed simplified formats lead in average to larger design solutions, i.e. increased construction costs. This is the price of the simplifications introduced. The structural dimensions are compared in Table 5.7 through the weighted average over-design $E[\Delta z]$, calculated from Eq. (5.17), where $z_{ijk}^{(SF)}$ is the design obtained by the simplified safety format proposed and $z_{ijk}^{(EC)}$ is the design according to Eurocode. It is important to highlight that the average increase in construction costs is lower than the $E[\Delta z]$ values in Table 5.7 since a large part of the construction costs is independent of the structural dimensions z. Weighted over-design averages were found higher for the case of dominant permanent loads. For variable loads dominating, it was found that the absolute maximum over-design was around 25 % for *SFI*, and very close to the average over-design for *SFII*. The maximum overdesigns were found to be around 60 % for cases where the permanent load is dominating.

$$E[\Delta z] = \sum_{i=1}^{6}\sum_{j=1}^{10}\sum_{k=1}^{10} w_{F,i}\, w_{\chi_G,j}\, w_{\chi_Q,k} \left[\frac{z_{ijk}^{(SF)}}{z_{ijk}^{(EC)}} - 1 \right] \tag{5.17}$$

It is important to note that the monetary benefit/loss associated with the use of simplified safety formats cannot be assessed by accounting the construction costs only. In fact, simplified safety formats can significantly reduce the effort in engineering work and associated costs. The quantification of these savings in a general way is not an easy task and is left to code-committees who will assess whether it is more efficient to use a simplified or a sophisticated format. The framework proposed in this paper will support this assessment in a rational way. Further, larger safety levels reduce the risk associated with the event of failure, where risk is defined as costs associated with failure times the probability of failure. The weighted average expected failure costs were found to be between 30 % and 60 % lower compared to the Eurocode. This is clearly a consequence of the higher safety levels reached with the simplified formats. The net benefit (or loss) obtained from the increase in construction costs and the decrease in both the engineering and failure costs can only be assessed by knowing the absolute values of these costs. However, this was beyond the scope of the work at hand.

Table 5.7. Weighted average over-design $E[\Delta z]$ (values in percentage).

Dominant material	*Dominant loads*	*Safety format*	*Case*			
			1 - Germany	*2 - Austria*	*3 - Denmark*	*4 - Norway*
ST	Permanent	SFI	+ 21.7	+ 21.3	+ 21.7	+ 21.3
		SFII	+ 21.7	+ 21.9	+ 21.7	+ 21.9
	Variable	SFI	+ 8.1	+ 5.4	+11.8	+ 8.4
		SFII	+ 10.0	+ 13.1	+ 13.2	+ 16.3
GL	Permanent	SFI	+ 22.6	+ 21.9	+ 22.6	+ 21.9
		SFII	+ 22.6	+ 22.5	+ 22.6	+ 22.5
	Variable	SFI	+ 5.4	+ 2.9	+ 9.0	+ 6.2
		SFII	+ 9.1	+ 15.9	+ 11.8	+ 19.1

5.6.2 Discussion

The resulting calibrated formats are shown to greatly reduce the number of load combinations with a minimal increase in structural dimensions and construction costs. This proves, as expected, that the complexity of the load combination rules provided in [87] does lead to more efficient structural design compared with the simplified formats. Therefore, it is important to emphasize that the formats proposed do not have the desire to substitute the existing combination rules, but rather to be alternatives that engineers can choose any time they need a rougher and faster design and/or they believe that these simpler formats reduce the engineering costs more than the increase in construction costs. In addition, simplified formats might be useful for checking the plausibility of results obtained from structural analyses performed by computer software with a large number of detailed load combinations. In this manner, analysis errors might be identified.

Both proposed safety formats with the calibrated reliability elements meet the requirement of simplifying design without decreasing the level of safety. Based on the performed calculations, the format *SFI* has the potential to be more economical in average but also leading to the largest absolute differences in design compared to the current version of the Eurocodes. The *SFII* includes a lower number of load combinations. In addition, *SFII* is expected to be easier implemented within the Eurocode framework, since it basically proposes to use the same load combination rules as used for the other materials. Hence, it follows the fundamental requirement of having material-independent load combinations. *SFII* can indeed be seen as a simplified way for accounting the load-duration effect on the material properties by dividing the material partial safety factor by a fixed factor (k'_{mod}).

The proposed formats were derived specifically for the cases with dominating variable loads, which are the most common for timber structures. As expected, they provide a balance between simplification and additional costs within this restriction. On the contrary, quite high over-design was obtained for the cases with dominating permanent load. These cases are seldom in timber structures and were mostly given for sake of completeness and for showing that, with different additional costs, the proposed formats lead to acceptable levels of safety in all cases. The work was limited to load combinations with snow, wind and permanent loads.

5.7 Conclusions

Two simplified safety formats have been proposed for simplifying the design of timber structures. Due to the timber specific load-duration effect on the material strength, the design of timber structures is more demanding compared to other construction materials. The first format consists of novel load combination rules maintaining the current modification factor values. On the contrary, the second format maintains the current combination rules while reducing the modification factor values to a single fixed one. Simplifications in design imply different design costs, different safety levels or both. For these reasons, the proposed formats have been calibrated in order to reach a satisfactory level of safety and limiting the increase in construction costs. The resulting calibrated formats greatly simplify the design. At the same time, they limit the additional costs and maintain (or increasing) the resulting safety level of the designed structures compared to the current Eurocodes.

The work at hand is expected to provide a generic framework applicable to further assessments and refinements of simplified safety formats. A higher degree of detail requires considering specific contexts including country-specific climates (see e.g. [100, 101]), load damage models, construction habits and normative requirements included in the National Annexes to the Eurocodes.

Although the investigations are strictly focusing on the Eurocodes, the proposed simplifications, concepts and calculations are in principle also applicable to other standards.

Acknowledgments

The work presented in this paper was partially funded by COST Action FP1402 "*Basis of Structural Design – from Research to Standards*" through the Short Term Scientific Mission (STSM) grant given to Michael Mikoschek, which allowed a successful and fruitful stay at the Norwegian University of Science and Technology.

Chapter 6 Paper V: On the Probabilistic Representation of Wind Climate for Calibration of Structural Design Standards

Paper

Authors: M. Baravalle[a], J. Köhler[a]

[a] Department of Structural Engineering, Norwegian University of Science and Technology, Trondheim

Submitted to an international scientific journal in April 2017.

6.1 Abstract

The article presents a contribution to the current debate on the probabilistic representation of the wind speed extremes for calibration of the partial safety factor covering wind action. The requirements for the probabilistic model are formulated. The Gumbel distribution is shown to represents best the 10-minutes mean wind velocity yearly maxima based on theoretical considerations and analyses of real data with different statistical techniques. Data from locations across a large geographical region indicate that the coefficient of variation of the distribution varies over the territory. A method is proposed for accounting this variation in order to calibrate a single partial safety factor for the whole territory. The distribution location is indirectly given in design standards through the georeferenced characteristic wind speed values. A solution for including the uncertainty affecting these values is suggested. The findings are implemented in an illustrative calibration exercise. The proposed methods and concepts might be applied to other environmental actions such as the snow loads.

Keywords: wind actions, probabilistic modelling, code calibration, partial safety factors, extremes.

6.2 Introduction

Modern structural design codes or standards as the Eurocodes [18] provide simple and safe basis for the design of structures. The simplicity is achieved mainly by the fact that structural safety is checked by comparing the design values of action effects with the design value of the resistance. Semi-probabilistic design equations in the Load Resistance Factor Design format (LRFD, see e.g. [5]) use partial safety factors (PSFs) applied on the resistance and action sides. These factors control the reliability of the corresponding design solutions. Their values are selected by code committees in order to achieve the desired level of safety [5, 7, 12, 25]. In the present version of the European Standards (The Eurocodes [18]), for example, one single partial safety factor ($\gamma_Q = 1.50$) is recommended for all unfavourable environmental variable actions such as snow and wind. However, it has been shown in [63] that a wind load dominated structure designed with $\gamma_Q = 1.50$ has a reliability lower than the Eurocode target, which requires a yearly target reliability index β_t equal to 4.70 (for consequence class 2). It also appears reasonable to differentiate the partial safety factors of the environmental actions, such as snow, wind and temperature, since these actions originate from different physical phenomena and are represented by different models involving various random variables.

Modern calibration methods are based on reliability theory considering fully probabilistic models [11, 12, 25]. If wind action is involved, this requires models representing the wind action on structures from the basic physical phenomenon (i.e. the geostrophic wind), and the representation of the governing variables, which may have a deterministic or a random nature. A widely accepted model is the Alan G. Davenport wind load chain [102] illustrated in Figure 6.1. Many semi-probabilistic codes such as the Eurocode 1 [15] represent wind actions on structures based on this model. The chain model includes five fundamental aspects, shortly: i) the *wind climate* comprising the weather systems generating geostrophic winds due to temperature gradients on the Earth surface; ii) the *influence of terrain,* which modifies the wind flow in the atmospheric boundary layer; iii) the *aerodynamic effects* depending on the structure shape; iv) the *dynamic effects* of the structure, and v) the *criteria* for verifying the predicted load models. More details are given in [103, 104].

Figure 6.1. Alan G. Davenport wind loading chain.

Although the model is widely accepted, challenges are still faced when defining the probabilistic models representing different aspects. In fact, several probabilistic models for representing the aspects in the Davenport chain have been proposed for calibration of design codes, see e.g. [105]. Therefore, this article discusses some open issues related to the stochastic modelling of the 10-minutes mean wind velocity yearly maxima ($V_{b,\max}$) used for representing the *wind climate* for code calibration purposes. In detail, the following aspects are addressed:

- *The selection of the type of distribution function representing* $V_{b,\max}$. This is still openly discussed in the scientific community since several distributions seem to fit well the available data, but they result in different calibrated safety factors due to the so-called tail sensitivity problem affecting the reliability analyses. Gumbel, Generalised extreme, Weibull, three-parameters Lognormal and other distributions are proposed in the literature, see for example [99, 104, 106].

- *The estimation of the distribution parameters that are relevant for the calibration of partial safety factors. These parameters are the coefficient of variation (COV) and the uncertainty on the distribution location*. The former should include the aleatory uncertainty (random nature of wind) and the epistemic uncertainties (originated by the lack of knowledge and a limited amount of information). The latter should include the uncertainties originated from the (surrogate) models utilised for creating the wind maps included in the design codes.
- *The representation and inclusion of the $V_{b,max}$ space-variation in the partial safety factor calibration*. This is required since a single partial safety factor for wind action is used for large geographical areas, although the wind climate is highly regional dependent.

The selection of the distribution type, the estimation of its parameters and their variation over a vast territory are addressed in Section 2 of the article. The second part of the article proposes a method for integrating, in the partial safety factor calibration, both the space-variation of the wind characteristics and the uncertainty on the distribution location. Wind speed records from five weather stations across Norway were analysed for catching the space-variation. The uncertainty on the distribution location was estimated based on measurements in several places over the territory. The findings are implemented in an illustrative calibration exercise.

6.3 Representation of the *wind climate*

6.3.1 Requirements of the model

The variation of the *wind climate* can be described by the wind velocity averaged over a period corresponding to frequencies in the spectral gap of the horizontal wind speed spectra [98, 103]. Periods of 10 minutes to 1 hour are typically used [107]. In the European Standard Eurocode 1 Part 1-4 (EC1-1-4) [15], the *wind climate* variation is represented by the basic wind velocity (V_b) which is defined as the 10-minutes mean wind velocity, irrespective of wind direction and time of the year, at 10 meters above the ground level in open terrain. The reliability assessment of a structure exposed to wind actions is a time-variant problem since the wind is varying in time. The reliability problem can be simplified to a time-invariant problem, if it can be assumed that the resistance is independent of the wind process, by the so-called time-integrated approach (see [5]) considering the V_b yearly maxima $V_{b,\max}$.

As any random variable, $V_{b,\max}$ might be represented by a distribution function, which is in general defined by the *type* of distribution and its *parameters*. The parameters determine the *location*, *scale* and *shape* of the distribution, while the *type* determines the tail behaviour.

The *type* of distribution and the *coefficient of variation* COV (i.e. the scale or scatter independent of the location) play an important role in reliability-based code calibration. This role can be observed in Eq. (6.1) where the partial safety factor for a Gumbel distributed variable X is determined using the design value method [18]. In the Equation, β_t is the target reliability, α is the sensitivity factor (see, e.g., [5]), p_k is the fractile corresponding to the characteristic value, $\Phi(\cdot)$ is the standard normal cumulative density function and $a_{EM} \cong 0.5772$ is the Euler-Mascheroni constant. The analytical expressions of the distributions functions utilised in the article are given in Section 6.7 at the end of the Chapter.

$$\gamma_X = \frac{6COV_X \ln\left\{-\ln\left[\Phi\left(\alpha\beta_t\right)\right]\right\} + 6a_{EM}\,COV_X - \pi\sqrt{6}}{6COV_X \ln\left\{-\ln\left[p_k\right]\right\} + 6a_{EM}\,COV_X - \pi\sqrt{6}} \tag{6.1}$$

The distributions *location* or magnitude is not affecting the partial safety factor when the extreme wind speeds are originated from a single physical phenomenon. In this case, standardised random variables can be used for PSF calibration as in [7]. For the wind, this is advantageous since the magnitude varies considerably in space due to different local climates and exposures. Design codes provide the regional magnitude or distribution location through the $V_{b,\max}$ characteristic value. In the Eurocode 1 [15], the characteristic value corresponds to the 98 % fractile (i.e. $p_k = 0.98$) of the yearly extreme value distribution and is referred to as the fundamental value of the basic wind velocity $v_{b,0}$. The regional distribution of $v_{b,0}$ is given in the Eurocode 1 National Annexes in the form of tables or maps. It has to be highlighted that the uncertainties affecting $v_{b,0}$ do influence the calibration of the partial safety factor. Thus, a good probabilistic representation of these uncertainties is of importance.

Correspondingly, in the authors' view, the distribution function representing $V_{b,\max}$ should have the following properties:

a) The distribution function type should represent $V_{b,\max}$ in the whole geographical application area of the standard at hand.
b) The distribution function type and parameters have to be validated by recorded time series over an adequate period, say, longer than 15 years [108].
c) The distribution function type must agree with the phenomena generating randomness.
d) The stochastic model should be suited for the reliability methods used in the calibration procedure. Usually, a parametric probability distribution is sought since the first order reliability method (FORM) is commonly used in calibration of partial safety factors because of its accuracy and its low computational cost.
e) It should include the statistical uncertainties which arise from the lack of data and the model uncertainties in order to estimate the predictive reliability index, see e.g. [109].
f) It should be accurate in the upper tail defined as the surroundings of the design point. The fractile corresponding to the design point is approximatively equal to $\Phi(\alpha \cdot \beta_t) = 5 \cdot 10^{-4}$, which is the fractile associated with the design point of the wind induced action obtained with $\alpha = 0.7$ and $\beta_t = 4.7$ according to [18].

In principle, different types of distributions can be fitted to the data upper tail, and the best one can be individuated by using statistical tools, probabilistic reasoning and judgment. Nevertheless, the point c) above is of particular importance especially due to the lack of observations in the surrounding of the design point. The application of extreme value theory (see e.g. [81, 110]) does limit the choice of distribution function type correspondingly, see also [111] for further discussion.

In the following, different analyses techniques are selected and utilised for individuating the distribution function representing the wind speed yearly maxima having all the properties listed above. These techniques differ in the basic assumptions, data considered and output. The techniques are divided into two main groups. The first group is based on the classical extreme value theory, which proposes different asymptotic distributions representing maxima under some specific assumptions that are discussed and assessed. The asymptotic convergence is improved when the parent distribution is considered. The distribution parameters are estimated from the yearly maxima, implying that one measurement for each year is considered only. The second group of techniques makes use of a larger amount of data by analysing the rate of threshold exceedance. These techniques allow to estimate the parameters as well as to evaluate the type of distribution that best represents the maxima.

The three-parameters lognormal (LN3) is proposed as a possible candidate distribution type for the representation of extreme wind phenomena [106]. The authors believe that, compared to other distributions discussed later, the distribution provides just a better fit to some samples of data due to the third parameter. In any case, the goodness of fit in the upper tail region of interest cannot be assessed due to lack of data. Nevertheless, the 3LN distribution was excluded because the distribution representing the N-years maxima ($V_{b,\max N}$) derived from LN3-distributed yearly maxima, as $F_{V_{b,\max N}} = F_{V_{b,\max}}^{N}$, is not of the type LN3. This is neither reasonable nor practicable since the type of distribution should not change with the selected reference period (for reference periods that are long enough to ensure independence between maxima). Therefore, this distribution is excluded in this paper since no theoretical background is found supporting its use.

6.3.2 Data set

Records from the Norwegian Meteorological Institute (MET) [112] of the highest hourly and 6-hours 10-minutes mean wind speed (MET code: *FX_1* and *FX*, respectively) were analysed. In detail, the 10-minutes mean wind speed was measured for each 10-minutes, and only the highest in each hour or in each 6-hours-period was recorded. *FX* records cover time periods between 25 and 58 years long. The data are of poor quality since the records are affected by rough rounding especially before 1980 (see Table 6.1). Nevertheless, no better data are available in Norway for periods long enough to support the probabilistic modelling of yearly maxima. Five stations across Norway were selected (see Figure 6.2) for representing different geographical regions. For illustration purposes, the data for Torsvåg Fyr (TOR) are reported in Table 6.1. *FX_1* records (Figure 6.3) are more accurate since rounded at $\pm 0.05\,m/s\,(=0.1kn)$ but they are available for periods not longer than 22 years. In general, a good agreement between *FX* and *FX_1* was observed in periods covered by both datasets. The data were quality checked, and two corrections were done for TOR data that included two entries equal to $45.2\,m/s$. These measurements were considered erroneous because of the extreme magnitude and due to the absence of reports on major storms in the corresponding period. Linear interpolation between previous and posterior entries was used for correcting the corresponding records.

Figure 6.2. Weather stations (from Google My Maps).

Table 6.1. FX values for TOR in m/s converted from knots (kn) (rounding: $\pm 2.31\,m/s\,(=4.5kn)$, $^{\S}\pm 1.80\,m/s\,(=3.5kn)$, $\pm 0.26\,m/s\,(=0.5kn)$ *otherwise).*

Year	v_b	Year	v_b	Year	v_b	Year	v_b
1957	26.75*	1969	22.64§	1981	30.87§	1993	36.01
1958	30.87§	1970	26.75*	1982	27.78	1994	22.64
1959	34.98*	1971	26.75*	1983	25.72	1995	26.75
1960	22.64§	1972	26.75*	1984	27.78	1996	34.98
1961	22.64§	1973	26.75*	1985	26.75	1997	34.98
1962	22.64§	1974	30.87§	1986	24.18	1998	27.78
1963	26.75*	1975	26.75*	1987	26.75	1999	22.12
1964	22.64§	1976	26.75*	1988	25.72	2000	29.32
1965	26.75*	1977	26.75*	1989	33.95	2001	26.24
1966	22.64§	1978	26.75*	1990	34.98	2002	24.18
1967	22.64§	1979	22.64§	1991	39.10	2003	26.75
1968	30.87§	1980	26.75*	1992	25.21	2004	23.15

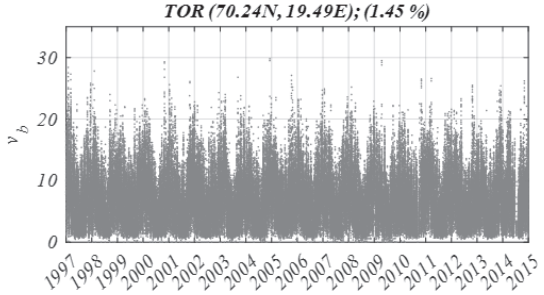

Figure 6.3. FX_1 series for TOR station with station coordinates and percentage of missing measurements (units: m/s).

6.3.3 Assumptions and limitations

The data were analysed under the following assumptions, limitations and simplifications.

a) Data from one location were considered sampled from the same population although the physical phenomena producing extreme wind velocity realisations might be different (e.g. extra-tropical cyclones, thunderstorms, etc.). This simplification was set to be consistent with the level of detail of the current version of the Eurocode 1, which includes a unique model for wind loads based on extra-tropical cyclone generated winds.

b) The *wind climate* was considered independent from the *influence of terrain* since the latter creates turbulences characterised by temporal frequencies that differ from the wind climate frequencies by one or two orders of magnitude, see e.g. [104]. This approximation is also considered in the Eurocode 1 [15].

c) Despite the fact that wind direction is important when the structural resistance and the wind are direction-dependent, see e.g. [113], wind directionality was not considered in the analyses. The reasons are that i) considering structures with direction-independent resistance only (or equivalently considering the wind worst direction) is conservative; ii)

directionality is highly location-dependent reducing the generality of the model which is sought; iii) the basic wind velocity in the Eurocode 1 is not conditional on a specific wind direction that is accounted by the direction factor.

d) The number of missing measurements is low for all the stations (see Figure 6.3) and it was assumed that the lack of registration was not correlated to extreme wind speeds.

e) The five selected measurement locations are located in small islands close to the shore or on the coast. The locations are surrounded by open terrain and by open sea. The latter has a lower roughness compared to open country. Nevertheless, when extreme wind speeds are registered, the sea is assumed in "ultimate limit state" and, hence, presenting the same roughness as the open country (see [107] Annex C). Therefore, the surroundings of the measuring stations are assumed to have a terrain roughness equivalent to the category II of the Eurocode 1, which is the reference category for deriving the basic wind velocity (V_b) according to [15].

f) The effects of the climate change on the wind speed are not considered, i.e. the wind is assumed to be an ergodic process. Although the climate change is predicted to affect the wind speed in future (see e.g. [114]), its inclusion in the design standards should involve several disciplines [30] and was not part of the current study.

6.3.4 Classical extreme value theory

According to the classical extreme value theory, the maxima of independent, identically distributed variables tend to a Gumbel distribution (see Eq. (6.11)) under the following assumptions [110]: *i*) the number of independent realisations is constant, and *ii*) the parent distribution has an exponential tail. These assumptions do not seem to be strictly verified for the 10-minutes mean wind speed since the number of independent weather systems and the parent distribution representing the 10-minutes mean wind speed differ from year to year. However, for practical analyses, the annual maxima present a linear behaviour in the Gumbel plot meaning that the assumptions are not strongly violated [108] and suggesting the Gumbel as the asymptotic distribution. The most accurate method for fitting the Gumbel distribution to the data is the so-called Gumbel-Lieblein method as shown in [115]. Nevertheless, the distribution parameters were estimated in this work utilizing the maximum likelihood (ML) method since it allows accounting for the rough rounding characterising the data at hand. The likelihood is formulated as a function of the distribution parameters conditional to the observations and the selected distribution function. The validity of the assumed distribution can be assessed based on the magnitude of the maximum (also relative to the maxima that correspond to different assumed distribution types). The deviation of the (unknown) real distribution is partly reflected (and considered) by the covariance of the parameters. In addition, the ML method provides the estimates of the parameters uncertainty which is integrated into the predictive distribution $f_X(x)$ in Eq. (6.2),

$$f_X(x) = \int_{\boldsymbol{\Theta}} f_{X|\boldsymbol{\Theta}}(x \mid \boldsymbol{\theta})\, f_{\boldsymbol{\Theta}}(\boldsymbol{\theta})\, d\boldsymbol{\theta} \tag{6.2}$$

where: $\boldsymbol{\Theta}$ is a vector with the distribution parameters and $f_{\boldsymbol{\Theta}}(\boldsymbol{\theta})$ is the joint density function representing the parameter uncertainties. These uncertainties might be significant when the data are limited in number or have poor quality. The ML method also allows considering the rounding and the left censoring by using the likelihood function reported in Eq. (6.12). The use

of left censored data allows to fit better the upper tail but it requires an adequate number of years of records for having a sufficient number of observations in the tail. The selection of the censoring threshold is not trivial. In fact, high thresholds lead to significant variance in the estimates while low thresholds produce estimations biased toward the central part of the distribution.

The distributions fitted to the measurements in TOR are illustrated in Figure 6.4. Data censoring improved the upper tail fit, and simultaneously increased the statistical uncertainty leading to a fatter tail of the predictive distribution. The predictive distributions were obtained with Eq. (6.2). The integral was approximated numerically by Monte Carlo (MC) sampling. Consequently, the predictive could not be represented in a closed form. Therefore, its upper tail was approximated by a Gumbel distribution obtained fitting the highest 30 % of the sampled values (i.e. the values characterised by $-\ln\left(-\ln\left(F_{V_{b,\max}}\right)\right) > 1.0$ in Figure 6.4) since these data were observed lying on a straight line in the Gumbel probability plot. The estimated *COVs* of the Gumbel distribution are displayed in Figure 6.5 as a function of the censoring threshold v_c. Their order of magnitude agrees with the values given in [13]. *FX* data were used only when the more precise *FX_1* data were missing. The largest censoring thresholds were approximatively corresponding to the 70 % fractile values.

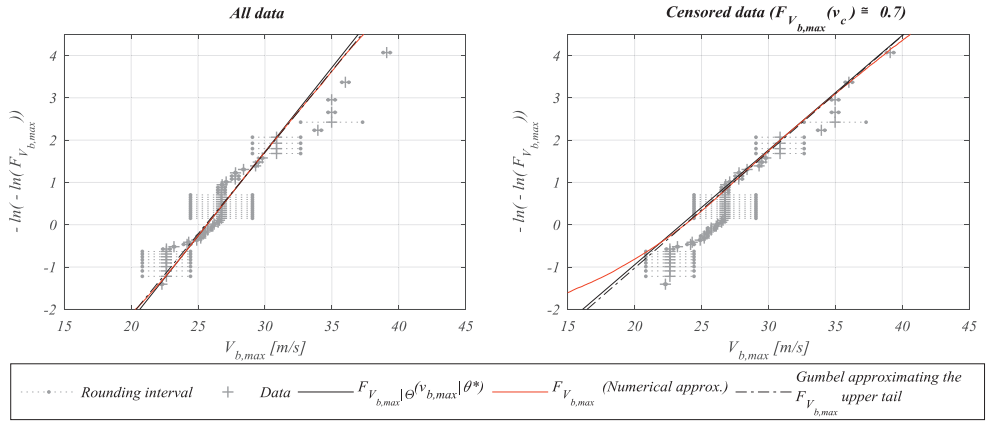

Figure 6.4. Gumbel probability plot with measured data (FX and FX_1) for weather station TOR and fitted Gumbel distributions. Data sorted according to the central values of the rounding intervals. Predictive distributions approximated by Montecarlo sampling with 10^5 simulations.

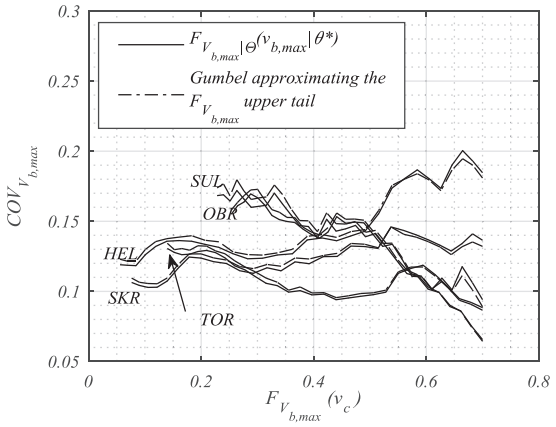

Figure 6.5. $COV_{V_{b,\max}}$ for Gumbel distributions estimated varying left-censoring threshold v_c on FX and FX_1.

6.3.4.1 Classical extreme value theory considering parent distribution

A significant amount of information contained in the weather data is not utilised when yearly maxima are analysed. Additional information can be included considering the underlying statistic. The probability distribution representing the 10-minutes mean wind speeds (i.e. the basic wind velocity V_b) is referred to as the "parent distribution" in the following. The parent distribution is the distribution from where the extreme wind speeds are "sampled". In Europe, the distribution that best represents V_b is the Weibull (see Eq. (6.14)) with shape parameter $b_w(V_b) \in [1.8, 2.2]$ as extensively reported in the literature and supported theoretically by the study of Harris and Cook [116]. It follows that the so-called preconditioned random variable $V_b^{b_w}$ is exponentially distributed (i.e. Weibull distributed with unitary shape parameter). The maxima of the exponentially distributed random variable $V_b^{b_w}$ converge faster than V_b to the Gumbel distribution. Consequently, the "*penultimate*" extreme value distribution for $V_b^{b_w}$ corresponds to the "*ultimate one*" [117] meaning that the error when using Gumbel asymptote is reduced. Cook introduced first this procedure considering a preconditioning parameter equal to 2 [24]. The obtained variable, V_b^2, is proportional to the 10-minutes mean wind pressure ($1/2\,\rho V_b^2$) and is represented by a Weibull distribution with $b_w(V_b^2) = b_w(V_b)/2$. $b_w(V_b^2)$ is close to one for $b_w(V_b) \in [1.8, 2.2]$ and, hence, V_b^2 is close to exponential distributed.

The Gumbel distribution *COVs* estimated from the preconditioned data were around double than for non-preconditioned data, see Figure 6.6. In addition, it was observed that the *COV* variation for different censoring thresholds and the variation among different weather stations were of the same order of magnitude. This made the selection of the censoring threshold less critical as a generalised representation of the *COV* was sought. The change of trends in Figure 6.5 and Figure 6.6 shows that the characteristics of the upper tail are caught by censoring fractiles above, approximatively, 50 %. For the data analysed, a censoring threshold corresponding to fractiles around 60 to 70 % was judged to balance the statistical uncertainty on the parameter estimates and the accuracy in the upper tail. In general, higher censoring thresholds might be selected when longer time series are available and data have better quality.

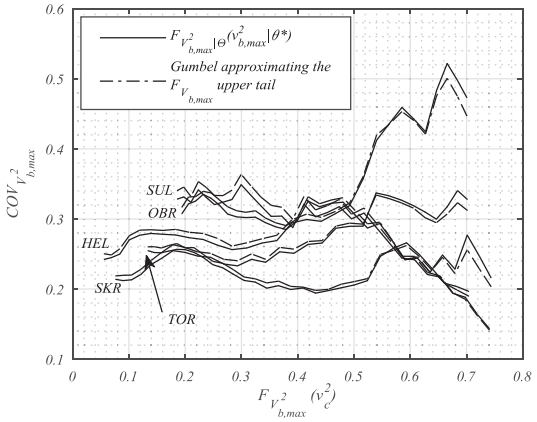

Figure 6.6. $COV_{V^2_{b,max}}$ for Gumbel distributions estimated varying left-censoring threshold v_c on FX and FX_1. Predictive distributions approximated by Montecarlo sampling with 10^5 simulations.

The knowledge on the parent distribution allows estimating the error affecting the use of asymptotic distributions. Assuming that the Weibull parent distribution F_X is known, the (theoretically) exact distribution of maxima is obtained from Eq. (6.3), where r is the number of independent events per years.

$$F_{X_{max}}(x) = \left[F_X(x \mid a_w, b_w)\right]^r \tag{6.3}$$

This derivation is not directly used since small errors on r, b_w, a_w lead to significant errors in $F_{X_{max}}$. Nevertheless, Eq. (6.3) can be utilised for estimating the errors induced by approximating the exact $F_{X_{max}}$ with a Gumbel distribution. The resulting error at the design point is depicted Figure 6.7 (reproduced after [117]). The error is in the order of $\pm 2\%$ for a Weibull distributed variate with $b_w \approx 1$ like V_b^2, and much larger for a variate with $b_w \approx 2$ like V_b. Therefore, it can be concluded that the use of the preconditioned wind speed is advantageous for calibration of codified design since the convergence error on the part of the upper tail of interest is almost eliminated. The values of $COV_{V^2_{b,max}}$ obtained from Eq. (6.3) are depicted in Figure 6.8 and are compared with the Gumbel asymptote obtained with asymptotic parameters given in [118]. They agree quite well with the values obtained in the data analysis, see Figure 6.5. This verifies the hierarchical model which considers Weibull parent and Gumbel maxima. More importantly, the results obtained from this hierarchical model (Figure 6.8) suggest that the $COV_{V^2_{b,max}}$ values over the territory of interest cannot differ much from the ones obtained analysing the five selected locations. Therefore, the use of few representative locations is sufficient for individuating a generic representation of the wind climate.

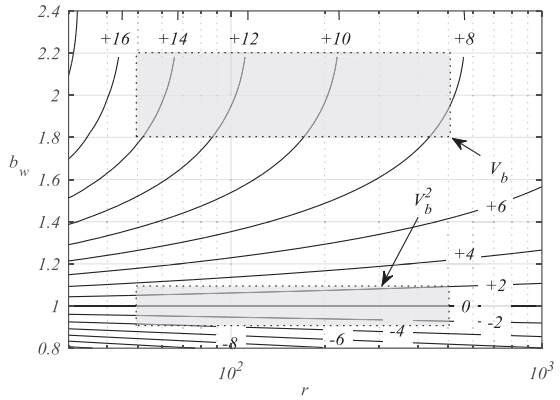

Figure 6.7. Error in percentage affecting the design value $x_d = F_{X_{max}}^{-1}\left(\Phi\left(\alpha \cdot \beta_t\right)\right)$ *for* $\alpha = 0.7$ *and* $\beta_t = 4.7$*, overestimation positive. Grey areas represent possible domains of* r *and* b_w *for wind speed.*

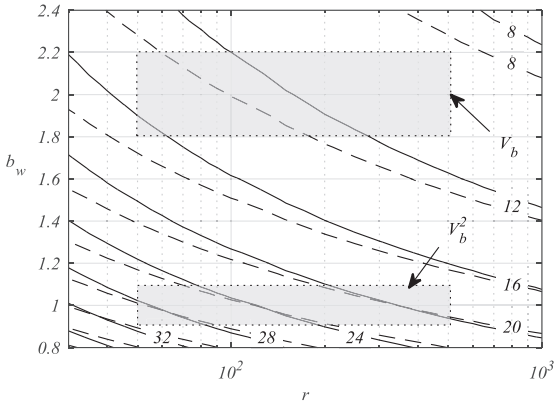

Figure 6.8. Yearly maxima distribution COV *from exact formula Eq. (6.3) (dashed line) and Gumbel asymptotic approximation (continuous line). Grey areas represent possible domains of* r *and* b_w *for wind speed.*

6.3.4.2 Generalised extreme value distribution

A more general application for the analysis of extreme wind velocity data makes use of the Generalised Extreme Value distribution which includes three types of distributions (Gumbel, Fréchet and Weibull maxima) characterised by three different tail behaviours. The data indicates which type of distribution is better through inference on the shape parameter (ξ_{GEV}) (see e.g. [81]). The uncertainty on the estimated parameter ($\hat{\xi}_{GEV}$) can be interpreted as the uncertainty on the distribution and tail type. It has to be noted that, when the statistical uncertainty is neglected, the GEV distribution always fits better the data compared with the Gumbel distribution due to the third additional parameter. Nevertheless, due to the asymptotic property of GEV, convergence errors still affect the estimate, see e.g. [117]. As reported in the

literature, $\xi_{GEV} < 0$ is typical for 10-minutes mean wind speed yearly maxima, implying that the distribution tail converges to a limit value being the domain right-bounded $\left(-\infty; a - b/\xi_{GEV}\right]$.

The GEV shape parameters estimated from the data were affected by high uncertainty. A standard deviation in the order of 0.3 was obtained. In addition, some most likely values of the shape parameters were positive (see Table 6.2) corresponding to distributions defined on a lower bounded domain. Unreasonable and very unstable COV and $\hat{\xi}_{GEV}$ were estimated from censored data with different censoring threshold. All these results were believed to be a consequence of the fact that the limited number of data points and their low quality led to considerably high statistical uncertainty on the parameter estimates. In fact, it is shown in the literature that a limited amount of data leads to unreasonable GEV parameters [119]. This deficiency is related to the ML estimation. In case the GEV distribution was to be used, the Bayesian estimation could have overcome this difficulty by selecting appropriate priors. However, this technique was not applied since the GEV distribution was excluded also based on the analyses presented in the remaining part of the article.

The results obtained from non-censored data need careful interpretation. The authors believe that GEV provides only a better empirical fit to the data for two reasons. The first is that the GEV distribution always provided greater Akaike Information Criteria (AIC) scores compared to the Gumbel and, thus, Gumbel is to be preferred [120]. The largest differences in AIC scores were observed for censored data. In detail, $AIC = 2k - 2\ln\left(\hat{L}\left(x \mid \hat{\boldsymbol{\theta}}, M\right)\right)$, where M is the selected statistical model with k parameters (e.g., Gumbel with $k = 2$, and GEV with $k = 3$), and $\hat{L}\left(x \mid \hat{\boldsymbol{\theta}}, M\right)$ is the maximum likelihood of the data x (corresponding to the parameters $\hat{\boldsymbol{\theta}}$ estimated with the ML). The second reason is that, as also commented in [117], the domain limits for GEV distributions representing $V_{b,\max}^2$ and $V_{b,max}$ were inconsistent, and did not correspond to the natural domain limits of the variables, see Table 2. For example, for OBR location, the parameters estimated from $V_{b,max}$ gave a domain upper bound equal to $44.1 m/s$, while the estimates from $V_{b,\max}^2$ gave an upper bound of $2746\left(m/s\right)^2 = (52.4\, m/s)^2$. Further, in [117] it was proven that Weibull parents with $b_w = 2$ and 1 give $\xi_{GEV} \cong -0.1$ and 0, respectively. The fact that the average values of $\hat{\xi}_{GEV}$ in Table 6.2 are very close to these values and that all the $\hat{\xi}_{GEV}$ 90 % confidence bounds contain -0.1 can be seen as an indirect proof that the assumption of a Weibull distributed parent and therefore asymptotically Gumbel distributed maxima leads to a good representation of data. Based on the observations above, the use of GEV distribution is excluded.

Table 6.2. Estimated GEV shape parameter and coefficient of variation from FX and FX_1.

	GEV – $V_{b,max}$			GEV – $V_{b,\max}^2$		
	$\hat{\xi}_{GEV}$	COV (conditional)	Domain	$\hat{\xi}_{GEV}$	COV (conditional)	Domain
HEL	-0.313	0.14	$(-\infty; 37.3]$	-0.256	0.26	$(-\infty; +1391]$
OBR	-0.191	0.13	$(-\infty; +44.1]$	-0.087	0.26	$(-\infty; +2746]$
SKR	0.068	0.11	$[-6.1; +\infty)$	0.161	0.25	$[-33.1; +\infty)$
TOR	0.135	0.14	$[+22.4; +\infty)$	0.234	0.32	$[+134.2; +\infty)$
SUL	-0.326	0.14	$(-\infty; +41.5]$	-0.209	0.28	$(-\infty; +1942]$

6.3.5 Threshold exceedance analysis

The analysis of yearly maxima excludes a significant amount of available data in contrast with methods based on analysing exceedances, exceedance rates and peaks over threshold as illustrated in Figure 6.9. Certain results are reported in this Section for the weather station TOR only, similar trends and behaviours were observed for the other four stations.

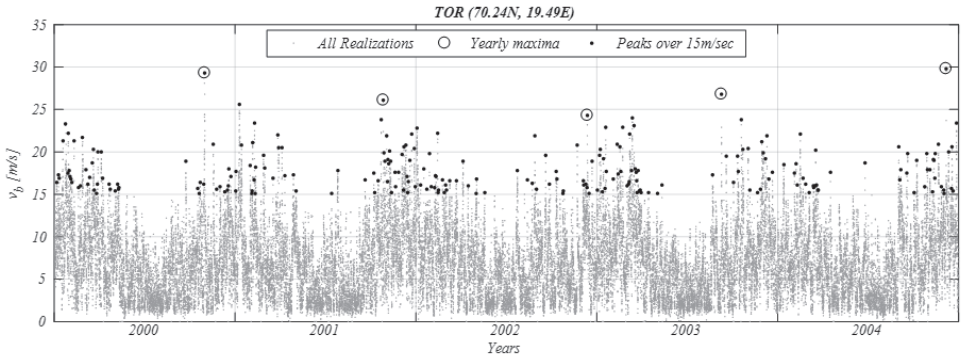

Figure 6.9. FX_1 time-series between 01-01-2000 and 31-12-2004 with all recorded values, yearly maxima and independent peaks over the threshold $v_t = 15\,m/\sec$.

6.3.5.1 The mean upcrossing rate

The mean upcrossing rate $\bar{\eta}^+(v_t)$ functional relationship with the threshold v_t provides significant information about the distribution of maxima. The starting point is Eq. (6.4) which relates $F_{V_{b,max}}$ to $\bar{\eta}^+(v_t)$, where T is the reference period equal to one year.

$$F_{V_{b,max}}(v_t) = \exp\left\{-\bar{\eta}^+(v_t)\cdot T\right\} \tag{6.4}$$

The up-crossing rate for large enough thresholds $v_t > v_{t,0}$ is usually related to v_t through a function of the form $\bar{\eta}^+(v_t) = \tilde{q}(v_t)\exp\left\{-a(v_t-b)^c\right\}$; where a,b,c are constants and $\tilde{q}(v_t)$ is near-constant [121]. The case $c=1$ gives $\ln\left(\bar{\eta}^+(v_t)\right)$ linear in v_t and corresponds to Gumbel asymptote. On the contrary, cases with $c \neq 1$ represent sub-asymptotic behaviours.

Up-crossings of a threshold are in general dependent. De-clustering is performed for extracting independent events considering clusters to start (and end) when at least n_c consecutive values are below a threshold v_t, see e.g. Coles [81]. The average number of up-crossings (or cluster) over a defined period (e.g., one year) is referred to as the average conditional exceedance rate (ACER) $\varepsilon_{n_c}(v_t)$. The empirical ACER functions are estimated from the data by the ACER method and can be used instead of $\bar{\eta}^+(v_t)$ in the above equations [122].

The plots of $\ln\left(\varepsilon_{n_c}(v_t)\right)$ versus v_t for the analysed data show the dependencies between up-crossings. It was observed that $n_c > 4$ eliminates the dependency without affecting the upper tail, see Figure 6.10. Thus, upcrossings separated by 4 or more hours are considered independent or, equivalently, belonging to different storm events. On the contrary, upcrossings separated by less than 4 hours might belong to the same storm and thus be dependent. This is in accordance with the average duration of a storm that is indicated in [13] to be in average 8 hours. For $n_c = 4$ the fitted line had $c \neq 1$ for V_b meaning sub-asymptotic behaviour and $c \cong 1$

for V_b^2. This further proves that the wind speed maxima are sub-asymptotic while the preconditioned wind speed converges to the asymptote in the tail.

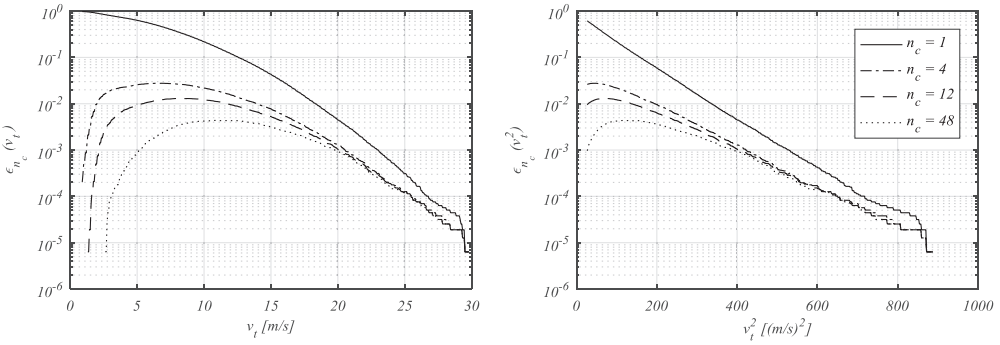

Figure 6.10. Logarithm of the ACER versus threshold for wind speed (right) and wind speed squared (left) at TOR weather station obtained with the Matlab-based free software [123]. Estimated parameters with $n_c = 4$ *for* v_t*:* $a = 0.20$, $b = 13.58$, $c = 1.27$, $q = 0.01$*; and for* v_t^2*:* $a = 0.01$, $b = 64.59$, $c = 1.00$, $q = 0.04$.

6.3.5.2 Peaks over threshold

Threshold exceedance analysis can also be utilised for evaluating the use of the GEV distribution and for estimating its parameters. In detail, the GEV shape parameter ξ_{GEV} is estimated by the Pickands method [124] analysing the peaks over threshold (POT). For large enough thresholds $v_t > v_{t,0}$ and under the assumptions that the realisations are independent, identically distributed and their maxima have a GEV domain of attraction, the distribution function of the exceedance $Y = V_b - v_t$ conditional on $V_b > v_t$ is represented by a generalised Pareto distribution (GPD). Pickands [124] proved that the GPD and the GEV distribution have the same shape parameter $\xi_{GEV} \equiv \xi_{GPD}$ asymptotically. Maximum likelihood estimates of $\hat{\xi}_{GPD}$ are reported in plots A in Figure 6.11. Data dependencies were eliminated by declustering data as described before. In this case, the largest value in each cluster was kept while the rest were discarded.

The POT analysis presents the non-trivial task of selecting the right threshold v_t. Different methods for threshold selection are proposed in the literature, see e.g. [125]. As discussed in [81], the following is valid for thresholds $v_t > v_{t,0}$: *i*) the mean of the exceedances $\bar{y}$ is linear in v_t; *ii*) $\hat{\xi}_{GPD}$ is near-constant and the Pareto scale parameter $\bar{\sigma}$ is linear in v_t; *iii*) the reparametrized GPD scale parameter $\sigma^* = \bar{\sigma}_{v_t} - \hat{\xi}_{GPD} v_t$ is constant. These three points can be used inversely for finding the appropriate $v_{t,0}$. For the TOR data, a minimum threshold $v_{t,0}$ of approximatively 15 m/sec was judged to satisfy all these three requirements as illustrated in plots B, C and D in Figure 6.11. Thresholds v_t larger than, but close to, $v_{t,0}$ should be selected for balancing statistical uncertainty and precision in the upper tail. Trends exactly equal to the theoretical ones cannot be expected due to inherent variability and the limited amount of data. The assessment of the appropriate threshold must be performed for each case and may be highly subjective and arduous in real problems.

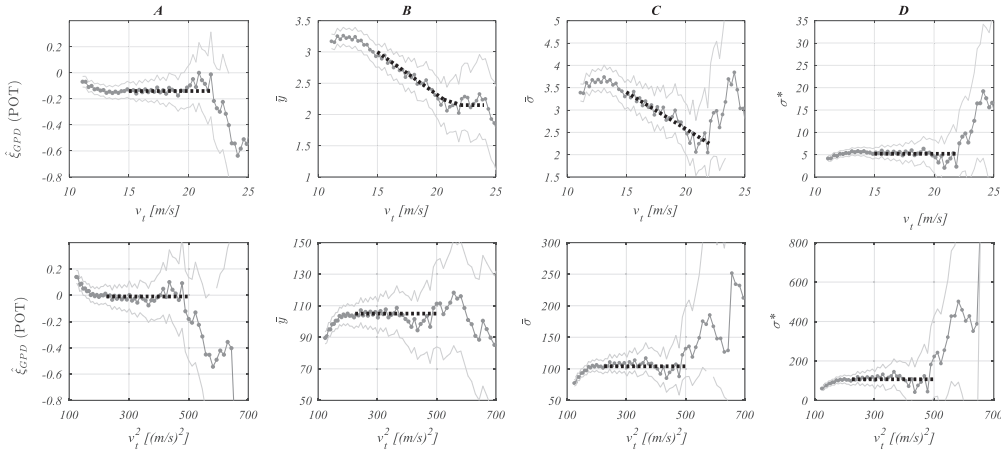

Figure 6.11. ML estimates of $\hat{\xi}_{GPD}$ from POT method (A) and plots for selecting threshold $v_{t,0}$ (B, C and D) for wind speed (top) and wind speed squared (bottom) for weather station TOR. 90 % confidence intervals drawn with light grey lines for illustrating the statistical uncertainty; dotted lines were drawn manually for representing identified trends.

The plots in Figure 6.11 present trends that further support the selection of the Gumbel for representing the extremes of a Weibull parent. In details, the signs of $\partial\overline{y}/\partial v_t$ are equal to $\hat{\xi}_{GPD}$ as expected when the parent is Weibull as demonstrated in [126]; $\partial\overline{y}/\partial v_t$ for V_b decreases to zero with increasing v_t, and it is (near-)constant for V_b^2. This is in accordance with the relations derived in [117] based on the assumption of Weibull parent, and the $\hat{\xi}_{GPD}$ is negative for V_b (around - 0.1) and close to zero for V_b^2 reflecting the behaviour shown in [117]. In conclusion, all results from exceedance analyses were consistent with the assumption of Weibull parent and indicated Gumbel for representing maxima, as concluded from the analysis of yearly extremes.

An alternative approach for identifying the distribution *type* uses the tail heaviness index that is proportional to the negative of the curvature of the minus log-exceedance plot [118, 127]. In the authors' view, the method is a useful decision-making tool for selecting the distribution representing maxima when lacking information on the underlying phenomenon and theoretical background supporting one or another distribution type. Consequently, application of this method was not documented in this article since the knowledge on the underlying phenomenon originating wind extremes allowed proofing theoretically that the Gumbel distribution is best for representing maxima.

6.4 Inclusion of wind climate spatial variation in code calibration

The first part of the article shows that the partial safety factor depends on the *COV* (see Eq. (6.1)) and that the *COV* varies in space. At the same time, semi-probabilistic codes typically include only one partial safety factor for the wind actions over the entire territory. Therefore, this Section proposes a framework for calibrating the wind partial safety factor and suggests a method for accounting the space-variation of the climatic actions.

6.4.1 Representation of the wind action on structures

Reliability-based calibration of the wind partial safety factor uses reliability analyses where the wind action is represented probabilistically. The models given in [13], that have been used in other calibration works [99], were adopted in this work. The model is based on the Alan G. Davenport wind load chain illustrated in Figure 6.1. The wind action on structure yearly maxima (W_{max}) is modelled as $W_{max} = 1/2\,\rho C_d\, C_r\, C_a\, C_g\, V_{b,max}^2$. The air density ($\rho$) is considered deterministic since its scatter is small at large wind speeds [128]. The *influence of the terrain* is accounted by the roughness factor C_r and by the gust factor C_g. The former describes the variation of the mean velocity pressure with height, the latter is the ratio between the peak velocity pressure to the mean velocity pressure. The *aerodynamic effect* is accounted for by the shape factor C_a that is named external pressure coefficient C_{pe} when W_{max} is the external pressure. Similarly, the internal pressure and friction are obtained with the corresponding factors C_{pi} and C_{fr}. The structural *dynamic effect* is accounted for by the dynamic factor C_d. The C-factors are affected by aleatory and epistemic uncertainties, the details on the stochastic models representing them can be found in [13].

6.4.2 Reliability-based calibration of partial safety factors

Following the methodology proposed by the JCSS [7], the partial safety factor (PSF) calibration is performed using a normalised and generalised limit state function as the one given in Eq. (6.5). The event of structural failure is characterised by $l(\mathbf{x}) < 0$.

$$l\left(x_R, r, g, c_d, c_{pe}, c_g, c_r, v_{b,max}^2\right) = z\, x_R\, r - \left[\delta g + (1-\delta) x_Q c_d c_{pe}\, c_g\, c_r\, v_{b,max}^2\right] \tag{6.5}$$

In the limit state function, δ is a parameter representing different proportions between permanent action g and wind action w, r is the material property dominating the failure mode, x_R is the resistance model uncertainty, x_Q the wind-load model uncertainty and z is the design variable governing the failure mode. This limit state function is generalised, i.e. it represents, with a satisfactory level of detail, different failure modes. For example, failure of a timber beam in bending is represented by r being the timber bending strength and x_R the model uncertainty on the bending capacity of timber elements. In addition, the limit state function is normalized, i.e. the random variables R, G and $V_{b,\max}^2$ have unitary mean. This allows for the simultaneous consideration of materials with different grades, and different load intensities. The normalisation and scaling of random variables, as for example by the factor $1/2\,\rho$, are 'absorbed' by z and simplify the problem without affecting the calibration outcome as discussed in the introduction.

The generic structural element is designed with a semi-probabilistic approach. An example of a design equation corresponding to the limit state equation in Eq. (6.5) is given in Eq. (6.6), where the Eurocode 0 [18] safety format is used. $\gamma_M, \gamma_G, \gamma_Q$ are the material, permanent action and variable action partial safety factors, respectively. The subscript "k" indicates the characteristic value of the random variable.

$$z = z\left(\gamma_M, \gamma_G, \gamma_Q\right) = \frac{\gamma_M}{r_k}\left[\delta g_k\, \gamma_G + (1-\delta)\gamma_Q\, c_{d,k} c_{pe,k}\, c_{g,k} c_{r,k} v_{b,0}^2\right] \tag{6.6}$$

In EC1-1-4, for example, the fundamental value of the basic wind velocity $v_{b,0}$ or velocity squared $v_{b,0}^2$ is defined as the 98 % fractile of $V_{b,\max}$ or $V_{b,\max}^2$, respectively. $v_{b,0}^2$ is calculated in Eq. (6.7) for the normalised $V_{b,\max}^2$ (i.e. $\mu_{V_{b,max}^2} = 1.00$) and a given geographical location (i.e.

known $COV_{V^2_{b,\max}}$). The statistical uncertainty is integrated into the distribution and therefore included in the coefficient of variation hereinafter.

$$v^2_{b,0} = v^2_{b,0}\left(COV_{V^2_{b,max}}\right) = -\frac{\left(6a_{EM}COV_{V^2_{b,max}} + 6\ln\left(-\ln\left(0.98\right)\right)COV_{V^2_{b,max}} - \pi\sqrt{6}\right)}{\sqrt{6}\pi} \tag{6.7}$$

The reliability index β associated with the limit state function in Eq. (6.5) is a function of the partial safety factors through the design parameter z, i.e. $\beta = \beta\left(z\left(\boldsymbol{\gamma}\right)\right)$. The calibrated safety factors are obtained imposing $\beta\left(z\left(\boldsymbol{\gamma}\right)\right) \equiv \beta_t$, where β_t is the target reliability index. When several design situations are considered simultaneously, calibration is performed by minimising the penalty function subject to the partial safety factors. Further details on calibration of design standards can be found in [5, 7, 11, 25, 45].

6.4.3 Wind action space-variation

Code calibration is generally performed for large interregional areas that correspond to the validity domain of the code format to be calibrated. In this area, the $COV_{V^2_{b,\max}}$ is varying as shown in Section 6.3 and this has to be taken into account in the calibration process. A possible strategy for providing a unique safety factor could be to choose conservatively a large $COV_{V^2_{b,\max}}$ which results in a large γ_Q. The selection of the largest value over the entire domain covered by the code at hand includes some obvious difficulties. Alternatively, the variation of the $COV_{V^2_{b,\max}}$ in space is accounted by treating the $COV_{V^2_{b,\max}}$ explicitly as a random variable in the limit state function. The variation of the $COV_{V^2_{b,\max}}$ can include not only the variation over the space but also the statistical uncertainty and the uncertainty related to the selection of the appropriate censoring threshold. The new limit state function is given in Eq. (6.8) was obtained by including Eq. (6.7) in Eq. (6.6) and by expressing the random variable $V^2_{b,\max}$ in Eq. (6.5) as a function of a normal standard variable U and the distribution parameters a and b.

$$l\left(x_R, r, g, c_d, c_{pe}, c_g, c_r, x_a, u\right) = z\, x_R\, r - \left[\delta g + \left(1-\delta\right) x_Q c_d c_{pe}\, c_g\, c_r \left[x_a a - b\ln\left(-\ln\left(\Phi\left(u\right)\right)\right)\right]\right] \tag{6.8}$$

The parameters a and b for the normalised $V^2_{b,\max}$ are a function of the random variable $COV_{V^2_{b,\max}}$: $b = COV_{V^2_{b,max}}\sqrt{6}/\pi$ and $a = 1 - a_{EM}COV_{V^2_{b,max}}\sqrt{6}/\pi$. It is highlighted that the $COV_{V^2_{b,\max}}$ enters the limit state function through both the design parameter and the wind action term. The $v_{b,0}$ (or $v^2_{b,0}$) value for a specific location is, indeed, obtained from Eq. (6.7) with the $COV_{V^2_{b,\max}}$ characterising the maxima in that location.

The random variable X_a in Eq. (6.8) represents the uncertainty on the location of the distribution function $F_{V^2_{b,\max}}$ or, equivalently, the uncertainty on the fundamental value of the basic wind velocity squared $v^2_{b,0}$ provided in wind maps and tables. Therefore, X_a depends on the model used by the code committees for deriving the $v_{b,0}$ or $v^2_{b,0}$ values over the territory. Statistical analyses of wind speed in several locations across the territory, or surrogate models (as in [129]) might be used to make the wind maps or the tables with $v_{b,0}$ or $v^2_{b,0}$ values.

6.4.4 Calibration example

A calibration example is reported in this Section for illustrating the application of the findings. The calibration was performed considering the design equation in Eq. (6.6) and the limit state function in Eq. (6.8). The probabilistic models and the PSFs are summarized in Table 6.3 at the end of this Chapter. All variables were assumed uncorrelated. Only structures loaded

by permanent load and external wind pressure without dynamic effects were considered, since they represent the most common design situations.

The partial safety factor covering wind actions for the Norwegian territory was calibrated. Therefore, the uncertainties X_a affecting the $v_{b,0}^2$ values corresponding to the $v_{b,0}$ values given in the Norwegian National Annex to EC1-1-4 were estimated. The $v_{b,0}$ values for the Norwegian territory were derived in [129] based on hindcast data collected at defined grid points over the North Sea, Norwegian Sea and Barents Sea for the period 1955-1997. In detail, sea surface pressure data were used to produce geostrophic wind data, and from the data the 10-minutes mean wind velocity averaged over area units of $75 \times 75\, km^2$ was determined four times a day (at 00, 6, 12 and 18 UTC). Successively, transformation parameters calibrated against real wind records were used to transform the data to point-in-time and point-in-space values for the standard terrain roughness ($z = 0.05\, m$). The Gumbel-Lieblein method was used to fit a Gumbel distribution to the generated wind speed squared data [117, 130] and deriving the $v_{b,0}^2$ values.

The uncertainty on the distribution location, X_a, is represented by a Lognormal distribution with parameters estimated with Maximum Likelihood method from the realisations $x_{a,i}$ computed according to Eq. (6.9), where $\left(v_{b,0}^2\right)_{M,i}$ and $\left(v_{b,0}^2\right)_{HC,i}$ are the characteristic values (98 % fractiles) obtained from in-land measured and hindcast-generated time series, respectively. The values in 21 locations on the Norwegian coast given in [129] were used for estimating the distribution parameters. The statistical uncertainty was integrated by Eq. (6.2), and the integral was approximated by Monte Carlo simulations. The parameters of the lognormal distribution approximating the predictive distribution were found to be $\mu_{X_a} = 0.96$ and $COV_{X_a} = 0.14$.

$$x_{a,i} = \frac{\left(v_{b,0}^2\right)_{M,i}}{\left(v_{b,0}^2\right)_{HC,i}} \tag{6.9}$$

The calibrated γ_Q was obtained solving the minimization problem in Eq. (6.10), where: β_i and $w_{\delta,i}$ are the reliability index and the weight associated with a certain δ_i; $w_{m,j}$ is the weight associated with the j^{th} material, and β_t is the target reliability. A target reliability $\beta_t = 4.7$ was chosen as given in [18] and in [10]. Three material properties were considered simultaneously: the structural steel yielding strength ($w_{m,1} = 0.4$), the reinforced concrete compression strength ($w_{m,2} = 0.4$) and the glulam timber bending strength ($w_{m,3} = 0.2$). These three construction materials are the most used in Europe. The associated weights were estimated subjectively. Ten values of δ equally spaced between 0 and 1 and equally weighted represented a broad range of design situations, from light structures ($\delta = 0$) to gravity-based structures ($\delta = 1$). The material and permanent load PSFs were fixed, see Table 6.3.

$$\underset{\gamma_Q}{\operatorname{argmin}} \left\{ \sum_{j=1}^{3} w_{m,j} \left[\sum_{i=1}^{10} w_{\delta,i} \left(\beta_i \left(z\left(\gamma_M, \gamma_G, \gamma_Q\right)\right) - \beta_t \right)^2 \right] \right\} \tag{6.10}$$

The solution of the minimization problem gave γ_Q values varying from 1.57 to 1.80 in the relevant range of $COV_{V_{b,\max}^2}$ values, say $[0.15, 0.5]$, see Figure 6.12. The selection of the $COV_{V_{b,\max}^2}$ was therefore crucial for the accurate calibration.

The limit state function in Eq. (6.8) with unknown $COV_{V_{b,\max}^2}$ represented by a normal distribution with $\mu_{COV_{V_{b,\max}^2}} = 0.25$ and $COV_{COV_{V_{b,\max}^2}} = 0.2$ gave $\gamma_Q \cong 1.60$. This value corresponds, with good approximation, to the PSF calibrated with known coefficient of

variation equal to the mean ($COV_{V^2_{b,max}} = 0.25$). In fact, the $COV_{V^2_{b,\max}}$ omission sensitivity factor [131] was found to be very close to 1, and the FORM sensitivity factor was approximatively equal to zero. Hence, the $COV_{V^2_{b,\max}}$ design point was close to its mean value. Therefore, the random variable could be substituted by its mean value in the limit state function. This made the distribution representing $COV_{V^2_{b,\max}}$ of little interest, and avoided the selection of a distribution type that is a non-trivial task since there is no theoretical evidence supporting one or another distribution. In addition, the use of the $COV_{V^2_{b,\max}}$ mean value reduced the possible values of the calibrated γ_Q to the range $[1.57, 1.65]$ (corresponding to $\mu_{COV_{V^2_{b,max}}} \in [0.2, 0.3]$). A conservative selection of $\mu_{COV_{V^2_{b,max}}} = 0.3$ led to $\gamma_Q = 1.65$ that could be considered an upper limit. The reliability indices before and after calibration are illustrated in Figure 6.13.

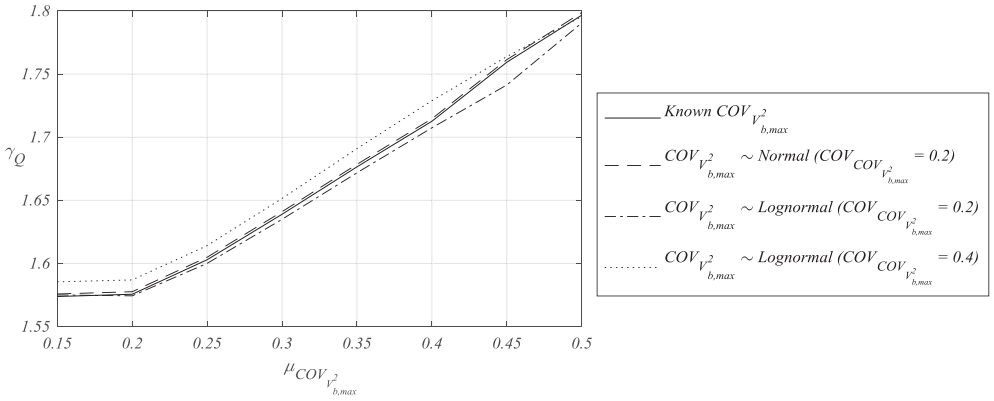

Figure 6.12. Calibrated partial safety factor for wind action from the accurate calibration with Eq. (6.10) and the limit state function in Eq. (6.8).

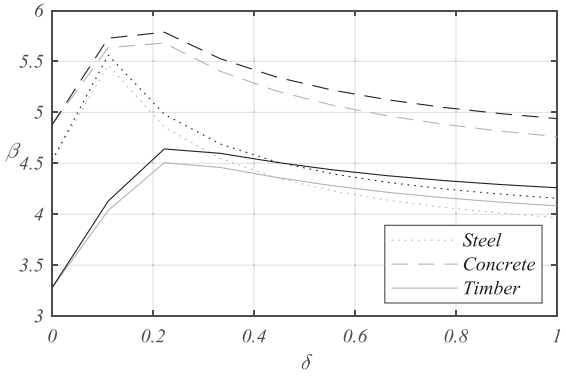

Figure 6.13. Reliability indices associated with $\gamma_Q = 1.50$ (grey lines) and $\gamma_Q = 1.60$ (black lines).

6.5 Discussion

The accuracy and goodness of the distribution representing the wind climate were not assessed in the classical absolute sense. However, the criteria related to the accuracy and

goodness were defined in Section 6.3.1, and a model that satisfies all these points was considered accurate, good in a Bayesian sense, i.e. as a basis for engineering decision making.

The calibration method and the probabilistic modelling approach proposed in the paper are able to account for the following epistemic uncertainties.

- The uncertainties on the choice of distribution type. These uncertainties are reduced by a careful and profound assessment of the phenomenon originating the wind and the underlying statistics. Different analyses techniques, based on various basic assumption, provide the same result.
- The uncertainties on the distribution parameters due to the limited number of measurements and the poor quality of measurements. These uncertainties are integrated into the distribution function.
- The uncertainty affecting the characteristic values of the wind maps for Norway due to their estimation with numerical model used. This uncertainty is represented by a stochastic variable that is included in the calibration of the safety factors.

The values of the partial safety factor proposed in the calculation example are sensitive to the chosen probabilistic models and are relative to the assumptions made. In particular, γ_Q is highly sensitive to both the resistance and the wind model biases (e.g. $\mu_{X_R}, \mu_{C_{pe}} \mu_{C_g} \mu_{C_r} \mu_{C_d} \mu_{X_Q}, \mu_{X_a}$). For example, the Eurocode 1 model includes hidden safety as reported in [99]. The inclusion of the model bias is crucial for an accurate calibration. Therefore, further research and investigations are needed for modelling probabilistically the *influence of terrain,* the *aerodynamic effects* and the *dynamic effects* links of the Davenport chain in order to calibrate γ_Q more accurately. In addition, the calibration of γ_Q was performed keeping the material and self-weight partial safety factors constant. More homogeneous reliability and a different value for γ_Q would be obtained optimising all the three partial safety factors simultaneously. Nevertheless, the scope of the example was to illustrate the proposed method, rather than proposing final values of γ_Q.

6.6 Conclusions

The analyses of the wind data with different statistical techniques indicated the use of Gumbel distribution for representing the 10-minutes mean wind speed squared yearly maxima $V^2_{b,\max}$ in reliability analyses for calibration of design codes. All techniques indicated that this distribution is accurate in the upper tail, consistent with the underlying statistic and minimising the asymptotic errors. No theoretical evidence was found supporting the use of the three-parameters Lognormal distributions. The variations of the distribution coefficient of variation COV in space and for different censoring thresholds were found to be of the same order of magnitude. Values between 0.20 and 0.35 were observed for the COV of $V^2_{b,\max}$ in the analyses. The location or magnitude of the distribution is given in design standards through tables or wind maps. The uncertainty affecting the values provided in the Norwegian National Annex to the Eurocode 1 was estimated. A method for accounting both this uncertainty and the space-variation of the distribution coefficient of variation in the calibration of partial safety factors was proposed. The method can be used for solving similar problems in code calibration such as the space-variation of the snow load characteristics.

In a calibration exercise, it was found that the space-variation can be accounted with good approximation by using the mean value of the coefficient of variation in the reliability analyses. The use of the average parameter avoided the need of modelling the parameters variation in

space probabilistically. The calibrated partial safety factor for wind actions was found to be around 1.60. The high sensitivity of the calibrated safety factor to the biases affecting the load and resistance models implemented in the codes was discussed, and the need for detailed probabilistic modelling of these uncertainties was highlighted. Although the present work focused on the European standards (Eurocodes), the analyses techniques, modelling principles and the proposed calibration method have general validity.

6.7 Appendix I to Chapter 6 - Equations and formulas

Generalised Extreme Value (GEV) distribution (support $x \in \left[a - b/\xi_{GEV}\right)$ for $\xi_{GEV} > 0$ (Fréchet); $x \in \left(-\infty, +\infty\right)$ for $\xi_{GEV} = 0$ (Gumbel) and $x \in \left(-\infty, a - b/\xi_{GEV}\right]$ for $\xi_{GEV} < 0$ (Reversed Weibull or Weibull maxima)):

$$F_X\left(x \mid \xi_{GEV}, a, b\right) = \begin{cases} \exp\left\{-\left[1 + \xi_{GEV}\left(\dfrac{x-a}{b}\right)\right]^{-1/\xi_{GEV}}\right\} & \xi_{GEV} \neq 0 \\ \exp\left\{-\exp\left[-\dfrac{x-a}{b}\right]\right\} & \xi_{GEV} = 0 \end{cases} \tag{6.11}$$

Likelihood for rounded values $\hat{x}_{r,i}$ corresponding to the (unknown) measured value $\hat{x}_i \in \left(\hat{x}_i^-; \hat{x}_i^+\right]$ with: $\hat{x}_i^- = \hat{x}_{r,i} - \Delta$, $\hat{x}_i^+ = \hat{x}_{r,i} + \Delta$ and Δ being half the rounding interval.

$$L\left(\boldsymbol{\theta} \mid \hat{\mathbf{x}}_r\right) = \prod_{i=1}^{n} L\left(\boldsymbol{\theta} \mid \hat{x}_{r,i}\right) \tag{6.12}$$

With:

$$L\left(\boldsymbol{\theta} \mid \hat{x}_{r,i}\right) = \begin{cases} F\left(\hat{x}_i^+ \mid \boldsymbol{\theta}\right) - F\left(\hat{x}_i^- \mid \boldsymbol{\theta}\right) & \text{if } \hat{x}_i^- \geq x_c \\ F\left(x_c \mid \boldsymbol{\theta}\right) & \text{if } \hat{x}_i^+ \leq x_c \\ F\left(x_c \mid \boldsymbol{\theta}\right) \cdot \Pr\left(\hat{x}_i \in \left(\hat{x}_i^-; x_c\right)\right) + \left[F\left(\hat{x}_i^+ \mid \boldsymbol{\theta}\right) - F\left(x_c \mid \boldsymbol{\theta}\right)\right] \cdot \Pr\left(\hat{x}_i \in \left(x_c; \hat{x}_i^+\right)\right) & \text{elsewhere} \end{cases} \tag{6.13}$$

where x_c is the censoring threshold, $\hat{\mathbf{x}}_r$ is the sample of rounded values, $\boldsymbol{\theta}$ is the vector of parameters and $\Pr\left(A\right)$ is the probability of the event A.

Weibull distribution (support $x \geq 0$):

$$F_X\left(x \mid a_w, b_w\right) = 1 - \exp\left[-\left(\frac{x}{a_w}\right)^{b_w}\right] \tag{6.14}$$

Generalised Pareto distribution (GPD) (support $x \geq 0$ for $\xi_{GPD} \geq 0$, $x \leq -\bar{\sigma}/\xi_{GPD}$ for $\xi_{GPD} < 0$):

$$F_X\left(x \mid \xi_{GPD}, \bar{\sigma}\right) = \begin{cases} 1 - \left(1 + \dfrac{\xi_{GPD} x}{\bar{\sigma}}\right)^{-1/\xi_{GPD}} & \xi_{GPD} \neq 0 \\ 1 - \exp\left(-\dfrac{x}{\bar{\sigma}}\right) & \xi_{GPD} = 0 \end{cases} \tag{6.15}$$

6.8 Appendix II to Chapter 6 - Stochastic models used in the example calibration

*Table 6.3. Stochastic models representing the basic random variables (from [13] unless otherwise stated) and partial safety factors ([a] [56] [b][132], [c][35], [d][133], [e][87], [f][134], [g][99], [h][18], [i][107], *range of possible values given in [13]).*

	Description		Distribution type	Mean	COV	Characteristic fractile	Partial safety factor (γ)
X_R	Model uncertainty	Structural steel element in compression [a]	Lognormal	1.15	5 %	/	/
		Reinforced concrete element in compression [a]	Lognormal	1.20	15 %	/	/
		Glulam timber element in bending	Lognormal	1.00	15 %	/	/
R	Material property	Struct. Steel yielding strength	Lognormal	1.00	7 %	5 %	1.00 [b]
		Concrete compression strength	Lognormal	1.00	15 % [c]	5 %	1.50 [d]
		Glulam timber bending strength	Lognormal	1.00	15 %	5 %	1.25 [e]
C_r	Roughness factor		Lognormal	0.80	15 % (10 to 20%)*	$F_{C_r}(\mu_{C_r})$	/
C_g	Gust factor		Lognormal	1.00	15 % (10 to 15%)*	$F_{C_g}(\mu_{C_g})$	/
C_{pe}	External pressure coefficient		Gumbel [f]	1.00	25 % [g] (10-30%)*	80 % [i]	/
G	Permanent action		Normal	1.00	10 %	50 %	*1.35* [h]
$V^2_{b,\max}$	Mean wind speed (1yr max)		Gumbel	1.00	$COV_{V^2_{b,max}}$	98 %	To be calibrated
X_a	$F_{V^2_{b,\max}}$ location uncertainty		Lognormal	0.96	0.14	$F_{X_a}(1)$	/
$COV_{V^2_{b,max}}$	$V^2_{b,\max}$ coefficient of variation		Normal	0.25	0.20	/	/
X_Q	Wind load model uncertainty [a]		Normal	0.80	0.20	$F_{X_Q}(1)$	/

Chapter 7 Paper VI: Risk and Reliability-Based Calibration of Design Codes for Submerged Floating Tunnels

Paper

Authors: M. Baravalle[a], J. Köhler[a]

[a] Department of Structural Engineering, Norwegian University of Science and Technology, Trondheim

In: *Procedia Engineering*, Volume 166, 2016, Pages 247-254.

7.1 Abstract

Submerged floating tunnels (SFTs), also known as Archimedes' bridges, allow crossing waterways where common bridges, underground tunnels or immersed tunnels are not feasible. In spite of this, no SFTs have been built yet in the world except for a prototype in China. The reasons are numerous and widely discussed in literature. The lack of past experience and ad hoc design codes or guidelines represents a great challenge in design. In fact, the direct use of target reliabilities and design codes, which are specifically developed for common structures and adapted through the years based on the gained experience, is questionable. This is because STFs might be characterised by different failure consequences and marginal safety costs. Optimal target reliabilities can be estimated through a full-risk assessment following the ISO standard 2394:2015 guidelines. Successively simpler design approaches and assessment of decisions such as reliability-based and semi-probabilistic design can be calibrated.

Keywords: risk, design codes, calibration, submerged floating tunnels.

7.2 Introduction

Submerged floating tunnels (SFTs) for crossing waterways have the potential to be a great technological solution allowing to cross water depths and spans which, nowadays, are impossible to cross with common bridge solutions. Although the first detailed studies on SFTs date back to the late Sixties no SFT have been built yet in the world except for a prototype for pedestrians in the Qiandao Lake (People's Republic of China). This is certainly due to several reasons; among them the lack of experience for this specific type of structures is probably the most important. In fact, the experience gained from other structures can be only partly used since the SFTs differ from common structures since in general they have:

- different relevant limit states. Water tightness and failure against submarine or boat impacts are two examples of relevant limit states that are rarely relevant in common structures.
- Different magnitude of the consequences associated to failure of a relevant limit states and different marginal safety costs, i.e. the costs for increasing the structural safety. Crack opening might for example lead to flooding of the SFT additionally to re-bars corrosion as in common structures. As it will be clear later, different consequence and safety costs affect the optimal safety level, which is defined as the safety level that minimizes the total expected costs. Moreover, different marginal safety costs result in different levels of acceptable safety.
- Different accuracy of the models predicting the structural response, which are associated with large epistemic uncertainty that, on its turn, is a consequence of the lack of past experience since only one pedestrian SFT has been built so far. This limits the back-assessment of the models and requires to glean information from laboratory test on down-scaled prototypes and/or to apply the know-how gained in similar, but not equal, structures.
- Different load scenarios such as the simultaneous action of traffic, currents, tide etc. leading to load combinations which rarely occur in other structures.

The use of semi-probabilistic codes such as the Eurocodes [18] greatly facilitates the engineering design work and standardize the structural safety level has shown during the past decades. Nevertheless, their use in designing non-common structures, i.e. structures they were not calibrated for, such as SFTs, might result into levels of safety that are in general non-optimal (i.e. uneconomic design) and, in the worst case, non-acceptable in terms of fatality risk. As discussed later, this can be avoided by using more general decision assessment approaches either directly in design or indirectly for specifically re-calibrating the existing codes for a certain type of structure.

The article summarizes first the link between the different design approaches and how higher level approaches can be used for calibrating lower levels. It then presents a tentative and qualitative estimation of the consequences and safety costs associated to the relevant limit states of a selected SFT concept. Further, the reliability of the design performed with existing codes is assessed and discussed.

It is worth mentioning that the article aims to open a discussion on the treated topics rather than providing final results.

Nomenclature

d	Reinforcement distance from outer fibre
$f_{c,t}$	Concrete tension resistance
r	Inner diameter

A_s	Reinforcement steel area
B	Buoyancy
C	Current
E_s, E_c	Steel and concrete Young's modulus
G_1	Permanent self-weight ($G_1 = \sum_{i=1}^{5} G_{1,i}$)
$G_{1,1}$	Weight of main structure
$G_{1,2}$	Weight of internal structural elements
$G_{1,3}$	Weight of permanent ballast
$G_{1,4}$	Weight of asphalt
$G_{1,5}$	Weight of equipment
G_2	Additional weight due to environment ($G_2 = \sum_{i=6}^{8} G_{2,i}$)
$G_{2,6}$	Marine growth
$G_{2,7}$	Water absorption main structure
$G_{2,8}$	Water absorption in ballast
$M_{E,y,[\cdot]}$	Bending moment @ y-axis induced by action $[\cdot]$
M_P	Pre-stressing bending moment
$N_{E,[\cdot]}$	Axial force induced by action $[\cdot]$
N_P	Pre-stressing axial force
R	Outer diameter
TR	Traffic
W	Waves
$X_{[\cdot]}$	Uncertainty on the model representing action $[\cdot]$
$X_{E,V}$	Model uncertainty for the structural response under environmental and traffic loads
$X_{E,G}$	Model uncertainty for the structural response under static loads
X_R	Model uncertainty for the resistance
γ_{Rd}	Partial safety factor (psf) covering uncertainty in the resistance model
$\gamma_{m,[\cdot]}$	Psf for the material property $[\cdot]$
γ_P	Psf for the prestressing action
γ_{Sd}	Psf covering uncertainties in the effect of actions
$\gamma_{f,[\cdot]}$	Psf for the action $[\cdot]$
$\sigma_{\max}$	Maximum stress
ψ	Load reduction factor
ΔP	Pre-stressing losses

7.3 Design approaches and code calibration

Structural design and assessment of decisions can be performed with three main approaches as included in the ISO 2394:2015 [10]. Each of them is supported by a specific type of standard and is subjected to limitations, see Figure 7.1.

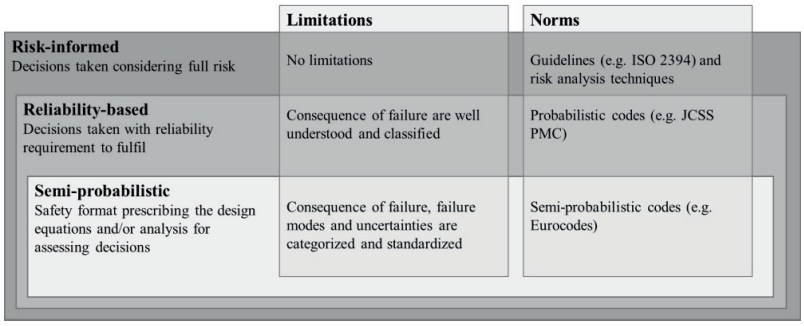

Figure 7.1. Design and assessment approaches with limitations and regulating norms according to ISO 2394:2015 [10].

7.3.1 Risk-based approach

The most general and widely applicable design approach is the identification of the optimal design alternative based on a full-risk analysis. Risk is defined as consequence associated to an event times the probability of occurrence of the event. The designer can find the optimal solution by playing on both the probability of occurrence of the event (e.g. failure probability) and the consequences given occurrence. The acceptability of optimum ($p_{acc} > p^*$) has to be assessed when life- and environmental-safety are relevant. Optimal decision can be adopted only when the corresponding safety level is above the minimum acceptable. An illustrative example of full-risk analysis is represented in Figure 7.2 where the risk is evaluated in monetary terms. The optimal decision (p^*) is associated with minimum-risk or, equivalently, minimum expected costs. Suboptimal structures ($p \neq p^*$) are associated with higher expected costs either due to large construction costs ($p > p^*$) or large expected failure costs due to large probability of failure ($p < p^*$).

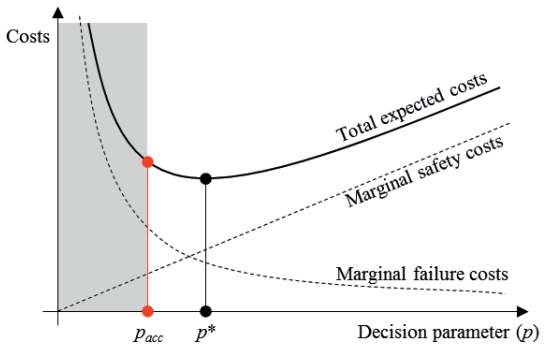

Figure 7.2. Total expected costs (thick black line) obtained adding the safety costs to the marginal failure costs calculated as probability of failure times the consequence of failure, from [10].

7.3.2 Reliability-based approach

Reliability-based design and assessment of decision are a simplification of the risk-based approach to be used when the consequence of failure and damage are well understood and in ordinary ranges. In detail, experts or standardization bodies individuate optimal reliabilities through a risk-based analysis for groups of similar structures in terms of construction, safety and failure costs, see Table 7.1. Structures are then designed so to fulfil the reliability requirement specified for the class they belong to. It is worth highlighting that no distinction between different magnitudes of reparation costs is made in Table 7.1. Reparation costs might be significant in a SFT and their inclusion in a risk-based analysis might result in different target reliabilities. As clearly stated in [10], structures characterised by very large consequence or structures whose failure and failure mechanisms are unknown or different than those considered for providing target values need to be designed following a risk-based approach.

Table 7.1. Tentative yearly target reliability indices and associated failure probabilities given by Joint Committee of Structural Safety [13].

		Ultimate limit states			***Irreversible serviceability limit states***
		Minor failure consequences	***Moderate failure consequences***	***Large failure consequences***	
Relative cost of safety measures	Large	3.1 ($P_{f,N} \approx 10^{-3}$)	3.3($P_{f,N} \approx 5 \cdot 10^{-4}$)	3.7 ($P_{f,N} \approx 10^{-4}$)	1.3 ($P_{f,N} \approx 10^{-1}$)
	Normal	3.7 ($P_{f,N} \approx 10^{-4}$)	4.2 ($P_{f,N} \approx 10^{-5}$)	4.4 ($P_{f,N} \approx 5 \cdot 10^{-6}$)	1.7 ($P_{f,N} \approx 5 \cdot 10^{-2}$)
	Small	4.2 ($P_{f,N} \approx 10^{-5}$)	4.4 ($P_{f,N} \approx 5 \cdot 10^{-6}$)	4.7 ($P_{f,N} \approx 10^{-6}$)	2.3 ($P_{f,N} \approx 10^{-2}$)

7.3.3 Semi-probabilistic approach

This approach consists in the design and assessment of decisions by means of semi-probabilistic design codes. It is a simplification of the reliability-based approach developed for categorized and standardized consequences, failure modes and uncertainty representation. As a consequence, semi-probabilistic codes are only to be used in the domain they were developed for.

Semi-probabilistic codes contain reliability elements such as the partial safety factors which control the reliability of the structures. These reliability elements are calibrated by code committee and/or experts and are valid only for the domain of applicability of the code. Code calibration is "[…] *the process of assigning values to the parameters in a design code.* […] *with a view to achieve a desired level of reliability in error-free structures*" [4]. In a broader sense, code calibration is the selection of the safety format of the design equation, the characteristic values, partial safety and load combination factors, load combination rules and all other reliability elements "*such that the level of reliability of all structures designed according to the design codes is homogeneous and independent of the choice of material and the prevailing loading, operational and environmental conditions.* […] *including the choice of the desired level of reliability or "target reliability"*" [5]. Calibration of a code is performed with higher level approaches such as reliability or risk-based approaches. Risk-based calibration consists in selecting the values of the reliability elements such that the corresponding design is associated with minimum risk. All consequences and hazards are explicitly considered in the calibration. Reliability-based calibration might be performed when the consequence of failure and damage

are well understood and in ordinary ranges. For each limit state or type of structure the reliability elements are calibrated with a target reliability corresponding to the appropriate class.

7.4 Case study: SFT with reinforced concrete structure

The concepts discussed above are applied to a SFT made of a reinforced concrete tube which is anchored to the seabed with tethers in tension, i.e. similar principle as e.g. for offshore tension leg platforms.

7.4.1 Relevant limit states

The relevant limit states are analysed in terms of consequences associated to failure, reparation costs after failure and cost of safety measure, i.e. the cost for increasing safety by varying the design parameter (or decision parameter). A summary of the analysis is reported in Table 7.2. The cost estimation has been performed with pure engineering judgment due to lack of detailed information. Higher levels of detail can be reached with a more detailed study and further research. The limits states reported in the table clearly show large differences of costs that result in different optimal safety levels.

Table 7.2. Relevant limit states for a SFT with qualitative estimation of costs of safety measures, failure and reparation.

Limit state / Definition of failure event	***Decision parameter / Cost of safety measure***	***Failure consequences / Associated costs***	***Reparation action / Associated costs***
Concrete tube water tightness (reversible) / Tension stresses larger than tension strength	Pre-stressing steel and pre-stressing forces / Low-medium	Minimum amount of water entering during a structural oscillation / Very low	No reparation required
Concrete tube water tightness (permanent) / Tension stresses in re-bars above yielding strength	Re-bars dimension and location / Low-medium	Depending on crack opening, pumping system capacity etc. / From low to high	Filling of permanent cracks / Medium-high
Slack of tethers / Tether(s) with no tension stresses	Permanent ballast / Low	For one tether (pontoon): overloading of other tethers / Low For two or more tethers (pontoons): overload of other tethers or pontoon, overload of tube / Medium-high	Tether re-gain tension after one oscillation / Very low. Reparation of concrete structure / Medium-high
Tether yielding	Tethers cross section, steel quality / Low-medium		Tether-SFT joint reparation / Low-medium Reparation of concrete structure / Medium-high
Loss of one tether or a tether group / Rupture of tethers of joints tether-SFT	Tether-to-SFT joint strength / Low-medium		Tether-SFT joint replacement / Medium-low Reparation of concrete structure / Medium-high
Foundation failure / Uplift of foundation	Foundation uplift capacity / Low		Foundation replacement, strengthening / Low Reparation of concrete structure / Medium-high
Pontoon freeboard lack / Lack of freeboard in one pontoon to absorb downward forces	Pontoon geometry and weight / Low		Pontoon replacements, modification / Low Reparation of concrete structure / Medium-high
Water ingress in pontoon / Punching or permanent cracks in pontoon	Pontoon wall reinforcement location and amount / Low-medium		Pontoon replacements, modification / Low-medium Reparation of concrete structure / Costs depends on degree of damage

7.4.2 Detailed reliability analysis and partial safety factor calibration for the reversible water tightness limit state

The reversible concrete tube water tightness limit state is studied more in detail. The reliability of the design performed with the partial safety factor taken from the Eurocodes is assessed.

The limit state equation is reported in Eq. (7.1) where tension stresses are considered positive, for symbols and probabilistic models see Table 7.3. The SFT cross section is represented as a circular tube with inner diameter r, outer diameter R and symmetrical reinforcement placed on the vertical axis at a distance d from the outer fibers, see Figure 7.3. Temperature variation, creep and shrinkage in concrete and water level variation are neglected in order to simplify the case study. Furthermore, the formation of through-thickness cracks and the time needed for water to penetrate is not considered. Instead, failure is considered when the inequality in Eq. (7.1) is satisfied in any point of the cross-section.

$$g(...) = f_{c,t} - \sigma_{\max} =$$
$$= X_R f_{c,t} - \left[\frac{N_P(1-\Delta P) + X_{E,V} N_{E,V}}{A_o} + \frac{M_P(1-\Delta P) + X_{E,V} M_{E,y,V} + X_{E,G} M_{E,y,G}}{I_{o,y}} R \right] < 0 \qquad (7.1)$$

In Eq. (7.1) $\sigma_{\max}$ is the maximum stress in the cross-section, $A_o = \pi(R^2 - r^2) + (E_s/E_c)2A_s$ and $I_{o,y} = \pi(R^4 - r^4)\frac{1}{4} + (E_s/E_c)2A_s(R-d)^2$ are the homogenized cross-sectional area and the moment of inertia; $N_{E,V} = X_C N_C + X_W N_W$ is the time-variant axial force induced by current and waves; $M_{E,y,V} = X_{TR} M_{TR} + X_W M_W$ is the time-variant bending moment induced by traffic and waves and $M_{E,y,G} = X_{G_1} M_{G_1} + X_{G_2} M_{G_2} + X_B M_B$ is the bending moment induced by permanent actions.

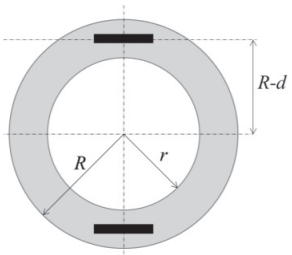

Figure 7.3. SFT cross-section (grey: concrete, black: reinforcement), not in scale.

The model uncertainties are expected to be low/medium for models where there is experience, e.g. resistance models (X_R) and structural response to static loads ($X_{E,G}$), while high model uncertainties might affect the models predicting the structural response under dynamic loads ($X_{E,V}$) as discussed previously.

The tube is designed "just safe", i.e. just satisfying the design equation written in the load and resistance factor design format reported in Eq. (7.2), where the subscripts k and d indicate the characteristic and design values, respectively. The decision parameters are the pre-stressing axial force and bending moment, N_P and M_P respectively. Due to infinite possible solutions one of the two decision parameters is arbitrarily fixed. Optimization studies or other limit states may individuate a unique and optimal couple of values.

$$\left[\frac{\gamma_P N_{P,k}(1-\Delta P_k) + N_{E,d}}{A_{o,d}} + \frac{\gamma_P M_{P,k}(1-\Delta P_k) + M_{E,y,d}}{I_{o,y,d}} R_d \right] - \frac{1}{\gamma_{Rd}} \frac{f_{c,t,k}}{\gamma_{m,f_{ct}}} < 0 \qquad (7.2)$$

The design values of the cross-sectional geometrical properties, axial force and bending moment are:

- $A_{o,d} = \pi(R_d^2 - r_d^2) + (\gamma_{m,E_c} E_{s,k} / \gamma_{m,E_s} E_{c,k}) 2A_{s,d}$,
- $I_{o,y,d} = \frac{1}{4}\pi(R_d^4 - r_d^4) + (\gamma_{m,E_c} E_{s,k} / \gamma_{m,E_s} E_{c,k}) 2A_{s,d}(R_d - d_d)^2$,
- $N_{E,d} = \gamma_{Sd}(\gamma_{f,C} N_{C,k} + \gamma_{f,W} N_{W,k})$,
- $M_{E,y,d} = \gamma_{Sd,V}(\gamma_{f,TR} M_{TR,k} + \gamma_{f,W} M_{W,k}) + \gamma_{Sd,G}(\gamma_{f,G_1} M_{G_1,k} + \gamma_{f,G_2} M_{G_2,k} + \gamma_{f,B} M_{B,k})$.

Three design situations are considered: 1) maximum sagging moment at tether-SFT joints, 2) maximum hogging moment in the free-spans and 3) unloaded design situation. The most

critical among them is seen to be the one with maximum positive moment (sagging) on a support and minimum axial compression force. This load scenario consists in waves and traffic actions giving sagging moment, G_1 giving hogging moment and G_2 loads (marine growth, water absorption etc.) absent.

Table 7.3. Probabilistic models representing random variables.

Random variable	***Distribution***	***Coefficient of variation***	***Characteristic fractile***
d	Lognormal	0.07	Mean
$f_{c,t}$	Lognormal	0.32	0.05
E_c	Lognormal	0.16	0.05
$G_{1,1}$	Normal	0.03	0.50
$G_{1,2}$	Normal	0.03	0.50
$G_{1,3}$	Normal	0.03	0.50
$G_{1,4}$	Normal	0.10	0.50
$G_{1,5}$	Normal	0.15	0.50
$G_{2,6}$	Lognormal	0.40	0.98
$G_{2,7}$	Lognormal	0.40	0.50
M_B	Lognormal	0.04	0.50
M_P	Normal	0.06	0.50
M_{TR}	Gumbel	0.40	0.999
N_C, M_C	Gumbel	0.30	0.99
N_P	Normal	0.06	0.50
N_W, M_W	Gumbel	0.30	0.99
$X_{E,G}$	Lognormal	0.05	/
$X_{E,V}$	Lognormal	0.15	/
X_R	Lognormal	0.11	/
R , r	Normal	0.03	0.50
ΔP	Lognormal	0.30	Mean

The limit state considered here is a Serviceability Limit State (SLS) so all partial safety factors are taken equal to unity ($\gamma_{Sd} = \gamma_f = \gamma_m = \gamma_{Rd} = 1.00$) as given in the Eurocodes. Load reduction factors (ψ) are assumed equal to 0.7 since no values are given in the used code. Three load combinations are considered, each of them has one time-varying action leading and the remaining two accompanying, see Table 7.4.

Table 7.4. Partial safety factors multiplying time varying variables.

		C	TR	W
LC1	C leading	$\gamma_f = 1.00$	$\gamma_f \psi = 1.00 \cdot 0.7$	$\gamma_f \psi = 1.00 \cdot 0.7$
LC2	TR leading	$\gamma_f \psi = 1.00 \cdot 0.7$	$\gamma_f = 1.00$	$\gamma_f \psi = 1.00 \cdot 0.7$
LC3	W leading	$\gamma_f \psi = 1.00 \cdot 0.7$	$\gamma_f \psi = 1.00 \cdot 0.7$	$\gamma_f = 1.00$

The reliability of the just safe design is assessed with FORM performed in Matlab® with the FERUM package [73]. All random variables are considered uncorrelated. The largest correlation is expected between the axial force and the bending moment induced by the waves (W), although the reliability index is seen to be not sensitive to it. Time-variant actions (C, W, TR) are combined following the Ferry Borges and Castanheta load combination rule. The loads are modelled with 90, 360, 720 repetitions a year, respectively.

7.4.2.1 Results

The yearly reliability index is found to be around 3.9 for different levels of N_P and associated M_P. The variation of reliability for different geometry, load proportions etc. is investigated. The reliability index is found, for example, to vary from around 3.6 to 4.2 for reinforcement ratios ($A_s / \pi\left(R^2 - r^2\right)$) varying from 1% to 4%, respectively.

Sensitivity factors from the FORM analysis are interesting outputs which allow to quantify how much a random variable affects the probability of failure. Random variables with sensitivity factors close to zero can be approximatively treated as deterministic variables simplifying the reliability calculations. On the contrary, random variables with large sensitivity factors might be further investigated in order to reduce the epistemic uncertainty affecting them (if there is any) through more research, measurements and/or using more refined models. The four highest sensitivity factors are found for the axial force induced by waves (N_W), the bending moment induced by buoyancy (M_B), the concrete tensile strength (f_{ct}) and the uncertainties on the model for calculating the response to dynamic loads ($X_{E,V}$).

Considering Table 7.1 valid for the SFT at hand we can conclude that the level of safety associated with the used partial safety factors (characteristic load combination and unitary material partial safety factors) is much higher than the optimal target that is equal to or lower than 2.30 for an irreversible SLS. This means that the partial safety factors used lead to an over-design and that partial safety factor calibration is required. If, contrarily, the validity of Table 7.1 for the studied SFT is in doubt, a full-risk assessment and optimization should be performed for estimating the optimal target level. In both cases, the calibration of the reliability elements should be performed considering different scenarios like, for example, different amount of reinforcement, intensities of loads and so on. In this way the calibrated partial safety factors will provide a level of safety as homogeneous as possible over the various scenarios.

7.5 Conclusion

Although the here reported results are just as good as the made assumptions, the article shows that further research is needed in the field. First of all, a detailed full-risk-based analysis is required for estimating tentative optimal target reliabilities for SFTs. The use of targets typically used for other types of structures might not be optimal due to different consequences and safety costs. Optimal target reliabilities might be used for reliability-based design or

reliability-based calibration of existing standards in order to use them for design. In fact, as shown in the case study, the use of partial safety factors (or reliability elements in general) given in a selected design standard leads to levels of safety that might not be optimal for a SFT. A calibration exercise, considering different geometries and load scenarios, is needed in order to provide partial safety factors giving homogeneous levels of safety over different SFTs. In fact, the reliability level is seen to vary consistently with the cross-section geometry, pre-stressing force and relative magnitude of the different loads.

The aforementioned assessments rely on a consistent amount of assumptions and subjective evaluations. This might lead to prefer typical target safety levels rather than undertaking a full-risk assessment and risk-optimization. Nevertheless, a large number of “hidden” assumptions are tacitly accepted and validated when typical targets are adopted.

Acknowledgments

This research has been supported by a Norwegian Public Roads Administration (NPRA) grant as part of the "Ferry-free coastal route E39" project.

References

1. Colling F., Mikoschek M. *Load combinations - State of the art and proposals for simplifications*. *Second workshop of COST action FP 1402*; Pamplona, Spain. 2015.
2. Gayton N., Mohamed A., Sørensen J.D., Pendola M., Lemaire M. Calibration methods for reliability-based design codes. *Structural Safety*. 2004; **26**(1), pp. 91-121.
3. Herczeg M., McKinnon D., Milios L., Bakas I., Klaassens E., Svatikova K., et al. *Resource efficiency in the building sector*. Rotterdam, The Netherlands: ECORYS,

Copenhagen Resource Institute; 2014, May 23rd.

4. Kübler O. *Applied decision-making in civil engineering* [Doctoral Thesis]. Zurich: Swiss federal Institute of Technology, ETH Zurich; 2007.
5. Melchers R.E. *Structural reliability: analysis and prediction.* Second ed. Chichester, England: John Wiley & Sons Ltd.; 1999.
6. Forssell C. Ekonomi och byggnadsvasen (Economy and construction). *Sunt Fornoft*. 1924; **4**, pp. 74-7. Translated in excerpts in Lind, S.M. *Structural reliability and codified design*, SM study No. 3, Solid Mechanics Division, University of Waterloo, Waterloo. 1970.
7. Faber M.H., Sørensen J.D. *Reliability based code calibration - The JCSS approach*. In: Der Kiureghian A., Madanat S., Pestana J.M., editors. *Proc of the 9th International Conference on Applications of Statistics and Probability in Civil Engineering*. San Francisco: Millpress; 2003. p. 927-35.
8. Rosenblueth E., Esteva L. Reliability basis for some mexican codes. *American Concrete Institute (ACI) Publication* 1972; **SP-31**
9. Lind N.C. *The design of structural design norms*. Waterloo, Ontario, Canada: University of Waterloo; 1971. Report No.: 89.
10. International Organization for Standardization (ISO). *ISO 2394:2015 General principles on reliability for structures*. Switzerland; March, 2015.
11. Ditlevsen O., Madsen H.O. *Structural Reliability Methods* [Monograph]: Department of Mechanical engineering at the Technical University of Denmark; 2007. Available from: http://od-website.dk//index-2.html/books.htm.
12. Madsen H.O., Krenk S., Lind N.C. *Methods of structural safety*. Mineaola, New York: Dover Publications; 2006. 407 p.
13. Joint Committee on Structural Safety (JCSS). *Probabilistic Model Code* 2001. Available from: http://www.jcss.byg.dtu.dk/Publications.
14. Schneider J. *Introduction to Safety and Reliability of Structures.* Second ed. International Association for Bridges and Structural Engineering (IABSE), editor. Zurich, Zwitzerland: IABSE-AIPC-IVBH; 2006.
15. European Committee for Standardization (CEN). *EN 1991-1-4:2005 Eurocode 1 - Actions on structures - Part 1-4: General actions - Wind actions*. Brussels; 2005.
16. Vrouwenvelder T. Developments towards full probabilistic design codes. *Structural Safety*. 2002; **24**(2–4), pp. 417-32.
17. Vrouwenvelder T. *Theory and applications of structural reliability Analysis*. In: Bucher C., Ellingwood B., Frangopol D.M., editors. Proc of the 12th Int Conf on Structural Safety and Reliability. Vienna, Austria: TU-Verlag Vienna; 2017. p. 1-16.

18. European Committee for Standardization (CEN). *EN 1990:2002/A1:2005/AC:2010 Eurocode 0 - Basis of structural design*. Brussels; 2002.

19. American Association of State Highway and Transportation Officials (AASHTO). *LRFD Bridge Design Specifications, U.S. Customary Units, 7th Edition, with 2015 and 2016 Interim Revisions* 2016.

20. American Society of Civil Engineers (ASCE). *AF&PA/ASCE 16-95 Standard for Load and Resistance Factor Design (LRFD) for Engineered Wood Construction*. New York, NY; 1996.

21. Det Norske Veritas (DNV). *DNV-OS-C101: Design of offshore steel structures, general (LRFD method)*. Online; July, 2011.

22. Fédération Internationale du Béton (fib). *fib Model Code for Concrete Structures 2010*. Lausanne, Switzerland: Ernst & Sons, a Wiley brand; 2013. Available from: http://dx.doi.org/10.1002/9783433604090.fmatter.

23. Vrouwenvelder T., Siemes A.J.M. Probabilistic calibration procedure for the derivation of partial safety factors for the Netherlands building codes. *HERON, 32 (4), 1987*. 1987;

24. Ravindra M., Galambos T.V. Load and resistance factor design for steel. *ASCE Journal of the Structural Division*. 1978; **104**(9), pp. 1337-53.

25. Lind N.C. *Reliability based structural codes, practical calibration*. In: Holand I., editor. *Safety of structures under dynamic loading*; Trondheim, Norway. Norwegian Institute of Technology; 1977. p. 149-60.

26. Ellingwood B.R. Probability-based codified design: past accomplishments and future challenges. *Structural Safety*. 1994; **13**(3), pp. 159-76.

27. Baker J.W., Schubert M., Faber M.H. On the assessment of robustness. *Structural Safety*. 2008; **30**(3), pp. 253-67.

28. European Commission. *M/515 EN - Mandate for amending existing eurocodes and extending the scope of structural eurocodes*. Brussels: European Commission - Enterprise and industry directorate; 2012.

29. Norwegian Public Roads administration (NPRA). *Mulighetsstudie - Krissing av Sognefjorden*. SVV, Prosjektavdelingen; 2010.

30. Madsen H.O. *Managing structural safety and reliability in adaptation to climate change*. In: Deodatis G., Ellingwood B.R., Frangopol D.M., editors. *Proc of the 11th International Conference on Structural Safety and Reliability*. London, UK: Taylor and Francis Group; 2014. p. 81-8.

31. Ditlevsen O. Structural reliability codes for probabilistic design — a debate paper based on elementary reliability and decision analysis concepts. *Structural Safety*. 1997; **19**(3), pp. 253-70.

32. Faber M.H., Sørensen J.D. *Reliability Based Code Calibration*. *JCSS Workshop on Reliability Based Code Calibration*; March, 2002; Zurich, Switzerland. 2002.

33. Ditlevsen O. Fundamental postulate in structural safety. *Journal of Engineering Mechanics*. 1983; **109**(4), pp. 1096-102. Export Date: 4 March 2016.

34. Henderson J.R., Blockley D.I. Logical analysis of assumptions in code calibration. *Structural Safety*. 1982; **1**(2), pp. 123-40.

35. Sørensen J.D., Hansen S.O., Nielsen T.A. *Calibration of partial safety factors for Danish structural codes*. *Proc IABSE Conf Safety, Risk and Reliability–Trends in Engineering, Malta, 2001*. Zurich, Switzerland: IABSE; 2001. p. 179-84.

36. Sørensen J.D., Kroon I.B., Faber M.H. Optimal reliability-based code calibration. *Structural Safety*. 1994; **15**(3), pp. 197-208.

37. SAKO. *Basis of design of structures - Proposal for modification of partial safety factors in Eurocodes*. Oslo, Norway: Joint Committee of NKB and INSTA-B (SAKO); 1999.

38. Ardillon E., Barthelet B., Sørensen J.D. Probabilistic calibration of safety factors for nuclear operating installations. *American Society of Mechanical Engineers, Pressure Vessels and Piping Division (Publication) PVP*. 1998; **376**, pp. 73-81. Export Date: 22 March 2016.

39. Eamon C.D., Nowak A.S., Ritter M.A. *LRFD calibration for wood bridges*. In: Melchers R.E., Stewart M.G., editors. *Proc of the 8th Int Confon Applications of Statistics and Probability in Civil Engineering*. 2. Rotterdam, The Netherlands: A.A. balkema; 2000.

40. Hansen P.H., Sørensen J.D. *Reliability-based code calibration of partial safety factors*. *JCSS Workshp on Reliability Based Code Calibration*; March 21-22, 2002; Zurich, Switzerland. 2002.

41. Kohler J., Fink G. *Reliability based code calibration of typical Eurocode 5 design equations*. In: Quenneville P., editor. *Proc of the World Conference on Timber Engineering 2012 (WCTE 2012)*. 4. Red Hook, USA: Curran Associate; 2012. p. 99-103.

42. Marková J., Holicky M. *Calibration of partial factors for design of concrete structures*. In: Faber M.H., Köhler J., Nishijima K., editors. *Proc of the 11th Int Conf on Applications of Statistics and Probability in civil engineering, Zurich, Switzerland, August 2011*: CRC Press; 2011. p. 986-90.

43. Maes M.A., Abdelatif S., Frederking R. Recalibration of partial load factors in the Canadian offshore structures standard CAN/CSAS-471. *Canadian Journal of Civil Engineering*. 2004; **31**(4), pp. 684-94.

44. Nowak A.S. Calibration of LRFD bridge code. *Journal of Structural Engineering (United States)*. 1995; **121**(8), pp. 1245-51.

45. Thoft-Christensen P., Baker M.J. *Structural reliability theory and its applications.* Berlin, Heidelberg: Springer Berlin Heidelberg; 1982.

46. von Neumann J., Morgenstern O. *Theory of games and economic behavior.* Princeton, USA: Princeton University Press; 1943. 776 p.

47. Rosenblueth E., Mendoza E. Reliability optimization in isostatic structures. *Journal of the Engineering Mechanics Division*. 1971; **97**(6), pp. 1625-42.

48. Rackwitz R. Optimization - the basis of code-making and reliability verification. *Structural Safety*. 2000; **22**(1), pp. 27-60.

49. Sørensen J.D. *Calibration of Partial Safety Factors in Danish Structural Codes*. *JCSS Workshop on Reliability Based Code Calibration*; March 21-22, 2002; Zurich, Switzerland. 2002.

50. Hasofer A.M. Design for infrequent overloads. *Earthquake Engineering & Structural Dynamics*. 1973; **2**(4), pp. 387-8.

51. Rosenblueth E. Optimum design for infrequent disturbances. *Journal of the Structural Division*. 1976; **102**(9), pp. 1807-25.

52. Seim W., Schick M., Eisenhut L. *Simplified design rules for timber structures - Drawback or progress*. In: Quenneville P., editor. *World Conference on Timber Engineering 2012 (WCTE 2012)*. 4. Red hook, USA: Curran Associate; 2012. p. 8-12.

53. Muttoni A., Ruiz M.F. Levels-of-approximation approach in codes of practice. *Struct Eng Int J Int Assoc Bridge Struct Eng*. 2012; **22**(2), pp. 190-4.

54. Dietsch P., Winter S. Eurocode 5 - Future Developments Towards a More Comprehensive Code on Timber Structures. *Structural Engineering International*. 2012; **22**(2), pp. 223-31.

55. Song R., Tjelta E., Bai Y. *Reliability-based calibration of safety factors for tubular joints design*. In: Grundy P., Koo J., Langen I., Roesset J.M., editors. *Proceedings of the Eighth International Offshore and Polar Engineering Conference, Vol 4*. Golden, Colorado, USA: International Society of Offshore and Polar Engineers; 1998. p. 435-41.

56. Holicky M., Sykora M. *Conventional probabilistic models for calibration of codes*. In: Faber M.H., Köhler J., Nishijima K., editors. *Proc of the 11th Int Conf on Applications of Statistics and Probability in civil engineering, Zurich, Switzerland, August 2011*: CRC Press; 2011. p. 969-76.

57. Sykora M., Holicky M. *Comparison of load combination models for probabilistic calibrations*. In: Faber M.H., Köhler J., Nishijima K., editors. *Proc of the 11th Int Conf on Applications of Statistics and Probability in civil engineering, Zurich, Switzerland, August 2011*: CRC Press; 2011. p. 977-85.

58. Sanpaolesi L. *The background document for snow loads*. *IABSE Colloquium on Basis of Design and Actions on Structures Background and application of Eurocode 1*; Delft, The Netherlands. 1996.

59. Wen Y.K. *Structural load modeling and combination for performance and safety evaluation.* Amsterdam, The Netherlands: Elsevier; 1990.

60. Sørensen J.D., Svensson S., Stang B.D. Reliability-based calibration of load duration factors for timber structures. *Structural Safety*. 2005; **27**(2), pp. 153-69.

61. Friis-Hansen P., Sørensen J.D. *Reliability-based code calibration of partial safety factors*. *JCSS Workshop on Reliability Based Code Calibration*; 21-22 March 2002; Zurich, Switzerland. 2002.

62. König G., Hosser D. *The simplified level II method and its application on the derivation of safety elements for level I. CEB Bulletin no 147 Conceptional preparation of future codes – Progress report*. Paris, France: Comité euro-international du béton; 1982.

63. Vrouwenvelder T., Scholten N. Assessment criteria for existing structures. *Structural Engineering International*. 2010; **1**, pp. 4.

64. Norwegian Public Roads administration (NPRA). *Costal Highway Route E39 - Project Overview* [Available from: https://www.vegvesen.no/vegprosjekter/ferjefriE39/english].

65. Nathwani J.S., Pandey M.D., Lind N.C. *Affordable safety by choice: the life quality method.* Waterloo, Canada: Institute for Risk Research, University of Waterloo; 1997.

66. Fischer K., Viljoen C., Faber M.H. *Deriving target reliabilities from the LQI*. *The LQI Symposium*; August 21-23, 2012; Kongens Lyngby, Denmark. 2012.

67. Baravalle M. *Matlab scripts for code calibration* 2017 [Available from: https://github.com/baravallemichele].

68. Cornell C.A. *Some comments on second-moment codes and on bayesian methods*. In: Freudenthal A.M., Shinozuka M., Konishi I., Kanazawa T., editors. *Reliability approach in structural engineering*. Maruzen, Tokyo; 1975. p. 17-26.

69. Ditlevsen O. *Uncertainty and Structural reliability. Hocus Pocus or Objective Modelling?* ABK D.t.H., editor. Lyngby1988.

70. Matheron G. *Estimating and Choosing: An Essay on Probability in Practice.* Springer Berlin Heidelberg; 2012.

71. Raiffa H., Schlaifer R. *Applied Statistical Decision Theory*. New York, USA: Wiley; 2000. 356 p.

72. Benjamin J.R., Cornell C.A. *Probability, statistics and decision for civil engineers*. New York, USA: McGraw-Hill; 1970.

73. Haukaas T., Der Kiureghian A. *FERUM - Finite Element Reliability Using Matlab*. Version 3.0; 1999. Available from: http://www.ce.berkeley.edu/projects/ferum/index.html.

74. Roscoe K., Diermanse F., Vrouwenvelder T. System reliability with correlated components: Accuracy of the equivalent planes method. *Structural Safety*. 2015; **57**, pp. 53-64.

75. Song J., Kang W.-H. System reliability and sensitivity under statistical dependence by matrix-based system reliability method. *Structural Safety*. 2009; **31**(2), pp. 148-56.

76. Pandey M.D., Nathwani J.S. Life quality index for the estimation of societal willingness-to-pay for safety. *Structural Safety*. 2004; **26**(2), pp. 181-99.

77. Fischer K., Faber M.H. *The LQI acceptance criterion and human compensation costs for monetary optimization - A discussion note*. *The LQI Symposium*; August 21-23, 2012; Kongens Lyngby, Denmark. 2012.

78. Rackwitz R. Optimization and risk acceptability based on the Life Quality Index. *Structural Safety*. 2002; **24**(2), pp. 297-331.

79. Baravalle M., Köhler J. A risk-based approach for calibration of design codes. *[Submitted manuscript]*. 2017;

80. Daniels H.E. The Statistical Theory of the Strength of Bundles of Threads. I. *Proceedings of the Royal Society of London Series A, Mathematical and Physical Sciences*. 1945; **183**(995), pp. 405-35.

81. Coles S. *An introduction to statistical modeling of extreme values*. London: Springer-Verlag 2004 2001. XIV, 209 p.

82. Baravalle M., Köhler J. *A framework for estimating the implicit safety level of existing design codes*. In: Bucher C., Ellingwood B., Frangopol D.M., editors. *Proc of the 12th International Conference on Structural Safety & Reliability (ICOSSAR2017)*. Vienna, Austria: TU-MV Media Verlag GmbH; 2017. p. 1037-46.

83. Fischer K., Virguez E., Sánchez-Silva M., Faber M.H. On the assessment of marginal life saving costs for risk acceptance criteria. *Structural Safety*. 2013; **44**(0), pp. 37-46.

84. Diamantidis D. *Report 32: Probabilistic Assessment of Existing Structures - A publication for the Joint Committee on Structural Safety (JCSS)*. RILEM; 2001.

85. Moan T. *Target levels for structural reliability and risk analysis of offshore structures*. In: Guedes S.C., editor. *Risk and Reliability in Marine Technology*. Rotterdam, The Netherlands: Balkema; 1998. p. 351-68.

86. Hauge L.H., Loseth R., Skjong R. *Optimal code calibration and probabilistic design*. In: Soares C.G., editor. *Proceedings of the 11th International Offshore Mechanics and Arctic Engineering Symposium*. 2. New York, USA: ASME; 1992. p. 191-9.

87. European Committee for Standardization (CEN). *EN 1995-1-1:2004/A1:2008 Eurocode 5: Design of timber structures. Part 1-1: General common rules and rules for buildings*. Brussels; 2004.

88. Nethercot D.A. Modern codes of practice: What is their effect, their value and their cost? *Struct Eng Int J Int Assoc Bridge Struct Eng*. 2012; **22**(2), pp. 176-81.

89. Colling F., Mikoschek M. *Simplified load combinations - Economic aspects and reliability*. *COST Action FP1402 - 3rd Workshop*; Stockholm, Sweden. 2016.

90. Gerhards C.C. *Time-Related Effects Of Loads On Strength Of Wood*. *Environmental Degradation of Engineering Materials Conference*; Blacksburg (Va.) , United States. 1977. p. 613-23.

91. Barrett J.D., Foschi R.O. Duration of Load and Probability of Failure in Wood - 2. Constant, Ramp, and Cyclic Loadings. *Canadian Journal of Civil Engineering*. 1978; **5**(4), pp. 515-32.

92. Barrett J.D., Foschi R.O. Duration of Load and Probability of Failure in Wood - 1. Modelling Creep Rupture. *Canadian Journal of Civil Engineering*. 1978; **5**(4), pp. 505-14.

93. Norsk Standard (NS). *NS-EN 1995-1-1:2004/A1:2008+NA:2010 Eurocode 5: Design of timber structures. Part 1-1: General common rules and rules for buildings*. Brussels; 2004.

94. German Institute for Standardization (DIN). *DIN 1052:2004-08. Entwurf, Berechnung und Bemessung von Holzbauwerken - Allgemeine Bemessungsregeln und Bemessungsregeln für den Hochbau*. Berlin; 2004.

95. Nowak A.S., Lind N.C. Practical code calibration procedures. *Canadian Journal of Civil Engineering*. 1979; **6**(1), pp. 112-9.

96. The MathWorks Inc. *MATLAB R2016a*. Version 9.0.0.341360; 2016.

97. Joint Committee on Structural Safety (JCSS). *CodeCal 03*. Version; 2003. Available from: http://www.jcss.byg.dtu.dk/Codecal.

98. Van der Hoven I. Power spectrum of horizontal wind speed in the frequency range from 0.0007 to 900 cycles per hour. *Journal of Meteorology*. 1957; **14**(2), pp. 160-4.

99. Hansen S.O., Pedersen M.L., Sørensen J.D. *Probability based calibration of pressure coefficients*. *Proc of the 14th International Conference on Wind Engineering*. Porto Alegre, Brazil; 2015.

100. Næss A., Leira B.J. *Long term stochastic modeling for combination of snow and wind load effects.* Rotterdam: Balkema; 2000.

101. Baravalle M., Köhler J. On the probabilistic representation of the wind climate for calibration of structural design standards. *Structural Safety*. 2018; **70**, pp. 115-27.

102. Davenport A.G. The relationship of reliability to wind loading. *Journal of Wind Engineering and Industrial Aerodynamics*. 1983; **13**(1–3), pp. 3-27.

103. Cook N.J. *The designer's guide to wind loading of building structures: static structures.* Building Research Establishment, Department of the Environment; 1990. 586 p.

104. Cook N.J. *The designer's guide to wind loading of building structures: Background, damage survey, wind data, and structural classfication.* Building Research Establishment, Department of the Environment; 1985. 371 p.

105. Botha J. *Probabilistic models of design wind loads in south africa* [Ph.D. Thesis]. Matieland, South Africa2016.

106. Holicky M., Sykora M. *Probabilistic models for wind actions*. *Proc of the Second International Symposium on Stochastic Models in Reliability Engineering, Life Science and Operations Management (SMRLO)*; 2016. p. 172-5.

107. International Organization for Standardization (ISO). *ISO 4354:2009 Wind actions on structures*. Lausanne, Switzerland; 2009.

108. Harris R.I. An improved method for the prediction of extreme values of wind effects on simple buildings and structures. *Journal of Wind Engineering and Industrial Aerodynamics*. 1982; **9**(3), pp. 343-79.

109. Der Kiureghian A. Analysis of structural reliability under parameter uncertainties. *Probabilistic Engineering Mechanics*. 2008; **23**(4), pp. 351-8.

110. Gumbel E.J. *Statistics of Extremes.* Columbia University Press; 1967.

111. Kruger A.C., Retief J.V., Goliger A.M. Strong winds in South Africa: Part 1 Application of estimation methods. *Journal of the South African Institution of Civil Engineering*. 2013; **55**(2), pp. 29-45.

112. Norwegian Meteorological Institute (MET). *eKlima* [Available from: http://sharki.oslo.dnmi.no/portal/page?_pageid=73,39035,73_39049&_dad=portal&_schema=PORTAL].

113. Wen Y.K. Wind direction and structural reliability. *Journal of Structural Engineering*. 1983; **109**(4), pp. 1028-41.

114. Grabemann I., Weisse R. Climate change impact on extreme wave conditions in the North Sea: an ensemble study. *Ocean Dynamics*. 2008; **58**(3), pp. 199-212.

115. Harris R.I. The accuracy of design values predicted from extreme value analysis. *Journal of Wind Engineering and Industrial Aerodynamics*. 2001; **89**(2), pp. 153-64.

116. Harris R.I., Cook N.J. The parent wind speed distribution: Why Weibull? *Journal of Wind Engineering and Industrial Aerodynamics*. 2014; **131**, pp. 72-87.

117. Cook N.J., Harris R.I. Exact and general FT1 penultimate distributions of extreme wind speeds drawn from tail-equivalent Weibull parents. *Structural Safety*. 2004; **26**(4), pp. 391-420.

118. Jordaan I. *Decisions Under Uncertainty: Probabilistic Analysis for Engineering Decisions.* Cambridge University Press; 2005.

119. Martins E.S., Stedinger J.R. Generalized maximum-likelihood generalized extreme-value quantile estimators for hydrologic data. *Water Resources Research*. 2000; **36**(3), pp. 737-44.

120. Akaike H. A new look at the statistical model identification. *IEEE Transactions on Automatic Control*. 1974; **19**(6), pp. 716-23.

121. Næss A., Gaidai O. Monte Carlo Methods for Estimating the Extreme Response of Dynamical Systems. *Journal of Engineering Mechanics*. 2008; **134**(8), pp. 628-36.

122. Karpa O., Naess A. Extreme value statistics of wind speed data by the ACER method. *Journal of Wind Engineering and Industrial Aerodynamics*. 2013; **112**(0), pp. 1-10.

123. Karpa O. *ACER User Guide* Online 2012 [Available from: http://folk.ntnu.no/karpa/ACER/ACER_User_guide.pdf].

124. Pickands J. Statistical inference using extreme order statistics. *The Annals of Statistics*. 1975; **3**(1), pp. 119-31.

125. Caers J., Maes M.A. Identifying tails, bounds and end-points of random variables. *Structural Safety*. 1998; **20**(1), pp. 1-23.

126. Davison A.C., Smith R.L. Models for Exceedances over High Thresholds. *Journal of the Royal Statistical Society Series B (Methodological)*. 1990; **52**(3), pp. 393-442.

127. Maes M.A. *Extrapolation into the unknown: modelling tails, extremes, and bounds*. 2003.

128. Kasperski M. Specification of the design wind load—A critical review of code concepts. *Journal of Wind Engineering and Industrial Aerodynamics*. 2009; **97**(7–8), pp. 335-57.

129. Harstveit K. *Extreme value analysis of hindcast wind data from the maritime areas surrounding Norway*. Norwegian Meteorological Institute; 2005, 29/11/20085. Report No.: 17/05.

130. Harris R.I. Gumbel re-visited - a new look at extreme value statistics applied to wind speeds. *Journal of Wind Engineering and Industrial Aerodynamics*. 1996; **59**(1), pp. 1-22.

131. Madsen H.O. Omission sensitivity factors. *Structural Safety*. 1988; **5**(1), pp. 35-45.

132. European Committee for Standardization (CEN). *EN 1993-1-1:2005 Eurocode 3 - Design of steel structures - Part 1-1: General rules and rules for buildings*. Brussels; 2005.

133. European Committee for Standardization (CEN). *EN 1992-1-1:2004 Eurocode 2: Design of concrete structures - Part 1-1: General rules and rules for buildings*. Brussels; 2004.

134. Cook N.J., Mayne J.R. A novel working approach to the assessment of wind loads for equivalent static design. *Journal of Wind Engineering and Industrial Aerodynamics*. 1979; **4**(2), pp. 149-64.

135. Ellingwood B., Galambos T.V., MacGregor J.G., Cornell C.A. *Development of a probability based load criterion for american national standard A58*. Washington: National Bureau of Standards; 1980.

136. European Committee for Standardization (CEN). *EN 1991-1-1:2002 Eurocode 1 - Actions on structures - Part 1-1: General actions - Densities, self-weight, imposed loads for buildings*. Brussels; 2002.

137. European Committee for Standardization (CEN). *EN 1991-1-3:2003 Eurocode 1: Actions on structures Part 1-3: General actions - Snow Loads*. Brussels; 2003.

138. European Committee for Standardization (CEN). *EN 1996-1-1:2005 Eurocode 6: Design of masonry structures Part 1-1: General rules for reinforced and unreinforced masonry structures*. Brussels; 2005.

139. Holmes J.D., Cochran L.S. Probability distributions of extreme pressure coefficients. *Journal of Wind Engineering and Industrial Aerodynamics*. 2003; **91**(7), pp. 893-901.

140. Kasperski M. Specification of the design wind load based on wind tunnel experiments. *Journal of Wind Engineering and Industrial Aerodynamics*. 2003; **91**(4), pp. 527-41.

141. Thiis T.K., O'Rourke M. Model for snow loading on gable roofs. *Journal of Structural Engineering*. 2015; **141**(12), pp. 04015051.

142. Corotis R., Sentler L. *CIB Report 116: Actions on structures - Live loads in buildings*. CIB; 1989.

Appendix A Penalty Functions for GOM and AM

The penalty functions (PF) proposed and utilised in the literature are summarized and compared in this Appendix.

A.1 Penalty functions

A.1.1 Penalty functions for the Global Optimisation Method (GOM)

The PFs for the generic j^{th} representative structure are listed below, the superscript number in brackets is introduced for distinguishing the functions.

- Squared deviations from β_t, see e.g. [7, 10]:

$$M_j^{(1)}\left(\mathbf{r},\beta_t\right)=\left(\beta_j\left(\mathbf{r}\right)-\beta_t\right)^2 \tag{A.1}$$

  Calibration objective: minimise the dispersion of β.
  Characteristic: symmetric in the β-domain.

- Squared deviations from $P_{f,t}$ [10]:

$$M_j^{(2)}\left(\mathbf{r},P_{f,t}\right)=\left(P_{f,j}\left(\mathbf{r}\right)-P_{f,t}\right)^2 \tag{A.2}$$

  Calibration objective: minimise the dispersion of P_f (since the expected failure consequences are proportional to P_f and not β).
  Characteristic: symmetric in the P_f-domain, highly non-symmetric in the β-domain.

- Cost optimisation [95]:

$$M_j^{(3)}\left(\mathbf{r},\beta_t,d\right)=\frac{\beta_j\left(\mathbf{r}\right)-\beta_t}{d}-1+\exp\left(-\frac{\beta_j\left(\mathbf{r}\right)-\beta_t}{d}\right)\qquad\left(d\approx 0.23\right) \tag{A.3}$$

  Calibration objective: minimise the total expected cost.
  Characteristics: the PF is derived modelling total expected costs as $C_T\left(\beta_j\right)=a\left(1+b\beta_j\right)+C_F\Phi^{-1}\left(-\beta_j\right)$ that is approximated as $a\left(1+b\beta_j\right)+C_F c\exp\left(-\beta_j/d\right)$, where: a,b are constants for modelling the initial costs, and c,d are constants for approximating the normal inverse cumulative density function. For differences $\beta_j\left(\mathbf{r}\right)-\beta_t$ close to zero, $M^{(3)}$ can be approximated by $c\cdot\left(\beta_j\left(\mathbf{r}\right)-\beta_{t,j}\right)^b$ where c and b are constants. The latter controls the skewness of the closeness function. For $c=1$ and $b=2$ $M^{(1)}$ is obtained [25].

- Generalised $M^{(3)}$ [25]:

$$M_j^{(4)}\left(\mathbf{r},\beta_t,k\right)=k\left(\beta_j\left(\mathbf{r}\right)-\beta_t\right)-1+\exp\left(-k\left(\beta_j\left(\mathbf{r}\right)-\beta_t\right)\right)\qquad\left(k>0\right) \tag{A.4}$$

  Calibration objective: control the asymmetry of the PF.

Characteristics: the PF is a generalization of $M^{(3)}$ that allows to control the asymmetry or skewness through the parameter k (the skewness increases with k). $M_j^{(4)}\left(\mathbf{r},\beta_t,k=1\right)$ is approximatively equal to $M^{(1)}$; while $M_j^{(4)}\left(\mathbf{r},\beta_t,k=1/d\right)$ is exactly equal to $M^{(3)}$.

- Unique calibration solution [36]:

$$M^{(5)}\left(\boldsymbol{\gamma},\beta_t,\varepsilon\right)=\left(\beta_j\left(\boldsymbol{\gamma}\right)-\beta_t\right)^2+\varepsilon\sum_i\left(\gamma_i-\gamma_{ji}^*\right)^2 \tag{A.5}$$

Calibration objective: account for the non-uniqueness problem into account and therefore providing a unique set of calibrated PSFs (In most calibration problems the solution is not unique since, in the LRFD, the material PSFs multiply the load PSFs leading to infinite sets of optimal PSFs).
Characteristics: The penalty functions force the PSF γ_i to be close to γ_{ji}^* that is the i[th] PSF estimated considering design situation j in isolation, ε weights the relative importance of the two terms and values of magnitude 1 are proposed. The summation in Eq. (A.5) is extended over all partial safety factors to be calibrated.

- Minimize dispersion [35]:

Calibration objectives: i) maintain the mean reliability equal to the previous version of the code and ii) minimise the scatter of reliability index. Since no PFs were explicitly reported in [35], the author proposes the following penalty function for reaching this objective:

$$M^{(6)}\left(\mathbf{r}^{(new)},\mathbf{r}^{(old)},\zeta\right)=\left(\mu_{\mathrm{B}}\left(\mathbf{r}^{(new)}\right)-\mu_{\mathrm{B}}\left(\mathbf{r}^{(old)}\right)\right)^2+\zeta\left(\sigma_{\mathrm{B}}\left(\mathbf{r}^{(new)}\right)\right)^2 \tag{A.6}$$

where $\mu_{\mathrm{B}}\left(\mathbf{r}\right)=\sum_{j=1}^m\beta_j\left(\mathbf{r}\right)\Big/m$ and $\sigma_{\mathrm{B}}\left(\mathbf{r}\right)=\sqrt{\sum_{j=1}^m\left(\beta_j\left(\mathbf{r}\right)-\beta_t\right)^2\Big/\left(m-1\right)}$ are the mean and standard deviation of the reliability indices associated to the different representative structures, respectively; the superscripts indicate the old and new code; and ζ controls the relative importance between minimizing the scatter and obtaining the same mean value.
Characteristics: an appropriate value of ζ is essential for reaching both the objectives. In fact, the absolute minimum scatter might be found for $\mu_{\mathrm{B}}\left(\mathbf{r}^{(new)}\right)\neq\mu_{\mathrm{B}}\left(\mathbf{r}^{(old)}\right)$. According with the author's experience the value of ζ depends on the case at hand.

- Squared deviations from $\log_{10}\left(P_{f,\mathrm{t}}\right)$ [34]:

$$M_j^{(7)}\left(\mathbf{r},\mathrm{P}_{f,t}\right)=\left\{\log_{10}\left(P_{f,j}\left(\mathbf{r}\right)\right)-\log_{10}\left(P_{f,\mathrm{t}}\right)\right\}^2 \tag{A.7}$$

Calibration objective: minimise the deviations of $\log_{10}\left(P_f\right)$, the use of logarithm is proposed since $\log_{10}\left(P_f\right)$ has a more linear relationship with the initial cost of the structure compared with P_f.
Characteristics: in the referenced article, $P_{f,t}$ is obtained from the existing version of code by $P_{f,\mathrm{t}}=\sum_j w_j P_{f,j}^{(old)}$ with $\sum_j w_j=1$.

- Maximum absolute scatter [25]:

$$M^{(8)}\left(\mathbf{r},\beta_t\right)=\max_j\left|\beta_t-\beta_j\left(\mathbf{r}\right)\right| \tag{A.8}$$

Calibration objective: minimizing the maximum absolute deviation from β_t.
Characteristics: the PF neither limit nor minimise the reliability index scatter.

- Squared deviations from target design [135]:

$$M^{(9)}(\mathbf{r}, z_t) = \left(p_j(\mathbf{r}) - p_{t,j}\right)^2 \tag{A.9}$$

Calibration objective: minimizing the deviation from the design p_t giving $\beta_j = \beta_t$.

A.1.2 Penalty functions for calibration with a AM

- PF $M^{(3)}$ adapted for AM [11]:

$$M_j^{(10)}\left(\hat{\boldsymbol{\alpha}}, \boldsymbol{\alpha}_j, \beta_{t,j}\right) = \left[\frac{\beta_{t,j}\left(\boldsymbol{\alpha}_j^T\hat{\boldsymbol{\alpha}} - 1\right)}{d} - 1 + \exp\left(\frac{\beta_{t,j}\left(\boldsymbol{\alpha}_j^T\hat{\boldsymbol{\alpha}} - 1\right)}{d}\right)\right] \tag{A.10}$$

  Calibration objective: see $M^{(3)}$.
  Characteristics: see $M^{(3)}$.

- PF $M^{(4)}$ adapted for AM [2].

$$M_j^{(11)}\left(\hat{\boldsymbol{\alpha}}, \beta_{t,j}, k\right) = \left[k\beta_{t,j}\left(\boldsymbol{\alpha}_j^T\hat{\boldsymbol{\alpha}} - 1\right) - 1 + \exp\left(-k\beta_{t,j}\left(\boldsymbol{\alpha}_j^T\hat{\boldsymbol{\alpha}} - 1\right)\right)\right] \qquad (k > 0) \tag{A.11}$$

  Calibration objective: see $M^{(4)}$.
  Characteristics: see $M^{(4)}$.

- Vrouwenvelder and Siemes [23]:

$$M_j^{(12)}\left(\mathbf{r}, \mathbf{x}_k, \beta_t, \boldsymbol{\mu}_X, \boldsymbol{\sigma}_X, \boldsymbol{\alpha}\right) = \sum_{j=1}^{n}\left\{\sum_{i=1}^{m+t}\alpha_{ji}\left\{\frac{r_i x_{k,i} - \mu_{X_i} + \alpha_{ji}\beta_t\sigma_{X_i}}{\sigma_{X_i}}\right\}\right\}\frac{\alpha_{jl}x_{k,l}}{\sigma_{X_l}} \tag{A.12}$$

  Where: $\mathbf{x}_k$ is the vector of characteristic or nominal values, $\boldsymbol{\mu}_X, \boldsymbol{\sigma}_X$ are the vectors of mean values and standard deviation values, and $\boldsymbol{\alpha}$ is the vector of FORM sensitivity factors ($\alpha > 0$ for resistance variables, $x_d = \gamma x_k$ for all variables).
  Calibration objective: minimise the squared differences between FORM design point coordinates and design value obtained as characteristic value multiplied by PSF $\gamma_i x_{i,k}$.

- PF $M^{(1)}$ adapted for AM:

$$M^{(13)}\left(\hat{\boldsymbol{\alpha}}, \beta_t\right) = \left[\beta_t\left(\boldsymbol{\alpha}_j^T\hat{\boldsymbol{\alpha}} - 1\right)\right]^2 \tag{A.13}$$

  Calibration objective: see $M^{(1)}$.
  Characteristics: see $M^{(1)}$.

A.2 Comparison of calibration methods and penalty functions

The AM and GOM applied with the different penalty functions are compared in an illustrative calibration exercise. The standardized limit state function in Eq. (A.14) and the related design equations in Eq. (A.15) based on the Eurocode semi-probabilistic safety format are considered. The random variables are summarized in Table A.1 together with the partial safety factors of the existing code.

$$g(\mathbf{X}, p) = p\Theta_i R_i - \delta G - (1 - \delta)Q \tag{A.14}$$

$$p = \frac{\gamma_{M,i}}{r_{k,i}}\left[\gamma_G \delta g_k + \gamma_Q (1-\delta) q_k\right] \tag{A.15}$$

In total 33 representative and equally weighted design situations are considered by varying $\delta = [0, 0.1, ...1]$ for three different materials. The FORM was used for calculating the reliability index by using the FERUM scripts [73] in Matlab [96]. The average reliability index with the PSFs given in Table A.1 was found to be $\mu_B(\mathbf{r}^{(old)}) \approx 4.42$ and the standard deviation $\sigma_B(\mathbf{r}^{(old)}) \approx 0.48$. All reliability indices refer to 1 year period.

Table A.1. Basic random variables, characteristic fractiles and initial partial safety factors.

	Distr.	μ_X	COV_X	$F_X(x_k)$	$\mathbf{r}^{(old)}$
R_1 - steel yielding strength	Logn.	1.00	7 %	0.05	γ_{M1} = 1.10
R_2 - concrete compression strength	Logn.		15 %	0.05	γ_{M2} = 1.50
R_3 - timber bending strength	Logn.		20 %	0.05	γ_{M3} = 1.30
Θ_1 - model unc. for steel elements	Logn.		5 %	$F_{\Theta_1}(\mu_{\Theta_1})$	/
Θ_2 - model unc. for concrete elements	Logn.		10 %	$F_{\Theta_2}(\mu_{\Theta_2})$	/
Θ_3 - model unc. for timber elements	Logn.		10 %	$F_{\Theta_3}(\mu_{\Theta_3})$	/
G - self-weight	Norm.		10 %	0.50	γ_G = 1.35
Q - variable load yearly maxima	Gumb.		40 %	0.98	γ_Q = 1.50

The following reliability elements are calibrated $\mathbf{r} = [\gamma_{M1}, \gamma_{M2}, \gamma_{M3}, \gamma_G, \gamma_Q]$, $\beta_t = 4.4$ was arbitrarily selected. The optimal vectors of PSFs are reported in Table A.3 and the results are compared in Figure A.1. Since the problem presents ∞^1 solutions, the condition $\gamma_G \equiv 1.35$ was imposed. The calibrated partial safety factors using different measures of closeness were similar except for penalty functions with large skewness ($M^{(2)}$ and $M^{(4)}$ with large k) that were leading to reliabilities close to or larger than the target beta. Larger differences on the calibrated partial safety factors are expected when the reliability index standard deviation over the considered design situations increases.

For the AM method, the $\boldsymbol{\alpha}_j$ were calculated choosing the design parameter p giving $\beta = \beta_t$. The elements of the $\hat{\boldsymbol{\alpha}}$-vector corresponding to the model uncertainty were fixed since the design values of the model uncertainty were set equal the mean. Moreover, the element of the $\hat{\boldsymbol{\alpha}}$-vector corresponding to the self-weight is fixed since γ_G is arbitrarily fixed to 1.35 for comparing the different methods.

The $\hat{\boldsymbol{\alpha}}$-vector at optimum utilizing the closeness function $M^{(10)}$ is reported in Table A.2 and is compared with the $\boldsymbol{\alpha}_j$ vectors in Figure A.2. The corresponding PSFs are $\mathbf{r} = [1.08 \quad 1.23 \quad 1.29 \quad 1.35 \quad 1.65]$. The $\hat{\boldsymbol{\alpha}}$-vector obtained with $\beta_t = 4.0$ (see Table A.2) results in partial safety factors for a target reliability of 4.4 equal to $\mathbf{r} = [1.05 \quad 1.19 \quad 1.25 \quad 1.39 \quad 1.70]$ that are similar to the ones calibrated before. This shows that the β_t used for determining $\hat{\boldsymbol{\alpha}}$-vector is of little importance. Thus, this calibration method very practical. The method proposed by Eurocode 0 [18] for calibrating partial safety factors based of test results is based on this method and makes use of fixed sensitivity factors which are independent of the target reliability.

Table A.2. Components of the $\hat{\boldsymbol{\alpha}}$-vector ($1/\beta_t \, \Phi^{-1}\left(F_{\Theta_i}\left(\theta_{d,i}\right)\right)$ with $\theta_{d,i} = \theta_{k,i} \cdot \gamma_{\Theta_i} = \mu_{\Theta_i} \cdot 1.0$; § $1/\beta_t \, \Phi^{-1}\left(F_{X_G}\left(g_d\right)\right)$ with $g_d = \gamma_G \cdot g_k = 1.35 \cdot \mu_G$; # $\hat{\boldsymbol{\alpha}}$-vector derived with $\beta_t = 4.0$).*

	$\hat{\alpha}_{Ri}$	$\hat{\alpha}_{\Theta i}$ *	$\hat{\alpha}_G$ §	$\hat{\alpha}_Q$
Steel	- 0.643 - 0.536#	- 0.006 - 0.006#		
Concrete	- 0.688 - 0.635#	- 0.011 - 0.013#	+ 0.800 + 0.875#	+ 0.783 +0.804#
Timber	- 0.669 - 0.629#	- 0.011 - 0.013#		

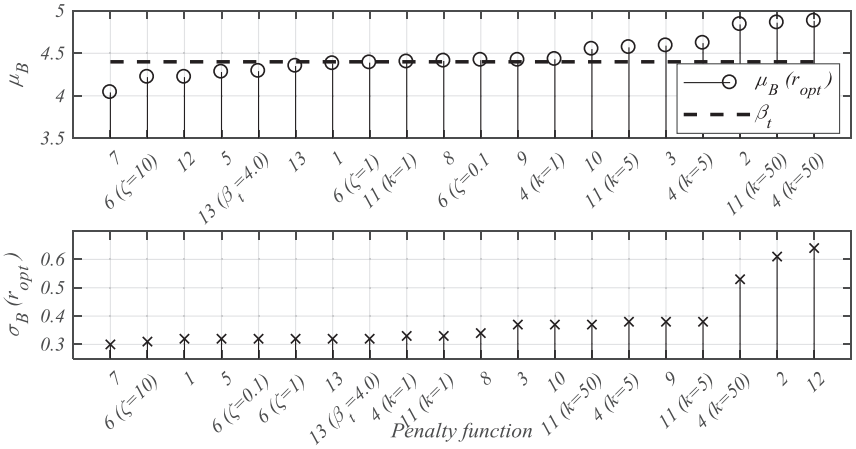

Figure A.1. Mean reliability index (top) representing the "conservativeness" of the penalty function and reliability index standard deviation (bottom) representing the "homogeneity" of the resulting reliability index.

Table A.3. Calibrated partial safety factors for different penalty functions with fixed $\gamma_G = 1.35$ (γ_G not fixed to 1.35; $^{\S} P_{f,\mathrm{t}} = \sum_j w_j P_{f,j}^{(old)} = 2.2 \cdot 10^{-5}$; $^{\#}\hat{\boldsymbol{\alpha}}$ calculated with $\beta_t = 4.0$).*

	$M(\,)$	γ_{M1}	γ_{M2}	γ_{M3}	γ_G	γ_Q	μ_{B}	σ_{B}
GOM	1	1.08	1.24	1.31	1.35	1.66	4.38	0.32
	2	1.41	1.44	1.51	1.35	1.46	4.84	0.61
	3	1.18	1.32	1.41	1.35	1.60	4.59	0.37
	4 ($k = 1$)	1.11	1.26	1.33	1.35	1.64	4.43	0.33
	4 ($k = 5$)	1.20	1.33	1.42	1.35	1.59	4.62	0.38
	4 ($k = 50$)	1.35	1.40	1.53	1.35	1.53	4.88	0.53
	5 ($\varepsilon = 1$)	1.14	1.31	1.39	1.24*	1.55	4.28	0.32
	6 ($\zeta = 0.1$)	1.09	1.25	1.32	1.35	1.67	4.42	0.32
	6 ($\zeta = 1$)	1.09	1.25	1.31	1.35	1.67	4.39	0.32
	6 ($\zeta = 10$)	1.06	1.21	1.26	1.35	1.61	4.22	0.31
	7[§]	1.03	1.16	1.21	1.59	1.57	4.04	0.30
	8	1.06	1.27	1.36	1.11	1.65	4.41	0.34
	9	1.10	1.16	1.20	1.35	1.82	4.42	0.38
AM	10 ($d = 0.23$)	1.18	1.30	1.39	1.35	1.59	4.55	0.37
	11 ($k = 1$)	1.11	1.25	1.32	1.35	1.63	4.40	0.33
	11 ($k = 5$)	1.20	1.31	1.40	1.35	1.58	4.57	0.38
	11 ($k = 50$)	1.21	1.38	1.50	1.35	1.70	4.86	0.37
	12	1.11	1.44	1.74	1.35	1.17	4.22	0.64
	13	1.08	1.23	1.29	1.35	1.65	4.35	0.32
	13[#]	1.08	1.19	1.25	1.39	1.70	4.29	0.32

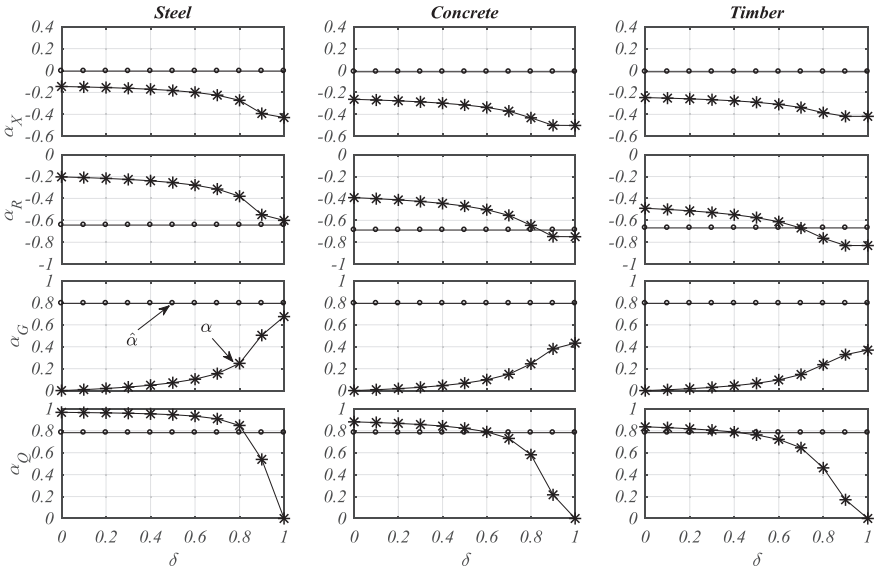

Figure A.2. FORM sensitivity factors and $\hat{\boldsymbol{\alpha}}$-vector for the three materials and the different representative structures.

Appendix B Reliability-Based Calibration of Partial Safety Factors in the Eurocodes

Report

Authors: M. Baravalle[a], J. Köhler[a] , J. D. Sørensen [b]
[a] Department of Structural Engineering, Norwegian University of Science and Technology, Trondheim
[b] Department of Civil Engineering, Aalborg University, Aalborg

This Appendix presents the preliminary calibration of the Partial Safety Factors (PSFs) in the Eurocodes performed in the CEN/TC250 Subcommittee 10 Working Group 1 (CEN/TC250-SC10-WG1). The calibration aims to reduce the variability of reliability among different example structures maintaining the current average reliability level.

To date, the Eurocodes recommend a unique PSF for all variable loads such as snow, wind and imposed loads. In this study, the PSFs are differentiated among the variable actions. This allows achieving a more uniform reliability after calibration. Further, it is investigated whether the safety factor for permanent actions should be differentiated between the permanent load and the self-weight of the load-bearing structure. In addition, the variable load PSF is calibrated for a generic time-variant action as a function of the coefficient of variations of the load yearly maxima and the load model uncertainty. A similar calibration is performed for a generic material. The obtained PSFs can be utilized when detailed information on the stochastic models representing the actions or the resistance are available. For the material side, the sensitivity factors to be used in the design value method (Annex C to EN 1990:2002) corresponding to the calibrated material PSFs are also calculated. Finally, the future work necessary to complete this preliminary study is discussed.

B.1 Introduction

This Appendix reports the calibration of the reliability elements in the Eurocodes. The work is part of the task of the CEN/TC250-SC10/WG1 and is still in a preliminary state since input from other Subcommittees and Working Groups are missing. At this stage, the document aims primarily at illustrating the methodology for calibrating the reliability elements. The final results could change after all input have been agreed.

The calibration aims to reduce the variability of reliability levels among different example structures. This is achieved by calibrating the partial safety factors (PSFs) with a target reliability equal to the average reliability index obtained with the partial factors recommended in the present version of the Eurocodes [15, 18, 87, 132, 133, 136, 137, 138]. The average reliability of the structures designed with the current reliability elements is considered satisfactory. Thus, it is outside the scope of this work to calibrate the partial load factors to an absolute reliability level.

The basic approach is to estimate the target reliability level using the stochastic models for the uncertain parameters, generic and simple limit state equations, and representative generic example structures.

B.2 Methods

The calibration is performed in two main steps. The first step aims at calibrating the partial factors on the load side that are later utilized for calibrating the PSFs on the resistance side by the committees revising the Eurocodes covering the different construction materials.

In the first part, the load PSFs are calibrating maintaining the PSFs on the resistance side and the load combination factors (ψ_0 and ξ in [18]) fixed and equal to the recommended values. A reduction of the reliability variability is achieved by differentiating the load partial safety factors. In the EN 1990:2002, a unique safety factor is recommended for the permanent load and the self-weight of the load-bearing structure ($\gamma_G = 1.35$), and a unique safety factor is recommended for all variable loads such as snow, wind and imposed load ($\gamma_Q = 1.50$). In the current work, different partial factors are calibrated for the mentioned loads. The calibration is performed for both load combination rules included in EN 1990:2002 [18]. These load combinations are given in the EN 1990:2002 in Eq. 6.10 and Eq. 6.10a&b. Thus, they are referred to as load combination "*6.10*" and "*6.10a&b*" in this work. Further, the PSF for a generic variable load is calibrated with the aim of providing a more detailed value of the safety factor for cases when precise information on the stochastic models representing the variable loads is known.

The second part of the work aims at calibrating the material partial safety factor (γ_M) and the sensitivity factor for the design point method in [18]. At this stage, the calibration is performed for a generic material for two reasons: i) illustrating the methodology that can be later applied by the committees responsible for revising the Eurocodes for the different materials and ii) provide detailed values of γ_M dependent on the uncertainties on the material property and on the resistance model. This part will be completed by considering material-dependent limit state functions representing specific failure modes in order to accurately calibrated the safety factors on the resistance side.

B.3 Calibration of the partial safety factors on the load side

B.3.1 Limit state function and design situations

A generic limit state function is utilized for calibrating the PSFs on the load side. The generality allows to catch all the most important details affecting the reliability problem and to cover a broad range of structures, failure modes and structural elements. Indeed, the load partial safety factors are material-independent thus they need to be calibrated considering all possible design situations (e.g., material properties, failure modes and so forth) simultaneously.

The limit state function representing a failure mode dominated by the material property R_i and under the effects of the self-weight (G_S), the permanent (G_P) and the variable (Q_j) loads is given in Eq. (B.1)

$$g_1\left(\mathbf{X}, p_{ij}\right) = p_{ij}\Theta_{R,i}R_i - \left(1-a_Q\right)\left[a_G G_{S,U} + \left(1-a_G\right)G_{P,U}\right] - a_Q\Theta_{Q,j}Q_j \tag{B.1}$$

where:

- The notation, the random variables and the probabilistic models are reported in Section B.3.2.
- a_Q is a parameter representing different proportions between variable and permanent loads ($a_Q = 1$ for variable load only). Ten equally spaced and equally weighted values in the ranges reported in Table B.1 are considered.
- a_G is a parameter representing different proportions between permanent load and self-weight ($a_G = 1$ for self-weight only). Three equally spaced and equally weighted values in the ranges reported in Table B.1 are considered.
- The six material properties listed in Table B.1 are considered.
- Wind ($j = 1$), snow ($j = 2$) and imposed ($j = 3$) loads are considered.
- The design variable p_{ij} in Eq. (B.1) is calculated with the design equations in the semi-probabilistic format for the material property i and the variable load j in Eq.(B.2) for "*6.10a&b*" and in Eq. (B.3) for "*6.10*".

$$p_{ij} = \max\left\{\begin{array}{l} \dfrac{\gamma_{M,i}}{\theta_{Ri,k}r_{i,k}}\left\{\left(1-a_Q\right)\left[a_G g_{S,k}\gamma_{GS} + \left(1-a_G\right)g_{P,k}\gamma_{GP}\right] + a_Q\psi_{0,j}\gamma_Q\theta_{Qj,k}q_{j,k}\right\} \\ \dfrac{\gamma_{M,i}}{\theta_{Ri,k}r_{i,k}}\left\{\left(1-a_Q\right)\left[a_G g_{S,k}\xi\gamma_{GS} + \left(1-a_G\right)g_{P,k}\xi\gamma_{GP}\right] + a_Q\gamma_Q\theta_{Qj,k}q_{j,k}\right\} \end{array}\right\} \tag{B.2}$$

$$p_{ij} = \frac{\gamma_M}{\theta_{Ri,k}r_{i,k}}\left\{\left(1-a_Q\right)\left[a_G g_{S,k}\gamma_{GS} + \left(1-a_G\right)g_{P,k}\gamma_{GP}\right] + a_Q\gamma_Q\theta_{Qj,k}q_{j,k}\right\} \tag{B.3}$$

Table B.1. Material properties, weights and ranges of variations of a_G and a_Q.

i	Mat. property	$w_{R,i}$ (weight)	a_G ranges	a_Q ranges	$\gamma_{M,i}$ recommended in current Eurocodes
1	Structural steel yielding strength	40 %	[0.6; 1.0]	[0.2; 0.8]	1.00 [132]
2	Concrete compressive strength	15 %		[0.1; 0.7]	1.50 [133]
3	Re-bar yield strength	25 %		[0.1; 0.7]	1.15 [133]
4	Glulam timber bending strength	7.5 %		[0.2; 0.8]	1.25 [87]
5	Solid timber bending strength	2.5 %		[0.2; 0.8]	1.30 [87]
6	Masonry compression strength	10 %		[0.1; 0.7]	1.50 [138]

The limit state in Eq. (B.1), the values of the parameters, the loads and the material properties were selected with the aim of covering the most common design situations for normal buildings whereas bridges and other types of structures were excluded from this work. For example, the failure of reinforced concrete elements (beams and columns) due to the failure of concrete in compression under different proportions of actions induced by the live load, self-weight and permanent loads are accounted by R_i representing the concrete compression strength.

B.3.2 Stochastic models

The random variables and the stochastic models for the reliability analysis agreed in the CEN/TC250-SC10/WG1 and mainly based on [9] are summarised in Table B.2. The level of detail of the set of probabilistic models selected fits to the level of detail of the limit sate function utilized in this part of the work.

*Table B.2. Stochastic models based on [13] unless otherwise specified (*yearly maxima).*

Random variable		Distr. type	Mean (μ)	COV	Ch. Fract. (value)	Ref. and notes
Resistance model unc. (steel)	$\Theta_{R,1}$	Logn.	1.00	0.05	(μ)	
Resistance model unc. (concrete)	$\Theta_{R,2}$	Logn.	1.00	0.10	(μ)	
Resistance model unc. (rebar)	$\Theta_{R,3}$	Logn.	1.00	0.10	(μ)	
Resistance model unc. (glulam)	$\Theta_{R,4}$	Logn.	1.00	0.10	(μ)	
Resistance model unc. (solid timber)	$\Theta_{R,5}$	Logn.	1.00	0.10	(μ)	
Resistance model unc. (masonry)	$\Theta_{R,6}$	Logn.	1.16	0.175	(μ)	
Mat. property (steel yielding strength)	R_1	Logn.	1.00	0.07	$\mu-2\sigma$	
Mat. property (concrete compr. capacity)	R_2	Logn.	1.00	0.15	0.05	
Mat. Property (rebar yielding strength)	R_3	Logn.	1.00	0.07	0.05	
Mat. property (glulam bending strength)	R_4	Logn.	1.00	0.15	0.05	
Mat. property (solid timber bending strength)	R_5	Logn.	1.00	0.20	0.05	
Mat. property (masonry compr. strength)	R_6	Logn.	1.00	0.16	0.05	
Self-weight (steel)	$G_{S,1}$	Norm.	1.00	0.04	0.50	See B.3.2.1
Self-weight (concrete)	$G_{S,2}$	Norm.	1.00	0.05	0.50	
Self-weight (rebar)	$G_{S,3}$	Norm.	1.00	0.05	0.50	
Self-weight (glulam)	$G_{S,4}$	Norm.	1.00	0.10	0.50	
Self-weight (solid timber)	$G_{S,5}$	Norm.	1.00	0.10	0.50	
Self-weight (masonry)	$G_{S,6}$	Norm.	1.00	0.065	0.50	
Permanent load	G_P	Norm.	1.00	0.10	0.50	
Permanent load (large COV)	G_P^*	Norm.	1.00	0.20	0.95	
Wind time-invariant part (gust C_g ,pressure C_{pe} and roughness C_r coefficients)	Θ_{Q_1}	Logn.*	0.79*	0.24*	(1.095)*	* Parameters of the Logn. distribution approximating the upper tail (> 0.90 fractile) of the distribution representing $\Theta_Q = C_g C_r C_{pe}$ with: C_{pe} Gumbel [134, 139], $\mu_{C_{pe}} = 1; COV_{C_{pe}} = 0.15$ and ch. fractile 0.78 [99, 140] (0.80 is suggested in [107]); C_r Logn., $\mu_{C_r} = 0.80; COV_{C_r} = 0.15$ and ch. value = 1.00; C_g Logn., $\mu_{C_g} = 1; COV_{C_g} = 0.10$ and ch. value = 1.00.
Snow time-invariant part (model uncertainty and shape coefficient)	Θ_{Q_2}	Logn.	1.00	0.30	($\mu+\sigma$)	Ch. value equal to $\mu+\sigma$ given in [13, 141]; ch. Value equal to the mean given in [58].
Wind mean reference velocity pressure *	Q_1	Gumb.	1.00	0.25	0.98	When the COV varies over the country and only one PSFs is sought the mean COV over the country can be used, see [101]. Alternatively, PSFs can vary over the territory; this is a national choice.
Snow load on roof *	Q_2	Gumb.	1.00	0.40	0.98	
Imposed load model uncertainty	Θ_{Q_3}	Logn.	1.00	0.10	(1.00)	The COV is assumed since no data are found in the literature. To be further assessed. [Not yet discussed in CEN/TC250-SC10/WG1].
Imposed load *	Q_3	Gumb.	1.00	0.53	0.98	See B.3.2.2. [Not yet discussed in CEN/TC250-SC10/WG1].

B.3.2.1 Stochastic models representing the self-weight of the load-bearing structure

In the JCSS Probabilistic Model Code [13] (PMC) Section 2.1, the self-weight of structural elements of the material i is modelled as

$$G_{S,i} = \int_{Vol} \rho_i \, dV \tag{B.4}$$

where:

- ρ_i is the weight density which is uncertain, and
- Vol is the volume of the structural element which is affected by deviations from the nominal values which are material-dependent.

The geometrical dimensions (thickness, cross-sectional area and so forth) are modelled as $d = d_{nom} + \delta$ where d_{nom} is the nominal dimension (deterministic) and δ is the deviation which is represented by a normal distribution with parameters μ_δ, COV_δ. It follows that d is also normally distributed with parameters $\mu_d = d_{nom} + \mu_\delta; \sigma_d = \sigma_\delta$.

The self-weight of a generic structural element of a specific material is needed in the current calibration. Therefore, a random variable $G_{S,i}$ representing the deviation of the self-weight from its nominal value for a generic element of the i^{th} material is obtained fitting a Normal distribution to the values sampled with crude Monte Carlo for different types of elements and absolute dimensions. The self-weight is normalised with respect to the nominal dimensions and the mean density (i.e. in the following, ρ is the weight density divided by its mean value and Vol is the volume divided by the nominal volume). The uncertainties related to the assumed sampling frequencies and the "empirical fit" might be accounted for by rounding up the coefficient of variation.

Assuming statistical independence, the self-weight of n elements is $G_{S,i} = \sum_{j=1}^{n} G_{S,ij}$ which has $COV_{G_{S,i}} < COV_{G_{S,ij}}$. Thus, using the coefficient of variation for the self-weight of one element might be conservative.

Results

The concrete normalized weight density is represented by a Normal distribution $\rho \sim N\left(\mu_\rho = 1.00; COV_\rho = 0.04\right)$ [13]. The self-weight of a concrete element of length l and cross-section $d_1 \times d_2$ is $G_S = d_1 d_2 l \rho$. The parameters of the Normal distribution representing the self-weight G_S of a generic concrete element estimated from the samples are: $\mu_{G_S} = 1.00; COV_{G_S} = 0.044 \approx 0.05$ (obtained with the stochastic models and sampling frequencies in Table B.3 and d_1, d_2 uncorrelated). The weight of the reinforcement was accounted increasing density of concrete.

Table B.3. Concrete elements cross-section dimensions and sampling frequencies (Assumed approximatively one third of the in-situ tolerances).*

		Geometrical dimension		
Type of element	Relative sampling frequency w_k (assumed)	Symbol	Mean μ	COV
Large elements casted in-situ $1000mm < d_{i,nom} < 2000mm$	20 %	$d_i \ (i=1,2)$	$d_{nom} + 3mm$	$\frac{10mm}{d_{nom} + 3mm}$
Small elements casted in situ $100mm < d_{i,nom} < 1000mm$	50 %	$d_i \ (i=1,2)$	$d_{nom}(1+0.003)$	$\frac{4 + 0.006 d_{nom}}{d_{nom}(1+0.003)}$
Large precast elements	20 %	$d_i \ (i=1,2)$	$d_{nom} + 1mm$ *	$\frac{3mm}{d_{nom} + 1mm}$
Small precast elements	10 %	$d_i \ (i=1,2)$	$d_{nom}(1+0.001)$ *	$\frac{1 + 0.002 d_{nom}}{d_{nom}(1+0.001)}$

The structural steel normalized weight density is represented by $\rho \sim N\left(\mu_\rho = 1.00; COV_\rho = 0.01\right)$ [13]. The self-weight of a steel profile with length l and cross-section area A is equal to $G_s = Al\rho$. The self-weight of a plate of thickness t and dimensions $l_1 \times l_2$ is $G_s = l_1 l_2 t \rho$. The parameters of the Normal distribution representing the self-weight G_S of a generic steel element estimated from the samples are: $\mu_{G_S} = 1.00; COV_{G_S} = 0.033 \approx 0.04$ (obtained with the stochastic models and sampling frequencies in Table B.4 and $l = l_1 = l_2 = 1$). The COV is rounded up to 0.04 accounting for welds, bolts, stiffeners and so on.

Table B.4. Steel elements cross-section dimensions and sampling frequencies.

		Geometrical dimension		
Type of element	Relative sampling frequency w_k (assumed)	Symbol	μ	COV
Profiles	50 %	Cross-sectional area A	$A_{nom}(1+0.01)$	$\frac{0.04 A_{nom}}{A_{nom}(1+0.01)}$
Plates	50 %	Thickness t	$t_{nom}(1+0.01)$	$\frac{0.02 t_{nom}}{t_{nom}(1+0.01)}$

The timber normalized weight density is represented by $\rho \sim N\left(\mu_\rho = 1.00; COV_\rho = 0.1\right)$ [13]. The self-weight of a timber element of length l and cross-section $d_1 \times d_2$ is $G_s = d_1 d_2 l \rho$. The parameters of the Normal distribution representing the self-weight G_S of a generic timber element estimated from the samples are: $\mu_{G_S} = 1.00; COV_{G_S} = 0.105 \approx 0.10$ (obtained with the stochastic models and sampling frequencies in Table B.5 and $l = 1$). The steel elements in the joints (e.g., bolts and dowels) are not accounted.

Table B.5. Timber elements cross-section dimensions and sampling frequencies.

	Relative sampling frequency w_k (assumed)	Geometrical dimension	μ	COV
Sawn $(0.05m < (d_1, d_2) < 0.45m)$	10 %	$d_i \ (i = 1,2)$	$d_{nom}(1+0.05)$	$\frac{2mm}{d_{nom}(1+0.05)}$
Glulam ($0.05m < d_1 < 1.55m$; $0.05m < d_2 < 0.45m$)	90 %	$d_i \ (i = 1,2)$	d_{nom}	$\frac{1mm}{d_{nom}}$

B.3.2.2 Stochastic models representing the imposed load

According to the JCSS PMC, the live load is modelled as the sum of equivalent uniformly distributed sustained (Q) and intermittent (P) loads where:

- The sustained load intensity is modelled as $Q \sim Gamma\left(\mu_Q = m_Q; \sigma_Q = \sqrt{\sigma_V^2 + \sigma_U^2 \kappa A_0 / A}\right)$. The load process is modelled as a Poisson rectangular pulse process with mean duration $\mu_{d,Q} = 1/\lambda_Q$. The sustained load is always "on" in the sense that probability of a non-zero realisation is equal to 1.
- The intermittent load intensity given non-zero realisation is modelled as $P \sim Exponential\left(\mu_P = \sigma_P = m_P\right)$. The load is modelled as a Poisson rectangular pulse process with mean duration $\mu_{d,P} = 1/\lambda_P$ (λ_P is the mean occurrence rate of zero and non-zero realisation). The probability of a non-zero realisation is equal to p_0. The mean occurrence rate of the non-zero realisations is $\upsilon_P = p_0 \lambda_P$.

The spatial variability of the loads is accounted by using an equivalent uniformly distributed load (EUDL) as described in the PMC Section 2.0.5.2.

The parameters of the distribution representing the maxima over a specific time period are estimated fitting a Gumbel distribution to the maxima sampled with crude Monte Carlo. The Gumbel is fitted to the upper tail of the cumulative density (fractiles larger than 0.75). The estimated parameters are summarised in Table B.7, the input for its derivation are summarised in Table B.6. One sampled time history is illustrated in Figure B.1. The cumulative density functions are shown in Figure B.2.

Table B.6. Parameters of the Poisson processes representing the sustained and intermittent loads.

	Q. Sustained load				P - Intermittent load			
Use	m_Q $[N/m^2]$	σ_V $[N/m^2]$	σ_U $[N/m^2]$	$\mu_{d,Q} = 1/\lambda_Q$ $[a]$	m_P $[N/m^2]$	$\mu_{d,P} = 1/\lambda_P$ $[days]$	$1/\upsilon_P$ $[a]$	$p_0 = \upsilon_P / \lambda_P$
Office	500	300	600	5	200	2	0.3	0.018

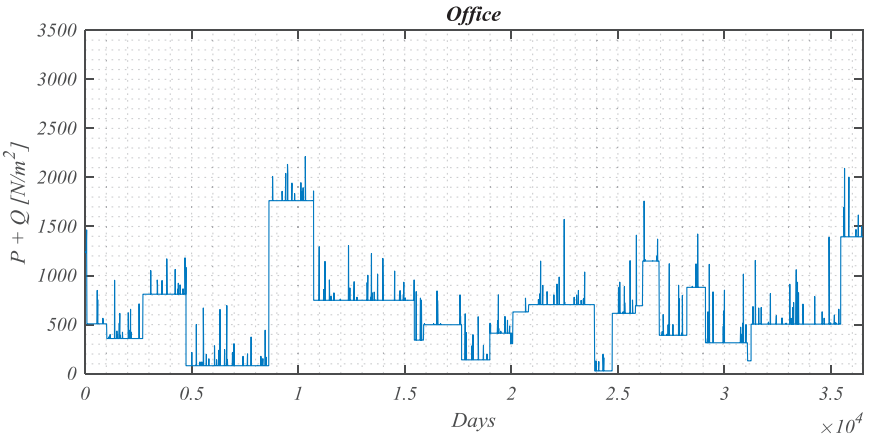

Figure B.1. Sampled time history of the sustained and intermittent load for an office space.

Table B.7. Parameters of the distributions representing the yearly and 50-years maxima for sustained and intermittent loads (parameters of the Poisson processes as in Table B.6).

	Yearly maxima - Gumbel approx. based on MC sampling			50-years maxima - Gumbel approx. based on MC sampling		Models proposed in [142] Table 5.7 ([142] was used as basis for the Eurocodes)		Characteristic values given in the Eurocode 1
Use	μ $[N/m^2]$	COV	Ch. value (98 % fractile) $[N/m^2]$	μ $[N/m^2]$	COV	μ $[N/m^2]$	COV	$[N/m^2]$
Office	839	0.53	1992	1918	0.22	2640	0.19	Cat B 2.00-3.00

The sustained load has a low renewal rate. Therefore, the dependence among the live load maxima in subsequent years might not be negligible as shown in the results. In fact, the distribution representing the 50-years maxima derived from the yearly maxima and assuming independence among years has mean 2196 N/m and COV = 0.20. The mean value is significantly different from the one derived from Monte Carlo simulations (i.e. $\mu = 1918\, N/m^2$), while the COVs are approximatively similar.

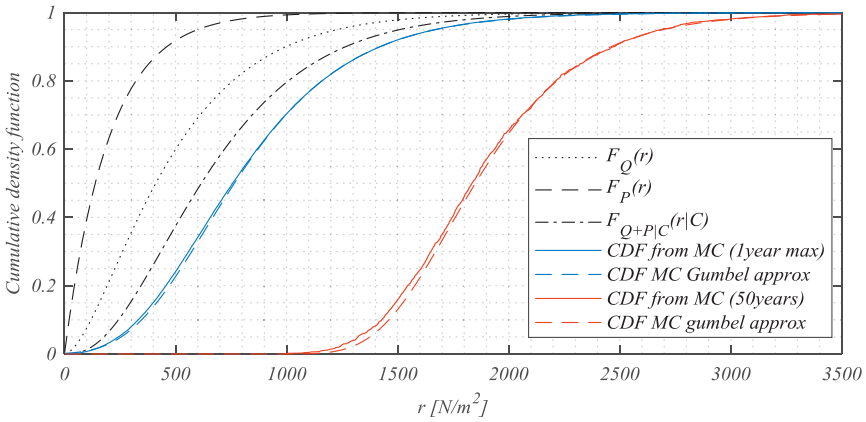

Figure B.2. Cumulative density functions for the live load process for an office space ($F_{Q+P|C}$ is the cumulative density function of the sum $Q+P$ given coincidence of Q and P).

B.3.3 Calibration strategy

The reliability-based calibration of the load partial safety factors is performed solving the following minimisation problem

$$\boldsymbol{\gamma}_{opt} = \arg\min_{\boldsymbol{\gamma}} \left\{ \left[\sum_{i=1}^{6} \sum_{j=1}^{3} \sum_{i_{aG}=1}^{3} \sum_{i_{aQ}=1}^{10} w_{i,j,i_{aG},i_{aQ}} \cdot \left(\beta_{i,j,i_{aG},i_{aQ}}(\boldsymbol{\gamma}) - \beta_t \right)^2 \right] \right\} \tag{B.5}$$

where:

- $\boldsymbol{\gamma} = \left[\gamma_{GS}, \gamma_{GP}, \gamma_{Q1}, \gamma_{Q2}, \gamma_{Q3} \right]$ are the PSFs on the load side.
- The target reliability β_t is equal to the weighted reliability associated to the Eurocode recommended reliability elements:

$$\beta_t = \mu_\beta(\boldsymbol{\gamma}_{EC}) = \frac{1}{\sum_{i=1}^{6} \sum_{j=1}^{3} \sum_{i_{aG}=1}^{3} \sum_{i_{aQ}=1}^{10} w_{i,j,i_{aG},i_{aQ}}} \sum_{i=1}^{6} \sum_{j=1}^{3} \sum_{i_{aG}=1}^{3} \sum_{i_{aQ}=1}^{10} w_{i,j,i_{aG},i_{aQ}} \beta_{i,j,i_{aG},i_{aQ}}(\boldsymbol{\gamma}_{EC}) \tag{B.6}$$

- The recommended reliability elements in the current versions of the Eurocodes ($\boldsymbol{\gamma}_{EC}$) are:
  - $\gamma_{M,i}$ given in the last column in Table B.1;
  - γ_{GP} and γ_{GS} are equal to $\gamma_G = 1.35$ [18];
  - $\gamma_{Q1} = \gamma_{Q2} = \gamma_{Q3} = 1.50$ [18];
  - $\psi_{0,Q1} = 0.6; \psi_{0,Q2} = 0.7; \psi_{0,Q3} = 0.7$ and $\xi = 0.85$ [18].
- The weights are calculated as $w_{i,j,i_{aG},i_{aQ}} = w_{R,i} w_{Q,j} w_{i_{aG}} w_{i_{aQ}}$ with:
  - $w_{R,i}$ are given in Table B.1;
  - $w_{Q_1} = w_{Q_2} = w_{Q_3} = 1/3$;
  - $w_{i_{aG}}$ and $w_{i_{aQ}}$ are equal for all $\left(i_{aG}, i_{aQ}\right)$ and giving the sum of all weights equal to 1.

B.3.4 Results

The calibrated partial load factors and the corresponding reliability levels are summarised in Table B.8. The reliability indices before and after calibration are illustrated in Figure B.3. As observed in the Table B.8, the calibration provides more similar average reliabilities among the variable loads. The differences in average reliability over the materials are almost unchanged since the material PSFs were not optimised.

The results are depending on the assumed stochastic models and the weighting between the different materials and between the loads. The assumptions made are considered representative, but comments from SC1 on the models representing environmental loads and also changes in the models representing the resistance could imply some modifications. The resulting average reliability index with a one-year reference period is determined to 4.08, close to the target reliability index recommended in ISO 2394:2015 [10].

Table B.8. Calibrated partial factors (in bold) and associated yearly reliability levels ($^{\#}$ reliability index averaged over the load or the material property in the brackets).

	Eq. 6.10a&b		Eq. 6.10	
	Eurocode recommended values	Calibrated values	Eurocode recommended values	Calibrated values
γ_M	$\gamma_M = [1.00; 1.50; 1.15; 1.25; 1.30; 1.50]$			
γ_{GS}	1.35	**1.19**	1.35	**1.16**
γ_{GP}	1.35	**1.23**	1.35	**1.22**
ξ	0.85	0.85	/	/
γ_Q (wind)	1.50	**1.42**	1.50	**1.43**
γ_Q (snow)	1.50	**1.71**	1.50	**1.76**
γ_Q (imposed)	1.50	**1.73**	1.50	**1.76**
β_t	/	4.08	/	4.27
μ_β	4.08	4.08	4.27	4.27
σ_β	0.54	0.42	0.60	0.44
COV_β	0.13	0.10	0.14	0.10
$\beta_{\min}$	3.30	3.62	3.33	3.70
$\beta_{\max}$	5.39	5.04	5.90	5.41
μ_β $^{\#}$ (steel)	3.70	3.74	3.87	3.91
μ_β (concrete)	4.81	4.78	5.00	4.97
μ_β (re-bar)	3.96	3.91	4.19	4.14
μ_β (glulam)	4.16	4.20	4.32	4.36
μ_β (sol timber)	4.21	4.24	4.35	4.39
μ_β (masonry)	4.73	4.71	4.91	4.88
μ_β (wind)	4.46	4.16	4.70	4.38
μ_β (snow)	3.91	4.05	4.06	4.22
μ_β (imposed)	3.87	4.04	4.05	4.22
Penalty function	0.2877	0.1780	0.3655	0.1963

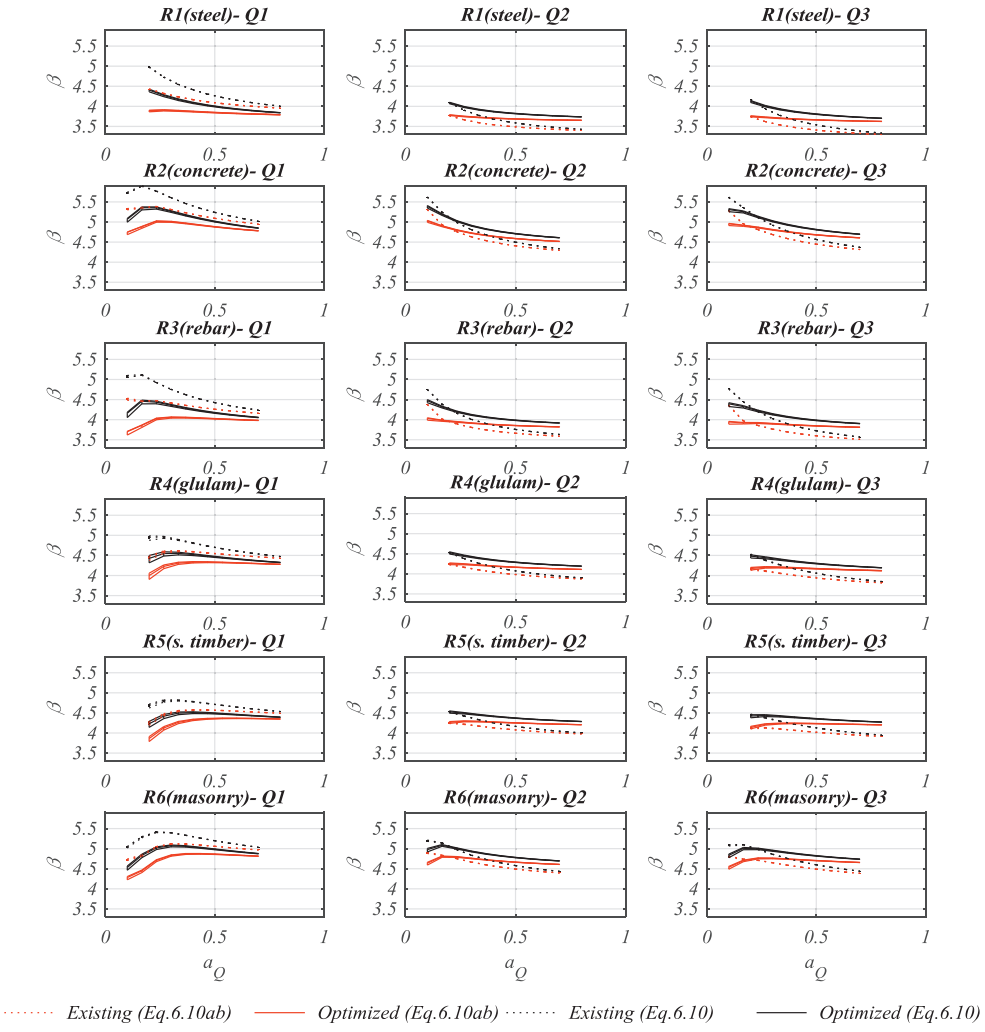

Figure B.3. Yearly reliability indices before and after calibration of the load partial safety factors.

B.3.5 Sensitivity to the resistance model biases

The influence of the biases of the resistance models is investigated. As an example, the calibration is performed with a model resistance for steel elements $\Theta_{R,1}$ represented by a Lognormal distribution with mean $\mu_{\Theta_{R,1}} = 1.10$, coefficient of variation $COV_{\Theta_{R,1}} = 0.05$ and characteristic value $\theta_{R,1,k} = 1.00$.

As expected, the partial safety factors on the load side are almost insensitive to the biases on the resistance side, see Table B.9. This is a consequence of the fact that the model bias is included both in the determination of the target reliability and in the calibration of the PSFs. A similar behaviour is expected for the load combination "*6.10*". Obviously, the average reliability index for steel structures is affected by the bias.

Table B.9. Calibrated partial safety factors (in bold) and associated yearly reliability levels for steel resistance model with 10 % bias.

	Eq. 6.10a&b	
	Eurocode recommended values	Calibrated values
γ_M	$\gamma_M = [1.00; 1.50; 1.15; 1.25; 1.30; 1.50]$	
γ_{GS}	1.35	**1.20**
γ_{GP}	1.35	**1.23**
ξ	0.85	0.85
γ_Q (wind)	1.50	**1.41**
γ_Q (snow)	1.50	**1.72**
γ_Q (imposed)	1.50	**1.72**
β_t	/	4.20
μ_β	4.20	4.20
σ_β	0.48	0.35
COV_β	0.11	0.08
$\beta_{\min}$	3.51	3.63
$\beta_{\max}$	5.39	5.06
μ_β (steel)	4.00	4.04
μ_β (concrete)	4.81	4.78
μ_β (re-bar)	3.96	3.91
μ_β (glulam)	4.16	4.20
μ_β (sol timber)	4.21	4.24
μ_β (masonry)	4.73	4.71
μ_β (wind)	4.60	4.29
μ_β (snow)	4.02	4.16
μ_β (imposed)	3.99	4.16
Penalty function	0.2318	0.1212

B.3.6 Sensitivity to the time reference period

This section shows the results of the calibration performed with the 50-years reliability index. The distributions representing the 50-years maxima of the time-variant loads are derived from the yearly maxima considering independent maxima over the years. This assumption might be only approximative for the imposed load due to the sustained load that renews in average every five years, see Table B.6. The mean and the standard deviation of the Gumbel distribution representing 50-years maxima are calculated from the distribution representing the yearly maxima in Eq. (B.7). The coefficient of variation for the 50-years maxima is lower than the COV for the yearly maxima since $\mu_{50} > \mu_1$ while the standard deviation is constant.

$$\mu_{50} = \mu_1 + \frac{\sqrt{6}}{\pi}\sigma_{50}\ln(50); \quad \sigma_{50} = \sigma_1 \tag{B.7}$$

Table B.10. Calibrated partial safety factors in bold and associated 50-years reliability levels.

	Eq. 6.10a&b		Eq. 6.10	
	Eurocode recommended values	Calibrated values	Eurocode recommended values	Calibrated values
γ_M	$\gamma_M = [1.00; 1.50; 1.15; 1.25; 1.30; 1.50]$			
γ_{GS}	1.35	**1.16**	1.35	**1.13**
γ_{GP}	1.35	**1.22**	1.35	**1.21**
ξ	0.85	/	/	/
γ_Q (wind)	1.50	**1.40**	1.50	**1.41**
γ_Q (snow)	1.50	**1.70**	1.50	**1.77**
γ_Q (imposed)	1.50	**1.77**	1.50	**1.81**
β_t	/	3.12	/	3.35
μ_β	3.12	3.12	3.35	3.35
σ_β	0.70	0.53	0.77	0.55
COV_β	0.23	0.17	0.23	0.16
$\beta_{\min}$	2.01	2.55	2.06	2.65
$\beta_{\max}$	4.98	4.32	5.38	4.71
μ_β (steel)	2.62	2.67	2.84	2.89
μ_β (concrete)	4.02	3.98	4.24	4.20
μ_β (re-bar)	2.99	2.93	3.26	3.19
μ_β (glulam)	3.25	3.30	3.43	3.48
μ_β (sol timber)	3.33	3.38	3.49	3.54
μ_β (masonry)	3.98	3.95	4.18	4.15
μ_β (wind)	3.64	3.22	3.90	3.46
μ_β (snow)	2.94	3.08	3.11	3.29
μ_β (imposed)	2.80	3.07	3.03	3.30
Penalty function	0.4957	0.2856	0.5920	0.3030

The calibrate PSFs are practically similar to the ones obtained for in the calibration with the yearly reliability index in Table B.8. The change of the time reference period was expected to influence more the "redistribution" of safety factors between the resistance and the load sides since the 50-years maxima have lower COVs than the yearly maxima and thus their contribution to the failure probability decreases. Consequently, larger material safety factor and lower load safety factors might be expected using the 50-years reliability in the calibration. However, the material PSFs were fixed in the calculations presented here so this "redistribution" was not possible.

B.3.7 Permanent load with large COV G_P^*

The PSF for a time-invariant load with a large coefficient of variation ($\gamma_{G_P^*}$) is calibrated in this Section. The permanent load G_P^* is represented by a Normal distribution with $COV_{G_P^*} = 0.20$. The characteristic value is $g_{P,k}^* = F_{G_P^*}^{-1}(0.95)$. Permanent loads with large uncertainties are not currently treated in EN 1990:2002 [18]. However, they might be relevant for cases such as a roof supporting a garden. Therefore, the target reliability is set equal to

$\mu_\beta(\boldsymbol{\gamma}_{EC})$ calculated with a permanent load $G_P \sim Normal\left(\mu_{G_P}=1; COV_{G_P}=0.10\right)$ and characteristic fractile 0.50.

The results are shown in Table B.11. It is seen that using "*6.10a&b*" the two partial factors for permanent load are $\gamma_{G_P}=1.17$ (for low COV and 50% fractile) and $\gamma_{G_P^*}=1.21$ (for large COV and 95% fractile), i.e. only a small difference from the PSFs in Table B.8. Using "*6.10*" results in a slightly larger difference. Thus, $\gamma_{G_P^*}=\gamma_{GP}$ can be suggested for practical applications.

Table B.11. Calibrated partial safety factors (in bold) and associated yearly reliability levels for the case with a permanent load with large uncertainty.

	Eq. 6.10a&b		Eq. 6.10	
	Eurocode recommended values $G_P \sim N(1.0;10\%)$	Calibrated values $G_P^* \sim N(1.0;20\%)$	Eurocode recommended values	Calibrated values $G_P^* \sim N(1.0;20\%)$
γ_M	$\gamma_M = [1.00; 1.50; 1.15; 1.25; 1.30; 1.50]$			
γ_{GS}	1.35	**1.17**	1.35	**1.14**
γ_{GP}	1.35	/	1.35	/
γ_{GP^*} (large COV)	/	**1.21**	/	**1.19**
ξ	0.85	0.85	/	/
γ_Q (wind)	1.50	**1.39**	1.50	**1.39**
γ_Q (snow)	1.50	**1.67**	1.50	**1.72**
γ_Q (imposed)	1.50	**1.69**	1.50	1.72
β_t	/	4.08	/	4.27
μ_β	4.08	4.08	4.27	4.27
σ_β	0.54	0.44	0.60	0.47
COV_β	0.13	0.11	0.14	0.11
$\beta_{\min}$	3.30	3.50	3.33	3.63
$\beta_{\max}$	5.39	5.29	5.90	5.62
μ_β (steel)	3.70	3.73	3.87	3.90
μ_β (concrete)	4.81	4.78	5.00	4.98
μ_β (re-bar)	3.96	3.92	4.19	4.15
μ_β (glulam)	4.16	4.19	4.32	4.35
μ_β (sol timber)	4.21	4.23	4.35	4.38
μ_β (masonry)	4.73	4.71	4.91	4.89
μ_β (wind)	4.46	4.17	4.70	4.38
μ_β (snow)	3.91	4.04	4.06	4.21
μ_β (imposed)	3.87	4.03	4.05	4.22
Penalty function	0.2877	0.1915	0.3655	0.2193

B.4 Evaluation of the reliability of the design with the calibrated load partial safety factors for cases with two variable loads acting simultaneously

This Section reports the assessment of the reliability level for cases with two variable loads acting simultaneously and with the load partial safety factors calibrated in Section B.3.4. Three load scenarios (LS) are considered:

- LS 1: Wind and Snow,
- LS 2: Wind and Imposed load, and
- LS 3: Snow and Imposed load.

The three LSs are equally weighted.

B.4.1 Limit state function and design situations

Generic limit state functions are utilised for representing a broad range of design situations as before. The load combination is approximated by the Ferry-Borges and Castanheta combination rule (see [5, 11] and Section B.4.2 for details on the processes and the combination rule). According to the combination rule, the failure under loads Q_j and Q_t acting simultaneously corresponds to the union of four failure events:

- load j acting alone,
- load t acting alone,
- load j leading and t accompanying, and
- load t leading and j accompanying.

It is assumed that one event is always dominating, so the system failure is approximated as the failure event with the highest probability of occurrence. The limit state functions representing the four failure events are given in Eqs. (B.8) to (B.11)

$$g_2\left(\mathbf{X}, p_{ijt}\right) = p_{ijt}\Theta_{R,i}R_i - \left(1-a_Q\right)\left[a_G G_{S,U} + \left(1-a_G\right)G_{P,U}\right] - a_Q\left[\Theta_{Q,j}Q_j a_{Q1Q2} + 0\right] \quad \text{(B.8)}$$

$$g_3\left(\mathbf{X}, p_{ijt}\right) = p_{ijt}\Theta_{R,i}R_i - \left(1-a_Q\right)\left[a_G G_{S,U} + \left(1-a_G\right)G_{P,U}\right] - a_Q\left[0 + \Theta_{Q,t}Q_t\left(1-a_{Q1Q2}\right)\right] \quad \text{(B.9)}$$

$$\begin{aligned} g_4\left(\mathbf{X}, p_{ijt}\right) = {} & p_{ijt}\Theta_{R,i}R_i - \left(1-a_Q\right)\left[a_G G_{S,U} + \left(1-a_G\right)G_{P,U}\right] + \\ & - a_Q\left[\Theta_{Q,j}Q_j^{(L)}a_{Q1Q2} + \Theta_{Q,t}Q_t^{(A)}\left(1-a_{Q1Q2}\right)\right] \end{aligned} \quad \text{(B.10)}$$

$$\begin{aligned} g_5\left(\mathbf{X}, p_{ijt}\right) = {} & p_{ijt}\Theta_{R,i}R_i - \left(1-a_Q\right)\left[a_G G_{S,U} + \left(1-a_G\right)G_{P,U}\right] + \\ & - a_Q\left[\Theta_{Q,j}Q_j^{(A)}a_{Q1Q2} + \Theta_{Q,t}Q_t^{(L)}\left(1-a_{Q1Q2}\right)\right] \end{aligned} \quad \text{(B.11)}$$

where:

- a_{Q1Q2} is a parameter representing different proportions between the two variable loads considered ($a_{Q1Q2}=1$ for the first variable load only). Ten values equally spaced and equally weighted between 0 and 1 for all materials and load combinations are considered.
- Q_j is the yearly maxima of the variable load j.
- $Q^{(L)}, Q^{(A)}$ stand for the random variables representing the leading and accompanying loads, respectively. These random variables represent the maxima of different reference periods

(shorter than or equal to 1 year) derived according to the Ferry-Borges and Castanheta rule (see Section B.4.2).

- The design variable p_{ijt} is calculated according to the EN 1990:2002 semi-probabilistic design format in Eq. (B.12) for "*6.10a&b*" and in Eq. (B.13) for "*6.10*".

$$p_{ijt} = \max \left\{ \begin{array}{l} \dfrac{\gamma_{M,i}}{\theta_{Ri,k} r_{i,k}} \left\{ \begin{array}{l} \left(1-a_Q\right)\left[a_G g_{S,k}\gamma_{GS} + \left(1-a_G\right) g_{P,k}\gamma_{GP}\right] + \\ +a_Q\left[\alpha_{Q1Q2}\gamma_{Q_j}\psi_{o,j}\theta_{Q_j,k} q_{j,k} + \left(1-\alpha_{Q1Q2}\right)\gamma_{Q_t}\psi_{0,t}\theta_{Q_t,k} q_{t,k}\right] \end{array} \right\} \\ \dfrac{\gamma_{M,i}}{\theta_{Ri,k} r_{i,k}} \left\{ \begin{array}{l} \left(1-a_Q\right)\left[a_G g_{S,k}\xi\gamma_{GS} + \left(1-a_G\right) g_{P,k}\xi\gamma_{GP}\right] + \\ +a_Q\left[\alpha_{Q1Q2}\gamma_{Q_j}\theta_{Q_j,k} q_{j,k} + \left(1-\alpha_{Q1Q2}\right)\gamma_{Q_t}\psi_{0,t}\theta_{Q_t,k} q_{t,k}\right] \end{array} \right\} \end{array} \right\} \quad \text{(B.12)}$$

$$p_{ijt} = \frac{\gamma_{M,i}}{\theta_{Ri,k} r_{i,k}} \left\{ \begin{array}{l} \left(1-a_Q\right)\left[a_G g_{S,k}\gamma_{GS} + \left(1-a_G\right) g_{P,k}\gamma_{GP}\right] + \\ a_Q\left[\alpha_{Q1Q2}\gamma_{Q_j}\theta_{Q_j,k} q_{j,k} + \left(1-\alpha_{Q1Q2}\right)\gamma_{Q_t}\psi_{0,t}\theta_{Q_t,k} q_{t,k}\right] \end{array} \right\} \quad \text{(B.13)}$$

B.4.2 Details for the Ferry Borges and Castanheta combination rule

Only the simultaneous presence of two of the three loads is considered in the calibration. The rectangular pulse processes representing Q_j and Q_t has the following properties:

- Duration of one repetition (see Table B.12 for the parameters n_p and n_r):
  - $d_j = \dfrac{n_{p,j}}{n_{r,j}}; d_t = \dfrac{n_{p,t}}{n_{r,t}}$
- Period of load coincidence (both loads are present):
  - $n_{p,\min} = \min\left(n_{p,j}, n_{p,t}\right)$

The distributions representing the load maxima in the limit state functions in Eqs. (B.8) to (B.11) are given below:

- Limit state function with Q_j only:
  - Distribution representing Q_j yearly maxima (F_{Q_j} , see Table B.2)
- Limit state function with Q_t only:
  - Distribution representing Q_t yearly maxima (F_{Q_t} , see Table B.2)
- Limit state function with Q_j leading and Q_t accompanying:
  - Maxima of Q_j over $n_{p,\min}$ combined with the maxima of Q_t over $\max\left(d_j, d_t\right)$
  - Distributions representing maxima: $F_{Q_j^{(L)}} = \left(F_{Q_j}\right)^{n_j}$ and $F_{Q_t^{(A)}} = \left(F_{Q_t}\right)^{n_t}$ (with: $n_j = n_{p,\min}/n_{p,j}$ and $n_t = \max\left(d_j, d_t\right)/n_{p,t}$).
- Limit state function with Q_t leading and Q_j accompanying:
  - Maxima of Q_t over $n_{p,\min}$ combined with the maxima of Q_j over $\max\left(d_j, d_t\right)$
  - Distributions representing maxima: $F_{Q_j^{(A)}} = \left(F_{Q_j}\right)^{n_j}$ and $F_{Q_t^{(L)}} = \left(F_{Q_t}\right)^{n_t}$ (with: $n_j = \max\left(d_j, d_t\right)/n_{p,j}$ and $n_t = n_{p,\min}/n_{p.t}$)

Table B.12. Representation of time-variant loads as rectangular pulse processes for the FBC combination.

Random variable		Yearly maxima distr. type	Number of days the load is present in 1 year n_p [days]	Number of repetitions within the presence period n_r
Wind mean reference velocity pressure *	Q_1	Gumbel	365	365
Snow load on roof*	Q_2	Gumbel	150	10
Imposed load *	Q_3	Gumbel	365	5

B.4.3 Results

The reliability indices obtained with the calibrated PSFs in Section B.3.4 are reported in Table B.13 and illustrated in Figure B.4.

Table B.13. Yearly reliability indices for cases of two variable loads acting simultaneously and design with calibrated PSFs.

	Eq. 6.10a&b		Eq. 6.10	
	Eurocode recommended values	Calibrated values	Eurocode recommended values	Calibrated values
γ_M	$\gamma_M = [1.00; 1.50; 1.15; 1.25; 1.30; 1.50]$			
γ_{GS}	1.35	**1.19**	1.35	**1.16**
γ_{GP^*}	1.35	**1.23**	1.35	**1.22**
ξ	0.85	/	/	0.85
γ_Q (wind)	1.50	**1.42**	1.50	**1.43**
γ_Q (snow)	1.50	**1.71**	1.50	**1.76**
γ_Q (imposed)	1.50	**1.73**	1.50	**1.76**
β_t	/	No calibration	/	No calibration
μ_β	4.42	4.43	4.62	4.63
σ_β	0.58	0.50	0.64	0.51
COV_β	0.13	0.11	0.14	0.11
$\beta_{\min}$	3.30	3.61	3.33	3.70
$\beta_{\max}$	6.01	5.81	6.39	6.12
μ_β (steel)	4.07	4.13	4.26	4.31
μ_β (concrete)	5.13	5.10	5.33	5.30
μ_β (re-bar)	4.31	4.26	4.54	4.49
μ_β (glulam)	4.48	4.53	4.64	4.69
μ_β (sol timber)	4.48	4.53	4.64	4.69
μ_β (masonry)	4.98	4.97	5.17	5.14
μ_β (wind + snow)	4.50	4.43	4.69	4.63
μ_β (wind + imposed)	4.46	4.40	4.68	4.61
μ_β (snow + imposed)	4.31	4.46	4.48	4.64

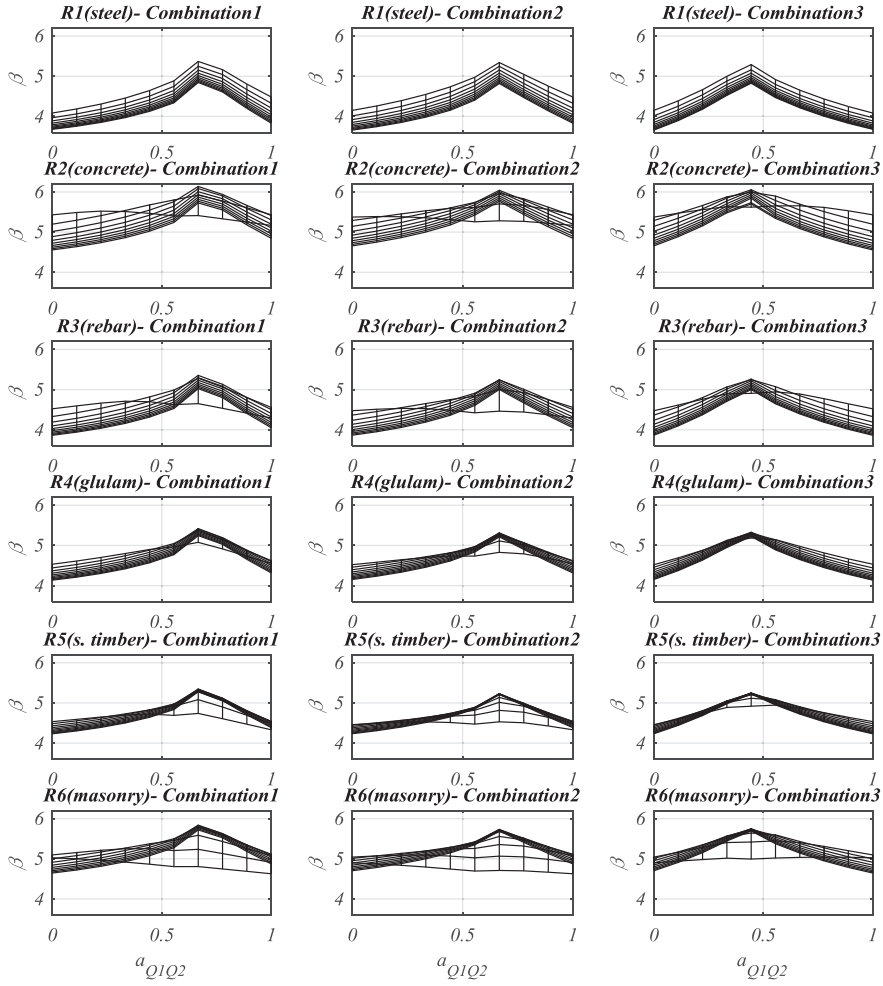

Figure B.4. Yearly reliability index for combinations of two variable loads, Eq. 6.10 and calibrated load partial safety factors. The curves represent the values for different a_Q *- values and* $a_G = 0.8$.

B.5 Calibration of the partial safety factor for a generic load

In this Section, the partial factor γ_Q for a generic variable load is calibrated for different combinations of COV_Q and COV_{Θ_Q} values. The output of this calibration allows differentiating the load partial factor when a detailed model for estimating the action effect is utilised. This case corresponds, for example, to the calculation of the wind load effect based on wind tunnel tests that provide a more accurate estimate (i.e. lower COV_{Θ_Q}) compared to the generic and simplified models included in the Eurocode 1. In addition, the load PSF can be adjusted when the COV_Q is precisely known as, for example, when weather records are analysed.

The variable load yearly maxima are represented by a Gumbel distribution with coefficient of variation COV_Q and characteristic fractile equal to 0.98. The load model uncertainty is $\Theta_Q \sim Ln\left(1.00, COV_{\Theta_Q}\right)$ with unitary characteristic value ($\theta_{Q,k} = 1.00$). The calibration is performed with the target reliability $\beta_t = 4.08$ (i.e. mean reliability with current PSFs and best estimate of stochastic models) and $\gamma_{GS} = 1.19, \gamma_{GP} = 1.23$ as calibrated in Section B.3.4, see Table B.8.

The results are summarized in Table B.14 and illustrated in Figure B.5. As expected, larger COVs imply larger load partial factor.

Table B.14. Calibrated γ_Q for Eq. 6.10a&b for a generic variable load.

		COV_{Θ_Q}				
		0.00	0.10	0.20	0.30	0.45
COV_Q	0.15	1.37	1.45	1.68	2.08	3.06
	0.25	1.46	1.53	1.75	2.12	3.02
	0.40	1.59	1.66	1.88	2.25	3.11
	0.60	1.72	1.79	2.02	2.40	3.26

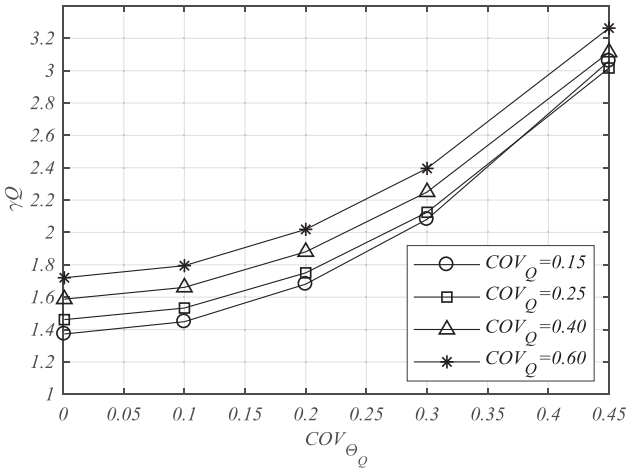

Figure B.5. Sensitivity of γ_Q with respect to COV_Q and COV_{Θ_Q}.

B.6 Calibration of the partial safety factor for a generic material

In this Section, a generic material is considered and the corresponding partial safety factor γ_M is calibrated. The output of this calibration allows selecting the proper resistance partial safety factor when the COV_R and the COV_{Θ_R} are known. The COV_R is known when measurements are available and could be relevant, for example, in the assessment of existing structures. Similarly, the γ_M could be selected based on the uncertainty of the model utilised for predicting the structural capacity, i.e. COV_{Θ_R}. This might be relevant when advanced finite element analysis is performed.

The material property governing the failure mode is represented by a Lognormal distribution with unitary mean and coefficient of variation COV_R. The characteristic value corresponds to the 5 % fractile. The resistance model uncertainty is represented by a Lognormal distribution with unitary mean and coefficient of variation COV_{Θ_R}. Two fractiles for the characteristic value are considered: the mean value and the 5 % fractile. The latter is accounted in the EN 1990:2002 Annex D which regulates design assisted by testing. The load PSFs calibrated in Section B.3.4 are utilized. The mean reliability with the current PSFs is utilized as a target, i.e. $\beta_t = 4.08$ for "*6.10 a&b*". The parameters representing the proportions among the weights are assumed varying in the ranges $a_G \in [0.6;1.0]$ and $a_Q \in [0.1;0.8]$. One variable load at a time is considered.

The calibrated material partial safety factors are summarised in Table B.15 and Table B.16. The relationship among the COVs and the partial material factor is illustrated in Figure B.6 and Figure B.7.

Table B.15. Calibrated γ_M for "Eq. 6.10a&b" and $\theta_{R,k} = 1.00$.

		COV_{Θ_R}				
		0	0.05	0.10	0.15	0.20
COV_R	0.05	1.06	1.09	1.17	1.29	1.47
	0.10	1.05	1.07	1.14	1.26	1.42
	0.15	1.07	1.09	1.15	1.26	1.41
	0.20	1.11	1.13	1.19	1.29	1.43
	0.25	1.17	1.19	1.24	1.34	1.47
	0.30	1.25	1.26	1.32	1.41	1.54
	0.35	1.34	1.35	1.41	1.50	1.63

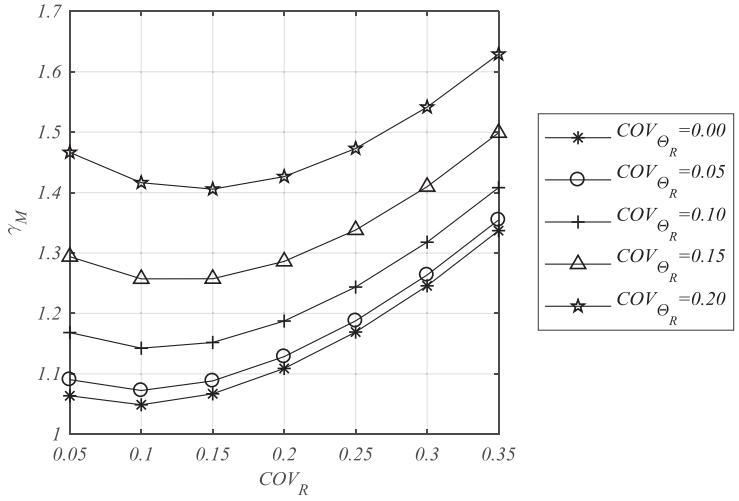

Figure B.6. Sensitivity of γ_M with respect to COV_R and COV_{Θ_R} for "Eq. 6.10a&b" and $\theta_{R,k} = 1.00$.

Table B.16. Calibrated γ_M for "6.10a&b" and $\theta_{R,k} = F_{\Theta_R}^{-1}(0.05)$.

		COV_{Θ_R}				
		0.00	0.05	0.10	0.15	0.20
COV_R	0.05	1.06	1.00	0.99	1.00	1.04
	0.10	1.05	0.99	0.96	0.97	1.00
	0.15	1.07	1.00	0.97	0.97	1.00
	0.20	1.11	1.04	1.00	1.00	1.01
	0.25	1.17	1.09	1.05	1.04	1.04
	0.30	1.24	1.16	1.11	1.09	1.09
	0.35	1.33	1.25	1.19	1.16	1.15

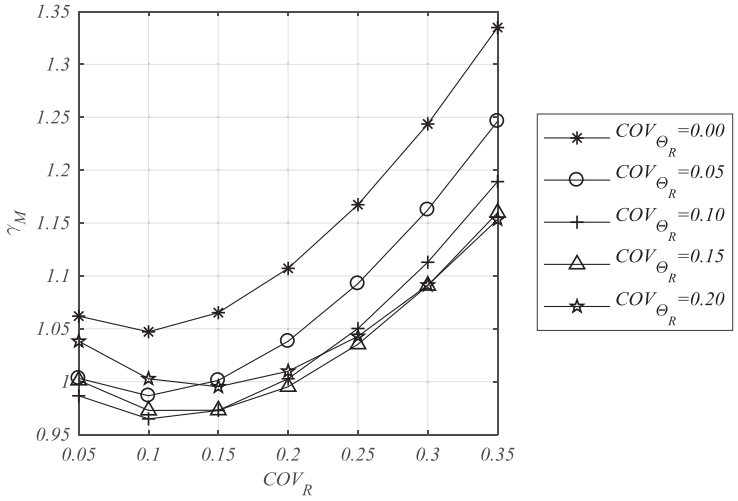

Figure B.7. Sensitivity of γ_M with respect to COV_R and COV_{Θ_R} for "6.10a&b" and $\theta_{R,k} = F_{\Theta_R}^{-1}(0.05)$.

The sensitivity factors for the resistance side (α_{Res}) corresponding to the calibrated γ_M are calculated. The aim is to provide values for α_{Res} to be used in the design point method included in the EN 1990:2002 Annex C. The α_{Res} is derived as follows:

- The random variable representing the resistance (including the model uncertainty) $R_\Theta = R \cdot \Theta_R$ is represented by a Lognormal distribution with $\mu_{R_\Theta} = \mu_R \cdot \mu_{\Theta_R}$ and $COV_{R_\Theta} = \sqrt{COV_R^2 + COV_{\Theta_R}^2 + COV_R^2 COV_{\Theta_R}^2}$.
- The design value of the resistance corresponding to the calibrated γ_M is:

$$r_{\theta,d} = r_d \theta_{R,d} = \frac{r_k}{\gamma_m} \frac{\theta_{R,k}}{\gamma_{Rd}} = \frac{F_R^{-1}(0.05)}{\gamma_m} \frac{\mu_{\Theta_R}}{\gamma_{Rd}} = \frac{F_R^{-1}(0.05)\,\mu_{\Theta_R}}{\gamma_M} \tag{B.14}$$

(considering $\theta_{R,k} = \mu_{\Theta_R}$)

- The sensitivity factor corresponding to R_Θ and to the calibrated γ_M is:

$$F_{R_\Theta}\left(r_d \theta_{R,d}\right) = \Phi\left(\alpha_{\text{Res}} \beta_t\right) \rightarrow \alpha_{\text{Res}} = \Phi^{-1}\left(F_{R_\Theta}\left(\frac{F_R^{-1}(0.05)\,\mu_{\Theta_R}}{\gamma_M}\right)\right)\frac{1}{\beta_t} \tag{B.15}$$

The calculated values are summarised in Table B.17. It is worth noting that the values of α_{Res} are not increasing with the coefficients of variations as it could be expected. This is a consequence of the fact that the PSFs on the load side are fixed. For the combination with low COVs, for example, the sensitivity factors should be low on the resistance side and high on the load side. However, the load PSFs are fixed and calibrated considering several design situations simultaneously. Therefore, the sensitivity factors on the load side that correspond to the calibrated PSFs are lower than the ones that would be obtained for the case with only one material with a low COV_{R_Θ}. Consequently, the α_{Res} are larger for compensating. The opposite is valid for large COV_{R_Θ}.

Table B.17. Sensitivity factors for R_Θ back-calculated from the calibrated PSFs in Table B.15.

		COV_{Θ_R}				
		0	0.05	0.10	0.15	0.20
COV_R	0.05	-0.69	-0.57	-0.50	-0.50	-0.52
	0.10	-0.51	-0.50	-0.49	-0.51	-0.53
	0.15	-0.50	-0.50	-0.51	-0.52	-0.55
	0.20	-0.52	-0.52	-0.53	-0.55	-0.56
	0.25	-0.54	-0.55	-0.56	-0.57	-0.58
	0.30	-0.57	-0.57	-0.58	-0.59	-0.60
	0.35	-0.60	-0.60	-0.60	-0.61	-0.62

B.7 Summary and future work

The calibration framework presented in this work aimed at providing more uniform reliability among structures subjected to different types of action and constructed with different materials. The calibration showed the following main results:

- The current partial safety factors (PSFs) recommended in the Eurocodes lead to higher reliability of design for structures dominated by wind actions compared with structure dominated by snow or imposed actions.
- The differentiation of the variable load safety factor can reduce the differences in reliability. The calibrated PSFs for wind, snow and imposed loads were found equal to approximatively 1.45, 1.70 and 1.75, respectively (with the assumed stochastic models and the currently recommended values for the PSFs on the resistance side).
- A unique partial safety factor equal to approximatively 1.2 can be utilised both for the self-weight and the permanent load. Thus, there is no need for differentiating the PSF for self-weight and permanent loads.
- A PSF of 1.2 can also be used for permanent actions with larger uncertainty when the characteristic value corresponds to the 0.95 fractile.
- The calibration results are almost insensitive to the reference time used in the time-integrated approach (1 year and 50 years). This is believed to be a consequence of the fact that the material PSFs were fixed. In addition, the results were insensitive to the resistance model biases as expected since the biases are accounted both in the estimation of the target reliability and in the calibration of the PSFs.

- The partial safety factor for a generic load was calibrated as a function of the COVs of the load maxima and the load model uncertainty. The PSF was increasing with the COV-values as expected.
- The partial safety factor for a generic material and failure mode was calibrated as a function of the COVs of the material property dominating the failure mode and the resistance model uncertainty. The PSFs was increasing with the COV-values as expected.

The present work should be continued and completed. For this reason, all the Matlab scripts utilised for these calculations are available at [67]. In detail:

- The stochastic models representing the environmental loads should be refined based on the Subcommittees input. In particular, the model biases (hidden safety) and the fractiles corresponding to the characteristic values provided in the corresponding Eurocodes should be accurately estimated. They are expected to influence considerably the calibration of the partial factors.
- A significant difference among the reliability levels of structures with different materials was observed. This difference can be reduced by calibrating the material partial safety factors. For this scope, material specific limit state functions representing the specific failure modes and detailed stochastic models representing the involved random variables should be utilised. The resistance model biases are expected to influence the results significantly. Making the reliability more uniform over the materials might lead to significant changes in the safety factors on the material side which might not be accepted nor trusted by the industry and the engineers.
- Other materials should be included in the calibration such as soil, structural glass and aluminium.

DEPARTMENT OF STRUCTURAL ENGINEERING
NORWEGIAN UNIVERSITY OF SCIENCE AND TECHNOLOGY

N–7491 TRONDHEIM, NORWAY
Telephone: +47 73 59 47 00 Telefax: +47 73 59 47 01

"Reliability Analysis of Structural Systems using Nonlinear Finite Element Methods",
C. A. Holm, 1990:23, ISBN 82-7119-178-0.

"Uniform Stratified Flow Interaction with a Submerged Horizontal Cylinder",
Ø. Arntsen, 1990:32, ISBN 82-7119-188-8.

"Large Displacement Analysis of Flexible and Rigid Systems Considering
Displacement-Dependent Loads and Nonlinear Constraints",
K. M. Mathisen, 1990:33, ISBN 82-7119-189-6.

"Solid Mechanics and Material Models including Large Deformations",
E. Levold, 1990:56, ISBN 82-7119-214-0, ISSN 0802-3271.

"Inelastic Deformation Capacity of Flexurally-Loaded Aluminium Alloy Structures",
T. Welo, 1990:62, ISBN 82-7119-220-5, ISSN 0802-3271.

"Visualization of Results from Mechanical Engineering Analysis",
K. Aamnes, 1990:63, ISBN 82-7119-221-3, ISSN 0802-3271.

"Object-Oriented Product Modeling for Structural Design",
S. I. Dale, 1991:6, ISBN 82-7119-258-2, ISSN 0802-3271.

"Parallel Techniques for Solving Finite Element Problems on Transputer Networks",
T. H. Hansen, 1991:19, ISBN 82-7119-273-6, ISSN 0802-3271.

"Statistical Description and Estimation of Ocean Drift Ice Environments",
R. Korsnes, 1991:24, ISBN 82-7119-278-7, ISSN 0802-3271.

“Properties of concrete related to fatigue damage: with emphasis on high strength
concrete”,
G. Petkovic, 1991:35, ISBN 82-7119-290-6, ISSN 0802-3271.

"Turbidity Current Modelling",
B. Brørs, 1991:38, ISBN 82-7119-293-0, ISSN 0802-3271.

"Zero-Slump Concrete: Rheology, Degree of Compaction and Strength. Effects of
Fillers as Part Cement-Replacement",
C. Sørensen, 1992:8, ISBN 82-7119-357-0, ISSN 0802-3271.

"Nonlinear Analysis of Reinforced Concrete Structures Exposed to Transient Loading",
K. V. Høiseth, 1992:15, ISBN 82-7119-364-3, ISSN 0802-3271.

"Finite Element Formulations and Solution Algorithms for Buckling and Collapse Analysis of Thin Shells",
R. O. Bjærum, 1992:30, ISBN 82-7119-380-5, ISSN 0802-3271.

"Response Statistics of Nonlinear Dynamic Systems",
J. M. Johnsen, 1992:42, ISBN 82-7119-393-7, ISSN 0802-3271.

"Digital Models in Engineering. A Study on why and how engineers build and operate digital models for decisison support",
J. Høyte, 1992:75, ISBN 82-7119-429-1, ISSN 0802-3271.

"Sparse Solution of Finite Element Equations",
A. C. Damhaug, 1992:76, ISBN 82-7119-430-5, ISSN 0802-3271.

"Some Aspects of Floating Ice Related to Sea Surface Operations in the Barents Sea",
S. Løset, 1992:95, ISBN 82-7119-452-6, ISSN 0802-3271.

"Modelling of Cyclic Plasticity with Application to Steel and Aluminium Structures",
O. S. Hopperstad, 1993:7, ISBN 82-7119-461-5, ISSN 0802-3271.

"The Free Formulation: Linear Theory and Extensions with Applications to Tetrahedral Elements
with Rotational Freedoms",
G. Skeie, 1993:17, ISBN 82-7119-472-0, ISSN 0802-3271.

"Høyfast betongs motstand mot piggdekkslitasje. Analyse av resultater fra prøving i Veisliter'n",
T. Tveter, 1993:62, ISBN 82-7119-522-0, ISSN 0802-3271.

"A Nonlinear Finite Element Based on Free Formulation Theory for Analysis of Sandwich Structures",
O. Aamlid, 1993:72, ISBN 82-7119-534-4, ISSN 0802-3271.

"The Effect of Curing Temperature and Silica Fume on Chloride Migration and Pore Structure of High Strength Concrete",
C. J. Hauck, 1993:90, ISBN 82-7119-553-0, ISSN 0802-3271.

"Failure of Concrete under Compressive Strain Gradients",
G. Markeset, 1993:110, ISBN 82-7119-575-1, ISSN 0802-3271.

"An experimental study of internal tidal amphidromes in Vestfjorden",
J. H. Nilsen, 1994:39, ISBN 82-7119-640-5, ISSN 0802-3271.

"Structural analysis of oil wells with emphasis on conductor design",
H. Larsen, 1994:46, ISBN 82-7119-648-0, ISSN 0802-3271.

"Adaptive methods for non-linear finite element analysis of shell structures",
K. M. Okstad, 1994:66, ISBN 82-7119-670-7, ISSN 0802-3271.

"On constitutive modelling in nonlinear analysis of concrete structures",
O. Fyrileiv, 1994:115, ISBN 82-7119-725-8, ISSN 0802-3271.

"Fluctuating wind load and response of a line-like engineering structure with emphasis on motion-induced wind forces",
J. Bogunovic Jakobsen, 1995:62, ISBN 82-7119-809-2, ISSN 0802-3271.

"An experimental study of beam-columns subjected to combined torsion, bending and axial actions",
A. Aalberg, 1995:66, ISBN 82-7119-813-0, ISSN 0802-3271.

"Scaling and cracking in unsealed freeze/thaw testing of Portland cement and silica fume concretes",
S. Jacobsen, 1995:101, ISBN 82-7119-851-3, ISSN 0802-3271.

"Damping of water waves by submerged vegetation. A case study of laminaria hyperborea",
A. M. Dubi, 1995:108, ISBN 82-7119-859-9, ISSN 0802-3271.

"The dynamics of a slope current in the Barents Sea",
Sheng Li, 1995:109, ISBN 82-7119-860-2, ISSN 0802-3271.

"Modellering av delmaterialenes betydning for betongens konsistens",
Ernst Mørtsell, 1996:12, ISBN 82-7119-894-7, ISSN 0802-3271.

"Bending of thin-walled aluminium extrusions",
Birgit Søvik Opheim, 1996:60, ISBN 82-7119-947-1, ISSN 0802-3271.

"Material modelling of aluminium for crashworthiness analysis",
Torodd Berstad, 1996:89, ISBN 82-7119-980-3, ISSN 0802-3271.

"Estimation of structural parameters from response measurements on submerged floating tunnels",
Rolf Magne Larssen, 1996:119, ISBN 82-471-0014-2, ISSN 0802-3271.

“Numerical modelling of plain and reinforced concrete by damage mechanics”,
Mario A. Polanco-Loria, 1997:20, ISBN 82-471-0049-5, ISSN 0802-3271.

“Nonlinear random vibrations - numerical analysis by path integration methods”,
Vibeke Moe, 1997:26, ISBN 82-471-0056-8, ISSN 0802-3271.

"Numerical prediction of vortex-induced vibration by the finite element method",
Joar Martin Dalheim, 1997:63, ISBN 82-471-0096-7, ISSN 0802-3271.

"Time domain calculations of buffeting response for wind sensitive structures",
Ketil Aas-Jakobsen, 1997:148, ISBN 82-471-0189-0, ISSN 0802-3271.

"A numerical study of flow about fixed and flexibly mounted circular cylinders",
Trond Stokka Meling, 1998:48, ISBN 82-471-0244-7, ISSN 0802-3271.

"Estimation of chloride penetration into concrete bridges in coastal areas",
Per Egil Steen, 1998:89, ISBN 82-471-0290-0, ISSN 0802-3271.

"Stress-resultant material models for reinforced concrete plates and shells",
Jan Arve Øverli, 1998:95, ISBN 82-471-0297-8, ISSN 0802-3271.

"Chloride binding in concrete. Effect of surrounding environment and concrete composition",
Claus Kenneth Larsen, 1998:101, ISBN 82-471-0337-0, ISSN 0802-3271.

"Rotational capacity of aluminium alloy beams",
Lars A. Moen, 1999:1, ISBN 82-471-0365-6, ISSN 0802-3271.

"Stretch Bending of Aluminium Extrusions",
Arild H. Clausen, 1999:29, ISBN 82-471-0396-6, ISSN 0802-3271.

"Aluminium and Steel Beams under Concentrated Loading",
Tore Tryland, 1999:30, ISBN 82-471-0397-4, ISSN 0802-3271.

"Engineering Models of Elastoplasticity and Fracture for Aluminium Alloys",
Odd-Geir Lademo, 1999:39, ISBN 82-471-0406-7, ISSN 0802-3271.

"Kapasitet og duktilitet av dybelforbindelser i trekonstruksjoner",
Jan Siem, 1999:46, ISBN 82-471-0414-8, ISSN 0802-3271.

"Etablering av distribuert ingeniørarbeid; Teknologiske og organisatoriske erfaringer fra en norsk ingeniørbedrift",
Lars Line, 1999:52, ISBN 82-471-0420-2, ISSN 0802-3271.

"Estimation of Earthquake-Induced Response",
Símon Ólafsson, 1999:73, ISBN 82-471-0443-1, ISSN 0802-3271.

"Coastal Concrete Bridges: Moisture State, Chloride Permeability and Aging Effects"
Ragnhild Holen Relling, 1999:74, ISBN 82-471-0445-8, ISSN 0802-3271.

"Capacity Assessment of Titanium Pipes Subjected to Bending and External Pressure",
Arve Bjørset, 1999:100, ISBN 82-471-0473-3, ISSN 0802-3271.

“Validation of Numerical Collapse Behaviour of Thin-Walled Corrugated Panels”,
Håvar Ilstad, 1999:101, ISBN 82-471-0474-1, ISSN 0802-3271.

“Strength and Ductility of Welded Structures in Aluminium Alloys”,
Miroslaw Matusiak, 1999:113, ISBN 82-471-0487-3, ISSN 0802-3271.

“Thermal Dilation and Autogenous Deformation as Driving Forces to Self-Induced Stresses in High Performance Concrete”,
Øyvind Bjøntegaard, 1999:121, ISBN 82-7984-002-8, ISSN 0802-3271.

“Some Aspects of Ski Base Sliding Friction and Ski Base Structure”,
Dag Anders Moldestad, 1999:137, ISBN 82-7984-019-2, ISSN 0802-3271.

"Electrode reactions and corrosion resistance for steel in mortar and concrete",
Roy Antonsen, 2000:10, ISBN 82-7984-030-3, ISSN 0802-3271.

"Hydro-Physical Conditions in Kelp Forests and the Effect on Wave Damping and Dune Erosion. A case study on Laminaria Hyperborea",
Stig Magnar Løvås, 2000:28, ISBN 82-7984-050-8, ISSN 0802-3271.

"Random Vibration and the Path Integral Method",
Christian Skaug, 2000:39, ISBN 82-7984-061-3, ISSN 0802-3271.

"Buckling and geometrical nonlinear beam-type analyses of timber structures",
Trond Even Eggen, 2000:56, ISBN 82-7984-081-8, ISSN 0802-3271.

”Structural Crashworthiness of Aluminium Foam-Based Components”,
Arve Grønsund Hanssen, 2000:76, ISBN 82-7984-102-4, ISSN 0809-103X.

“Measurements and simulations of the consolidation in first-year sea ice ridges, and some aspects of mechanical behaviour”,
Knut V. Høyland, 2000:94, ISBN 82-7984-121-0, ISSN 0809-103X.

”Kinematics in Regular and Irregular Waves based on a Lagrangian Formulation”,
Svein Helge Gjøsund, 2000-86, ISBN 82-7984-112-1, ISSN 0809-103X.

”Self-Induced Cracking Problems in Hardening Concrete Structures”,
Daniela Bosnjak, 2000-121, ISBN 82-7984-151-2, ISSN 0809-103X.

"Ballistic Penetration and Perforation of Steel Plates",
Tore Børvik, 2000:124, ISBN 82-7984-154-7, ISSN 0809-103X.

"Freeze-Thaw resistance of Concrete. Effect of: Curing Conditions, Moisture Exchange and Materials",
Terje Finnerup Rønning, 2001:14, ISBN 82-7984-165-2, ISSN 0809-103X

"Structural behaviour of post tensioned concrete structures. Flat slab. Slabs on ground",
Steinar Trygstad, 2001:52, ISBN 82-471-5314-9, ISSN 0809-103X.

"Slipforming of Vertical Concrete Structures. Friction between concrete and slipform panel",
Kjell Tore Fosså, 2001:61, ISBN 82-471-5325-4, ISSN 0809-103X.

"Some numerical methods for the simulation of laminar and turbulent incompressible flows",
Jens Holmen, 2002:6, ISBN 82-471-5396-3, ISSN 0809-103X.

“Improved Fatigue Performance of Threaded Drillstring Connections by Cold Rolling”,
Steinar Kristoffersen, 2002:11, ISBN: 82-421-5402-1, ISSN 0809-103X.

"Deformations in Concrete Cantilever Bridges: Observations and Theoretical Modelling",
Peter F. Takâcs, 2002:23, ISBN 82-471-5415-3, ISSN 0809-103X.

"Stiffened aluminium plates subjected to impact loading",
Hilde Giæver Hildrum, 2002:69, ISBN 82-471-5467-6, ISSN 0809-103X.

"Full- and model scale study of wind effects on a medium-rise building in a built up area",
Jónas Thór Snæbjørnsson, 2002:95, ISBN82-471-5495-1, ISSN 0809-103X.

“Evaluation of Concepts for Loading of Hydrocarbons in Ice-infested water”,
Arnor Jensen, 2002:114, ISBN 82-417-5506-0, ISSN 0809-103X.

”Numerical and Physical Modelling of Oil Spreading in Broken Ice”,
Janne K. Økland Gjøsteen, 2002:130, ISBN 82-471-5523-0, ISSN 0809-103X.

”Diagnosis and protection of corroding steel in concrete”,
Franz Pruckner, 20002:140, ISBN 82-471-5555-4, ISSN 0809-103X.

“Tensile and Compressive Creep of Young Concrete: Testing and Modelling”,
Dawood Atrushi, 2003:17, ISBN 82-471-5565-6, ISSN 0809-103X.

“Rheology of Particle Suspensions. Fresh Concrete, Mortar and Cement Paste with Various Types of Lignosulfonates”,
Jon Elvar Wallevik, 2003:18, ISBN 82-471-5566-4, ISSN 0809-103X.

“Oblique Loading of Aluminium Crash Components”,
Aase Reyes, 2003:15, ISBN 82-471-5562-1, ISSN 0809-103X.

“Utilization of Ethiopian Natural Pozzolans”,
Surafel Ketema Desta, 2003:26, ISSN 82-471-5574-5, ISSN:0809-103X.

“Behaviour and strength prediction of reinforced concrete structures with discontinuity regions”, Helge Brå, 2004:11, ISBN 82-471-6222-9, ISSN 1503-8181.

“High-strength steel plates subjected to projectile impact. An experimental and numerical study”, Sumita Dey, 2004:38, ISBN 82-471-6282-2 (printed version), ISBN 82-471-6281-4 (electronic version), ISSN 1503-8181.

“Alkali-reactive and inert fillers in concrete. Rheology of fresh mixtures and expansive reactions.”
Bård M. Pedersen, 2004:92, ISBN 82-471-6401-9 (printed version), ISBN 82-471-6400-0 (electronic version), ISSN 1503-8181.

“On the Shear Capacity of Steel Girders with Large Web Openings”.
Nils Christian Hagen, 2005:9 ISBN 82-471-6878-2 (printed version), ISBN 82-471-6877-4 (electronic version), ISSN 1503-8181.

”Behaviour of aluminium extrusions subjected to axial loading”.
Østen Jensen, 2005:7, ISBN 82-471-6873-1 (printed version), ISBN 82-471-6872-3 (electronic version), ISSN 1503-8181.

”Thermal Aspects of corrosion of Steel in Concrete”.
Jan-Magnus Østvik, 2005:5, ISBN 82-471-6869-3 (printed version), ISBN 82-471-6868 (electronic version), ISSN 1503-8181.

”Mechanical and adaptive behaviour of bone in relation to hip replacement.” A study of bone remodelling and bone grafting.
Sébastien Muller, 2005:34, ISBN 82-471-6933-9 (printed version), ISBN 82-471-6932-0 (electronic version), ISSN 1503-8181.

“Analysis of geometrical nonlinearities with applications to timber structures”.
Lars Wollebæk, 2005:74, ISBN 82-471-7050-5 (printed version), ISBN 82-471-7019-1 (electronic version), ISSN 1503-8181.

“Pedestrian induced lateral vibrations of slender footbridges”,
Anders Rönnquist, 2005:102, ISBN 82-471-7082-5 (printed version), ISBN 82-471-7081-7 (electronic version), ISSN 1503-8181.

“Initial Strength Development of Fly Ash and Limestone Blended Cements at Various Temperatures Predicted by Ultrasonic Pulse Velocity”,
Tom Ivar Fredvik, 2005:112, ISBN 82-471-7105-8 (printed version), ISBN 82-471-7103-1 (electronic version), ISSN 1503-8181.

“Behaviour and modelling of thin-walled cast components”,
Cato Dørum, 2005:128, ISBN 82-471-7140-6 (printed version), ISBN 82-471-7139-2 (electronic version), ISSN 1503-8181.

“Behaviour and modelling of selfpiercing riveted connections”,
Raffaele Porcaro, 2005:165, ISBN 82-471-7219-4 (printed version), ISBN 82-471-7218-6 (electronic version), ISSN 1503-8181.

”Behaviour and Modelling og Aluminium Plates subjected to Compressive Load”,
Lars Rønning, 2005:154, ISBN 82-471-7169-1 (printed version), ISBN 82-471-7195-3 (electronic version), ISSN 1503-8181.

”Bumper beam-longitudinal system subjected to offset impact loading”,
Satyanarayana Kokkula, 2005:193, ISBN 82-471-7280-1 (printed version), ISBN 82-471-7279-8 (electronic version), ISSN 1503-8181.

“Control of Chloride Penetration into Concrete Structures at Early Age”,
Guofei Liu, 2006:46, ISBN 82-471-7838-9 (printed version), ISBN 82-471-7837-0 (electronic version), ISSN 1503-8181.

“Modelling of Welded Thin-Walled Aluminium Structures”,
Ting Wang, 2006:78, ISBN 82-471-7907-5 (printed version), ISBN 82-471-7906-7 (electronic version), ISSN 1503-8181.

”Time-variant reliability of dynamic systems by importance sampling and probabilistic analysis of ice loads”,
Anna Ivanova Olsen, 2006:139, ISBN 82-471-8041-3 (printed version), ISBN 82-471-8040-5 (electronic version), ISSN 1503-8181.

“Fatigue life prediction of an aluminium alloy automotive component using finite element analysis of surface topography”.
Sigmund Kyrre Ås, 2006:25, ISBN 82-471-7791-9 (printed version), ISBN 82-471-7791-9 (electronic version), ISSN 1503-8181.

”Constitutive models of elastoplasticity and fracture for aluminium alloys under strain path change”,
Dasharatha Achani, 2006:76, ISBN 82-471-7903-2 (printed version), ISBN 82-471-7902-4 (electronic version), ISSN 1503-8181.

“Simulations of 2D dynamic brittle fracture by the Element-free Galerkin method and linear fracture mechanics”,
Tommy Karlsson, 2006:125, ISBN 82-471-8011-1 (printed version), ISBN 82-471-8010-3 (electronic version), ISSN 1503-8181.

“Penetration and Perforation of Granite Targets by Hard Projectiles”,
Chong Chiang Seah, 2006:188, ISBN 82-471-8150-9 (printed version), ISBN 82-471-8149-5 (electronic version), ISSN 1503-8181.

"Deformations, strain capacity and cracking of concrete in plastic and early hardening phases",
Tor Arne Hammer, 2007:234, ISBN 978-82-471-5191-4 (printed version), ISBN 978-82-471-5207-2 (electronic version), ISSN 1503-8181.

"Crashworthiness of dual-phase high-strength steel: Material and Component behaviour", Venkatapathi Tarigopula, 2007:230, ISBN 82-471-5076-4 (printed version), ISBN 82-471-5093-1 (electronic version), ISSN 1503-8181.

"Fibre reinforcement in load carrying concrete structures",
Åse Lyslo Døssland, 2008:50, ISBN 978-82-471-6910-0 (printed version), ISBN 978-82-471-6924-7 (electronic version), ISSN 1503-8181.

"Low-velocity penetration of aluminium plates",
Frode Grytten, 2008:46, ISBN 978-82-471-6826-4 (printed version), ISBN 978-82-471-6843-1 (electronic version), ISSN 1503-8181.

"Robustness studies of structures subjected to large deformations",
Ørjan Fyllingen, 2008:24, ISBN 978-82-471-6339-9 (printed version), ISBN 978-82-471-6342-9 (electronic version), ISSN 1503-8181.

"Constitutive modelling of morsellised bone",
Knut Birger Lunde, 2008:92, ISBN 978-82-471-7829-4 (printed version), ISBN 978-82-471-7832-4 (electronic version), ISSN 1503-8181.

"Experimental Investigations of Wind Loading on a Suspension Bridge Girder",
Bjørn Isaksen, 2008:131, ISBN 978-82-471-8656-5 (printed version), ISBN 978-82-471-8673-2 (electronic version), ISSN 1503-8181.

"Cracking Risk of Concrete Structures in The Hardening Phase",
Guomin Ji, 2008:198, ISBN 978-82-471-1079-9 (printed version), ISBN 978-82-471-1080-5 (electronic version), ISSN 1503-8181.

"Modelling and numerical analysis of the porcine and human mitral apparatus",
Victorien Emile Prot, 2008:249, ISBN 978-82-471-1192-5 (printed version), ISBN 978-82-471-1193-2 (electronic version), ISSN 1503-8181.

"Strength analysis of net structures",
Heidi Moe, 2009:48, ISBN 978-82-471-1468-1 (printed version), ISBN 978-82-471-1469-8 (electronic version), ISSN1503-8181.

"Numerical analysis of ductile fracture in surface cracked shells",
Espen Berg, 2009:80, ISBN 978-82-471-1537-4 (printed version), ISBN 978-82-471-1538-1 (electronic version), ISSN 1503-8181.

"Subject specific finite element analysis of bone – for evaluation of the healing of a leg lengthening and evaluation of femoral stem design",
Sune Hansborg Pettersen, 2009:99, ISBN 978-82-471-1579-4 (printed version), ISBN 978-82-471-1580-0 (electronic version), ISSN 1503-8181.

"Evaluation of fracture parameters for notched multi-layered structures",
Lingyun Shang, 2009:137, ISBN 978-82-471-1662-3 (printed version), ISBN 978-82-471-1663-0 (electronic version), ISSN 1503-8181.

"Modelling of Dynamic Material Behaviour and Fracture of Aluminium Alloys for Structural Applications"
Yan Chen, 2009:69, ISBN 978-82-471-1515-2 (printed version), ISBN 978-82 471-1516-9 (electronic version), ISSN 1503-8181.

"Nanomechanics of polymer and composite particles"
Jianying He 2009:213, ISBN 978-82-471-1828-3 (printed version), ISBN 978-82-471-1829-0 (electronic version), ISSN 1503-8181.

"Mechanical properties of clear wood from Norway spruce"
Kristian Berbom Dahl 2009:250, ISBN 978-82-471-1911-2 (printed version) ISBN 978-82-471-1912-9 (electronic version), ISSN 1503-8181.

"Modeling of the degradation of TiB_2 mechanical properties by residual stresses and liquid Al penetration along grain boundaries"
Micol Pezzotta 2009:254, ISBN 978-82-471-1923-5 (printed version) ISBN 978-82-471-1924-2 (electronic version) ISSN 1503-8181.

"Effect of welding residual stress on fracture"
Xiabo Ren 2010:77, ISBN 978-82-471-2115-3 (printed version) ISBN 978-82-471-2116-0 (electronic version), ISSN 1503-8181.

"Pan-based carbon fiber as anode material in cathodic protection system for concrete structures"
Mahdi Chini 2010:122, ISBN 978-82-471-2210-5 (printed version) ISBN 978-82-471-2213-6 (electronic version), ISSN 1503-8181.

"Structural Behaviour of deteriorated and retrofitted concrete structures"
Irina Vasililjeva Sæther 2010:171, ISBN 978-82-471-2315-7 (printed version) ISBN 978-82-471-2316-4 (electronic version) ISSN 1503-8181.

"Prediction of local snow loads on roofs"
Vivian Meløysund 2010:247, ISBN 978-82-471-2490-1 (printed version) ISBN 978-82-471-2491-8 (electronic version) ISSN 1503-8181.

"Behaviour and modelling of polymers for crash applications"
Virgile Delhaye 2010:251, ISBN 978-82-471-2501-4 (printed version) ISBN 978-82-471-2502-1 (electronic version) ISSN 1503-8181.

"Blended cement with reducted CO_2 emission – Utilizing the Fly Ash-Limestone Synergy",
Klaartje De Weerdt 2011:32, ISBN 978-82-471-2584-7 (printed version) ISBN 978-82-471-2584-4 (electronic version) ISSN 1503-8181.

"Chloride induced reinforcement corrosion in concrete" Concept of critical chloride content – methods and mechanisms.
Ueli Angst 2011:113, ISBN 978-82-471-2769-9 (printed version) ISBN 978-82-471-2763-6 (electronic version) ISSN 1503-8181.

"A thermo-electric-Mechanical study of the carbon anode and contact interface for Energy savings in the production of aluminium".
Dag Herman Andersen 2011:157, ISBN 978-82-471-2859-6 (printed version) ISBN 978-82-471-2860-2 (electronic version) ISSN 1503-8181.

"Structural Capacity of Anchorage Ties in Masonry Veneer Walls Subjected to Earthquake". The implications of Eurocode 8 and Eurocode 6 on a typical Norwegain veneer wall.
Ahmed Mohamed Yousry Hamed 2011:181, ISBN 978-82-471-2911-1 (printed version) ISBN 978-82-471-2912-8 (electronic ver.) ISSN 1503-8181.

"Work-hardening behaviour in age-hardenable Al-Zn-Mg(-Cu) alloys".
Ida Westermann , 2011:247, ISBN 978-82-471-3056-8 (printed ver.) ISBN 978-82-471-3057-5 (electronic ver.) ISSN 1503-8181.

"Behaviour and modelling of selfpiercing riveted connections using aluminium rivets".
Nguyen-Hieu Hoang, 2011:266, ISBN 978-82-471-3097-1 (printed ver.) ISBN 978-82-471-3099-5 (electronic ver.) ISSN 1503-8181.

"Fibre reinforced concrete".
Sindre Sandbakk, 2011:297, ISBN 978-82-471-3167-1 (printed ver.) ISBN 978-82-471-3168-8 (electronic ver) ISSN 1503:8181.

"Dynamic behaviour of cablesupported bridges subjected to strong natural wind".
Ole Andre Øiseth, 2011:315, ISBN 978-82-471-3209-8 (printed ver.) ISBN 978-82-471-3210-4 (electronic ver.) ISSN 1503-8181.

"Constitutive modeling of solargrade silicon materials"
Julien Cochard, 2011:307, ISBN 978-82-471-3189-3 (printed ver). ISBN 978-82-471-3190-9 (electronic ver.) ISSN 1503-8181.

"Constitutive behavior and fracture of shape memory alloys"
Jim Stian Olsen, 2012:57, ISBN 978-82-471-3382-8 (printed ver.) ISBN 978-82-471-3383-5 (electronic ver.) ISSN 1503-8181.

“Field measurements in mechanical testing using close-range photogrammetry and digital image analysis”
Egil Fagerholt, 2012:95, ISBN 978-82-471-3466-5 (printed ver.) ISBN 978-82-471-3467-2 (electronic ver.) ISSN 1503-8181.

“Towards a better under standing of the ultimate behaviour of lightweight aggregate concrete in compression and bending”,
Håvard Nedrelid, 2012:123, ISBN 978-82-471-3527-3 (printed ver.) ISBN 978-82-471-3528-0 (electronic ver.) ISSN 1503-8181.

“Numerical simulations of blood flow in the left side of the heart”
Sigrid Kaarstad Dahl, 2012:135, ISBN 978-82-471-3553-2 (printed ver.) ISBN 978-82-471-3555-6 (electronic ver.) ISSN 1503-8181.

“Moisture induced stresses in glulam”
Vanessa Angst-Nicollier, 2012:139, ISBN 978-82-471-3562-4 (printed ver.) ISBN 978-82-471-3563-1 (electronic ver.) ISSN 1503-8181.

“Biomechanical aspects of distraction osteogensis”
Valentina La Russa, 2012:250, ISBN 978-82-471-3807-6 (printed ver.) ISBN 978-82-471-3808-3 (electronic ver.) ISSN 1503-8181.

“Ductile fracture in dual-phase steel. Theoretical, experimental and numerical study”
Gaute Gruben, 2012:257, ISBN 978-82-471-3822-9 (printed ver.) ISBN 978-82-471-3823-6 (electronic ver.) ISSN 1503-8181.

“Damping in Timber Structures”
Nathalie Labonnote, 2012:263, ISBN 978-82-471-3836-6 (printed ver.) ISBN 978-82-471-3837-3 (electronic ver.) ISSN 1503-8181.

“Biomechanical modeling of fetal veins: The umbilical vein and ductus venosus bifurcation”
Paul Roger Leinan, 2012:299, ISBN 978-82-471-3915-8 (printed ver.) ISBN 978-82-471-3916-5 (electronic ver.) ISSN 1503-8181.

“Large-Deformation behaviour of thermoplastics at various stress states”
Anne Serine Ognedal, 2012:298, ISBN 978-82-471-3913-4 (printed ver.) ISBN 978-82-471-3914-1 (electronic ver.) ISSN 1503-8181.

“Hardening accelerator for fly ash blended cement”
Kien Dinh Hoang, 2012:366, ISBN 978-82-471-4063-5 (printed ver.) ISBN 978-82-471-4064-2 (electronic ver.) ISSN 1503-8181.

“From molecular structure to mechanical properties”
Jianyang Wu, 2013:186, ISBN 978-82-471-4485-5 (printed ver.) ISBN 978-82-471-4486-2 (electronic ver.) ISSN 1503-8181.

“Experimental and numerical study of hybrid concrete structures”
Linn Grepstad Nes, 2013:259, ISBN 978-82-471-4644-6 (printed ver.) ISBN 978-82-471-4645-3 (electronic ver.) ISSN 1503-8181.

“Mechanics of ultra-thin multi crystalline silicon wafers”
Saber Saffar, 2013:199, ISBN 978-82-471-4511-1 (printed ver.) ISBN 978-82-471-4513-5 (electronic ver). ISSN 1503-8181.

“Through process modelling of welded aluminium structures”
Anizahyati Alisibramulisi, 2013:325, ISBN 978-82-471-4788-7 (printed ver.) ISBN 978-82-471-4789-4 (electronic ver.) ISSN 1503-8181.

“Combined blast and fragment loading on steel plates”
Knut Gaarder Rakvåg, 2013:361, ISBN978-82-471-4872-3 (printed ver.) ISBN 978-82-4873-0 (electronic ver.). ISSN 1503-8181.

“Characterization and modelling of the anisotropic behaviour of high-strength aluminium alloy”
Marion Fourmeau, 2014:37, ISBN 978-82-326-0008-3 (printed ver.) ISBN 978-82-326-0009-0 (electronic ver.) ISSN 1503-8181.

“Behaviour of threated steel fasteners at elevated deformation rates”
Henning Fransplass, 2014:65, ISBN 978-82-326-0054-0 (printed ver.) ISBN 978-82-326-0055-7 (electronic ver.) ISSN 1503-8181.

“Sedimentation and Bleeding”
Ya Peng, 2014:89, ISBN 978-82-326-0102-8 (printed ver.) ISBN 978-82-326-0103-5 (electric ver.) ISSN 1503-8181.

“Impact against X65 offshore pipelines”
Martin Kristoffersen, 2014:362, ISBN 978-82-326-0636-8 (printed ver.) ISBN 978-82-326-0637-5 (electronic ver.) ISSN 1503-8181.

“Formability of aluminium alloy subjected to prestrain by rolling”
Dmitry Vysochinskiy, 2014:363,, ISBN 978-82-326-0638-2 (printed ver.) ISBN 978-82-326-0639-9 (electronic ver.) ISSN 1503-8181.

“Experimental and numerical study of Yielding, Work-Hardening and anisotropy in textured AA6xxx alloys using crystal plasticity models”
Mikhail Khadyko, 2015:28, ISBN 978-82-326-0724-2 (printed ver.) ISBN 978-82-326-0725-9 (electronic ver.) ISSN 1503-8181.

“Behaviour and Modelling of AA6xxx Aluminium Alloys Under a Wide Range of Temperatures and Strain Rates”
Vincent Vilamosa, 2015:63, ISBN 978-82-326-0786-0 (printed ver.) ISBN 978-82-326-0787-7 (electronic ver.) ISSN 1503-8181.

"A Probabilistic Approach in Failure Modelling of Aluminium High Pressure Die-Castings"
Octavian Knoll, 2015:137, ISBN 978-82-326-0930-7 (printed ver.) ISBN 978-82-326-0931-4 (electronic ver.) ISSN 1503-8181.

"Ice Abrasion on Marine Concrete Structures"
Egil Møen, 2015:189, ISBN 978-82-326-1034-1 (printed ver.) ISBN 978-82-326-1035-8 (electronic ver.) ISSN 1503-8181.

"Fibre Orientation in Steel-Fibre-Reinforced Concrete"
Giedrius Zirgulis, 2015:229, ISBN 978-82-326-1114-0 (printed ver.) ISBN 978-82-326-1115-7 (electronic ver.) ISSN 1503-8181.

"Effect of spatial variation and possible interference of localised corrosion on the residual capacity of a reinforced concrete beam"
Mohammad Mahdi Kioumarsi, 2015:282, ISBN 978-82-326-1220-8 (printed ver.) ISBN 978-82-1221-5 (electronic ver.) ISSN 1503-8181.

"The role of concrete resistivity in chloride-induced macro-cell corrosion"
Karla Horbostel, 2015:324, ISBN 978-82-326-1304-5 (printed ver.) ISBN 978-82-326-1305-2 (electonic ver.) ISSN 1503-8181.

"Flowable fibre-reinforced concrete for structural applications"
Elena Vidal Sarmiento, 2015-335, ISBN 978-82-326-1324-3 (printed ver.) ISBN 978-82-326-1325-0 (electronic ver.) ISSN 1503-8181.

"Development of chushed sand for concrete production with microproportioning"
Rolands Cepuritis, 2016:19, ISBN 978-82-326-1382-3 (printed ver.) ISBN 978-82-326-1383-0 (electronic ver.) ISSN 1503-8181.

"Withdrawal properties of threaded rods embedded in glued-laminated timer elements"
Haris Stamatopoulos, 2016:48, ISBN 978-82-326-1436-3 (printed ver.) ISBN 978-82-326-1437-0 (electronic ver.) ISSN 1503-8181.

"An Experimental and numerical study of thermoplastics at large deformation"
Marius Andersen, 2016:191, ISBN 978-82-326-1720-3 (printed ver.) ISBN 978-82-326-1721-0 (electronic ver.) ISSN 1503-8181.

"Modeling and Simulation of Ballistic Impact"
Jens Kristian Holmen, 2016:240, ISBN 978-82-326-1818-7 (printed ver). ISBN 978-82-326-1819-4 (electronic ver.) ISSN 1503-8181.

"Early age crack assessment of concrete structures"
Anja B. Estensen Klausen, 2016:256, ISBN 978-82-326-1850-7 (printed ver). ISBN 978-82-326-1851-4 (electronic ver.) ISSN 1503-8181.

“Uncertainty quantification and sensitivity analysis for cardiovascular models”
Vinzenz Gregor Eck, 2016:234, ISBN 978-82-326-1806-4 (printed ver.) ISBN 978-82-326-1807-1 (electronic ver.) ISSN 1503-8181.

“Dynamic behaviour of existing and new railway catenary systems under Norwegain conditions”
Petter Røe Nåvik, 2016:298, ISBN 978-82-326-1935-1 (printed ver.) ISBN 978-82-326-1934-4 (electronic ver.) ISSN 1503-8181.

“Mechanical behaviour of particle-filled elastomers at various temperatures”
Arne Ilseng, 2016-295, ISBN978-82-326-1928-3 (printed ver.) ISBN 978-82-326-1929-0 (electronic ver.) ISSN 1503-8181.

“Nanotechnology for Anti-Icing Application”
Zhiwei He, 2016:348, ISBN 978-82-326-2038-8 (printed ver.) ISBN 978-82-326-2019-5 (electronic ver.) ISSN 1503-8181.

“Conduction Mechanisms in Conductive Adhesives with Metal-Coated Polyer Spheres”
Sigurd Rolland Pettersen, 2016:349, ISBN 978-326-2040-1 (printed ver,) ISBN 978-82-326-2041-8 (electronic ver.) ISSN 1503-8181.

“The interaction between calcium lignosulfonate and cement”
Alessia Colombo, 2017:20, ISBN 978-82-326-2122-4 (printed ver.) ISBN 978-82-326-2123-1 (electronic ver.) ISSN 1503-8181.

“Behaviour and Modelling of Flexible Structures Subjected to Blast Loading”
Vegard Aune, 2017:101, ISBN 978-82-326-2274-0 (printed ver.) ISBN 978-82-326-2275-7 (electronic ver.) ISSN 1503-8181.

“Behaviour of steel connections under quasi-static and impact loading”
Erik Løhre Grimsmo, 2017:159, ISBN 978-82-326-2390-7 (printed ver.) ISBN 978-82-326-2391-4 (electronic ver.) ISSN 1503-8181.

“An experimental and numerical study of cortical bone at he macro and Nano-scale”
Masoud Ramenzanzadehkoldeh,, 2017:208, ISBN 978-82-326-2488-1 (printed ver.) ISBN 978-82-326-2489-8 (electronic ver.) ISSN 1503-8181.

“Optoelectrical Properties of a Novel Organic Semiconductor: 6,13-Dichloropentacene”
Mao Wang, 2017:130, ISBN 978-82-326-2332-7 (printed ver.) ISBN 978-82-326-2333-4) (electronic ver.) ISSN 1503-8181.

“Core-shell structured microgels and their behavior at oil and water interface”
Yi Gong, 2017:182, ISBN 978-82-326-2436-2 (printed. ver.) ISBN 978-82-326-2437-9 (electronic ver.) ISSN 1503-8181.

"Aspects of design of reinforced concrete structures using nonliear finite element analyses"
Morten Engen, 2017:149, ISBN 978-82-326-2370-9 (printed ver.) ISBN 978-82-326-2371-6 (electronic ver.) ISSN 1503-8181.

"Numerical studies on ductile failure of aluminium alloys"
Lars Edvard Dæhli, 2017:284, ISBN 978-82-326-2636-6 (printed ver.) ISBN 978-82-326-2637-3 (electronic ver.) ISSN 1503-8181.

"Modelling and Assessment of Hydrogen Embrittlement in Steels and Nickel Alloys"
Haiyang Yu, 2017:278, ISBN 978-82-326-2624-3 (printed. ver.) ISBN 978-82-326-2625-0 (electronic ver.) ISSN 1503-8181.

"Network arch timber bridges with light timber deck on transverse crossbeams"
Anna Weronika Ostrycharczyk, 2017:318, ISBN 978-82-326-2704-2 (printed ver.) ISBN 978-82-326-2705-9 (electronic ver.) ISSN 1503-8181.

"Splicing of Large Glued Laminated Timber Elements by Use of Long Threated Rods"
Martin Cepelka, 2017:320, ISBN 978-82-326-2708-0 (printed ver.) ISBN 978-82-326-2709-7 (electronic ver.) ISSN 1503-8181.

"Thermomechanical behaviour of semi-crystalline polymers: experiments, modelling and simulation"
Joakim Johnsen, 2017-317, ISBN 978-82-326-2702-8 (printed ver.) ISBN 978-82-326-2703-5 (electronic ver.) ISSN 1503-8181.